Swansea University
Prifysgol Abertawe

Cronfa
Setting Research Free

Swansea University E-Theses

The influence of elastomer support on machine behaviour.

Sim, Ling Fann

How to cite:

Sim, Ling Fann (2005) *The influence of elastomer support on machine behaviour..* thesis, Swansea University.
http://cronfa.swan.ac.uk/Record/cronfa43151

Use policy:

This item is brought to you by Swansea University. Any person downloading material is agreeing to abide by the terms of the repository licence: copies of full text items may be used or reproduced in any format or medium, without prior permission for personal research or study, educational or non-commercial purposes only. The copyright for any work remains with the original author unless otherwise specified. The full-text must not be sold in any format or medium without the formal permission of the copyright holder. Permission for multiple reproductions should be obtained from the original author.

Authors are personally responsible for adhering to copyright and publisher restrictions when uploading content to the repository.

Please link to the metadata record in the Swansea University repository, Cronfa (link given in the citation reference above.)

http://www.swansea.ac.uk/library/researchsupport/ris-support/

University of Wales Swansea
School of Engineering

THE INFLUENCE OF ELASTOMER SUPPORT ON MACHINE BEHAVIOUR

By

LING FANN SIM
B. Eng. (Hons.)

Thesis submitted to the University of Wales Swansea
for the degree of Master of Philosophy

ProQuest Number: 10821543

All rights reserved

INFORMATION TO ALL USERS
The quality of this reproduction is dependent upon the quality of the copy submitted.

In the unlikely event that the author did not send a complete manuscript
and there are missing pages, these will be noted. Also, if material had to be removed,
a note will indicate the deletion.

ProQuest 10821543

Published by ProQuest LLC (2018). Copyright of the Dissertation is held by the Author.

All rights reserved.
This work is protected against unauthorized copying under Title 17, United States Code
Microform Edition © ProQuest LLC.

ProQuest LLC.
789 East Eisenhower Parkway
P.O. Box 1346
Ann Arbor, MI 48106 – 1346

UNIVERSITY OF WALES SWANSEA
LIBRARY

Declaration

This work has not previously been accepted in substance for any degree and is not being concurrently submitted in candidature for any degree.

Signed (candidate): _____

Date: 17/5/2005

Statement 1

This thesis is the result of my own investigations, except where otherwise stated. Other sources are acknowledged by the use of explicit references. A list of references is included.

Signed (candidate): _____ _____

Date: 17/5/2005

Statement 2

I hereby give consent for my thesis, if accepted, to be available for photocopying and for inter-library loan, and for the title and summary to be made available to outside organisations.

Signed (candidate): _____ _____

Date: 17/5/2005

ACKNOWLEDGEMENTS

I wish to thank School of Engineering for the use of all their facilities throughout this project. I would like to express my gratitude to Prof. A. W. Lees for his guidance, supervision and support and for his careful checking and helpful comments on this thesis, to bring this work to an optimistic conclusion.

Special thanks to Dr Price and staff of the workshop at Swansea for their valuable help in the experimental work.

Finally, I would also like to thank my family, friends and housemate for their support and consistently cheering me up throughout my study at Swansea.

SUMMARY OF THESIS

The present research is concerned with the influence of elastomers on machine behaviour. Presently, applications of elastomers are receiving greater attention in both academic and industial communities, and hence the present study is carried out. In this thesis, the effects of elastomers on dynamic behaviour of machinery have been addressed, including a review of the relevant literature and an overview of the associated techniques for property identification.

For machinery involving elastomeric damper, it has been shown that the inclusion of elastomers can have a significant influence on the dynamic behaviour of the system. Three different types of tests (run-down test, hammer test and shaker test) have been carried out to accomplish the objective of this research work. It was shown that very different results were obtained when different numbers of layers of elastomers were used.

An identification technique for the influence of elastomer on machine behaviour has been presented. The size of elastomers used in the system can have a significant influence on machine behaviour. It was shown that the increment of elastomers in terms of thickness reduced the natural frequency, stiffness and damping properties of the system. Furthermore, it was also shown that the stiffness tends to increase and damping tends to decrease on increasing the excitation frequency. The identification technique was generally successful, with the measured hammer and shaker test results matching very closely in most cases.

CONTENTS

LIST OF FIGURES

NOMENCLATURE

θ	Rotational angle
x	Thickness of recesses of the bearing housing
r	Distance from the centre of bearing housing
M, C, K	Mass, damping and stiffness matrices
f	Force
C_t	Total Damping
C_i	Internal Damping
C_e	External Damping
r	Response of machine
K_b	Bearing stiffness
M_b	Bearing mass
k_e	Elastomer stiffness
c_e	Elastomer damping
I	Moment of inertia
Γ	Torsional Damping
χ	Torsional Stiffness
M	Moment
θ	Angular displacement
i	Imaginary number, $\sqrt{1}$
ω	Rotor running speed

e	Vector of the rotor unbalance parameters
t	time
a	Real part
b	Imaginary part

CHAPTER 1

INTRODUCTION

In the scientific literature, materials with long molecular chains are often referred to as elastomeric polymers. Due to their high deformability, damping capacity and wide range of obtainable mechanical properties, they have numerous applications in vibration control. Typically, elastomers show a non-linear elastic and dissipative behaviour. This means that stiffness and damping properties of elastomers are non-linear functions of displacement and frequencies when the elastomers are excited by periodic forces.

Presently, applications of elastomers are receiving greater attention in both academic and industrial communities. Industrial applications of elastomers have been successful in several sectors including aerospace, automobile, marine, construction, medical and power plants. There are various companies manufacturing different types compound/ingredient of elastomers for all types of industrial application such as automotive instrument panels, adhesives and sealant for machines, building and construction, etc. However, proper selection of elastomers is essential since a difference in elastomer compounds or ingredients will provide different applications. These factors can improve specific chemical or thermal properties, improve dynamic performance, reduce cost, improve electrical properties, reduce friction or sticking, and many other aspects of seal performance.

Elastomer dampers are also an attractive alternative to the squeeze film for rotating machinery due to their simplicity, inherent combination of stiffness and damping, their compactness and lack of need for seals or oil supply. Elastomers in the form of O-rings or cartridges are being

considered for low-cost engine applications, turbopumps and also for helicopter transmission shafting.

Dynamic systems suffering from instability or resonance problems often lack sufficient damping to reduce the vibration to an acceptable level. Elastomers are particularly suitable to provide the necessary damping for rotors. There is a trend towards small light machines, a case in point being high-speed vacuum pumps, which have been considered recently. These are mounted on elastomers, which provide damping but have properties that vary with a number of external parameters.

Considering the high demand on the application of elastomers, accurate knowledge of the dynamic characteristics is becoming more important. The available knowledge is only the chemical and sealing properties, for example, hardness, performance during different temperature, elongation etc. Nevertheless the dynamic characteristic such as stiffness and damping coefficient are not readily available. Two factors, which resist the growth in the application of elastomers, are the limited availability of the data on their dynamic behaviour and limited qualification of the problems to be encountered in their application [14].

Therefore, the main aim of the project is to describe and quantify the dynamic properties of elastomers on machine behaviour by using experimental and data analysis techniques. Techniques for property identification under operating conditions will be developed in this research work.

In this research, a small rotor rig was build to define the dynamic properties of elastomers. Measurements are obtained from this test rig. The experimental apparatus will be discussed in Chapter 5.

1.1 Thesis Overview

The present chapter serves as a general introduction and gives detailed objectives and highlights the advantages of the present studies. The organisation of the thesis is as follows.

Chapter 2 gives an overview on the recent developments and background in the field of elastomer properties.

Chapter 3 explains the theoretical techniques for identifying the elastomer's dynamic properties from hammer and shaker tests.

Chapter 4 describes the design and commissioning of the run-down experimental rotor rig used to verify the dynamic characteristic of elastomers. As well as the development of the machine itself, the associated data acquisition system and corresponding signal processing issues are also considered. The experimental results of run-down tests are discusses in this chapter.

Chapter 5 gives details of the experimental apparatus for the hammer tests used to verify the identification method presented in Chapter 3. The experimental results of hammer/impact test are discussed in this chapter.

Chapter 6 gives the details of the shaker test experimental test rig used to verify the results of the hammer tests. The experimental results from the shaker tests are also discussed in this chapter.

Chapters 7 discusses and compares the experimental results obtained from hammer/impact test and shaker tests.

Chapter 8 provides a summary of the work presented in this thesis together with some general conclusions and recommendations for future work.

CHAPTER 2

LITERATURE REVIEW

The main aim of this chapter is to provide an insight into recent developments in the field of elastomer properties and literature relating to elastomers. At the present time, research in elastomer properties is receiving greater attention in both academic and industrial communities. Industrial applications have been successful in several sectors including aerospace, automobile, marine, construction and power plant.

The factor, which resists the growth of the application of elastomer dampers, is the limited availability of the information on elastomer properties. Hence, this research is carried out to study and quantify the influence of the dynamics properties of elastomers on machine behaviour.

Research on the subject of elastomer properties is vast and wide ranging. Recently, blending of polymers has become a favourite area of research activity. Blending of two or more types of polymer is a useful technique for the preparation and development of materials with properties superior to those of the individual constituent [1].

Elastomer blends are used for many reasons such as lowering the compound cost, for ease of fabrication and to improve the performance of industrial rubber. There have been numerous papers written on this subject. Research work focused on elastomer/rubber blends has been performed by e.g. *Findik et al.* [1], *Silva et al.* [2], *Louis et al.* [3] and *Zheng Ming Huang et al* [4]. These articles focus on different kinds of research area such as mechanical and physical [1], rheological [2], morphological, thermal and mechanical [3] and stress and strain [4] behaviours of the blended elastomer/rubber.

Since then it has been found that a material with unique mechanical properties is produced from heated natural gum mixed with sulphur. This material had found an indisputable role in many mechanical applications. One of the reasons is that rubber is generally soft and withstands high deformation up to several hundred percent while resuming it original shape after stress release. This elastic property facilitates its wide use as vibration isolators, suspensions and flexible joints in machines.

Elastomeric materials such as rubbers are commonly used as isolators. Therefore, an understanding of the dynamic properties of rubber isolators is necessary for the vibration analysis and optimization of many resilient mounting systems. *Tan and Weng* [5] have developed an identification scheme to investigate the dynamic behaviour of isolated structures in which laminated rubber bearings are used. A few years later, *Richards and Singh* [6] clarified the non-linear stiffness characterization issues of rubber isolators. A process is proposed that includes experiments in single and multi-degree-of-freedom configurations while different types of excitation are applied. It was found that the size and shape of rubbers are giving significant influence on the vibration of the system. The thickness of the rubber also affects the damping characteristics of the system [6]. The finding of this paper [6] is in good agreement with the findings in this work.

At the same time, *Kim and Singh* [7] present a new experimental identification method for extracting the frequency-dependent multi-dimensional dynamic stiffness of an isolator (rubber). The proposed characterization method uses two inertia elements and an isolator, and a refined multi-dimensional mobility synthesis formulation is developed for estimating the properties of the system.

Engineering knowledge of elastomer/rubber properties is often rather poor, despite it being so commonly used. This is probably due to

its complex behaviour where mechanical properties such as dynamic hardness, stiffness and damping are dependent not only on additives in the material but also on temperature, frequency and amplitude of motion [8]. This knowledge is essential when elements composed of elastomer are included in dynamic systems.

The rubber compound frequently has carbon black fillers added. Inclusion of fillers increases material hardness, abrasion resistance and material damping [8]. *Sjőberg and Kari* [8] investigated the nonlinear excitation effects on dynamic stiffness and damping of a filled rubber isolator through measurements.

At present, the problem of controlling the propagation of vibration and shock waves in building construction, car industry, aeronautics and railway track applications are of concern [9]. The measurement of the dynamic stiffness was performed on recycled rubber based railway track mats by *Lapčik et al* [9]. Measurements were performed at three static pre-loads, 0.0, 0.06 and 0.1 MPa in the frequency range 10-100 Hz. A steady increase in the dynamic stiffness with increasing frequency was observed in the samples studied. At the same time, the measured dynamic stiffness shifted to higher absolute values with increasing static pre-load.

The analysis and study of the performance of elastomers in industrial applications is becoming critical in terms of both production and maintenance. It is not surprising as faults in machinery represent crucial aspect of the subject, receiving ever more attention.

Recently, the need has increased for vibration isolation in very important buildings and sensitive semiconductor equipment. An elastomer/rubber is widely used as a vibration damper and an isolator. Base isolation offers the most effective method to reduce vibration transmitted from the ground to the structures. The key point in the

design of an effective base isolation system is the understanding of the isolator characteristics.

One example of an isolator, which is the laminated rubber bearing, has gained wide acceptance in engineering applications. The main characteristic of laminated rubber bearings is that they provide high vertical stiffness to sustain structural weight while maintaining flexibility in the horizontal direction, discussed earlier by Chang [10], the laminated rubber bearings have been modelled using an analytical stiffness matrix. A laminated rubber bearing consists of several layers of rubber bonded to interleaving steel shims. The total number of rubber layers and steel shims is changeable. The variation of stiffness was studied by changing the total number of rubber layers [10]. Using the same experimental concept (laminated rubber bearing consists of rubber layers and steel shims), the influence of the shape factor on the stress distributions and stress concentrations of laminated elastomeric bearings subjected to vertical load is discussed by Imbimbo and De Luca [11].

2.1 Previous Literature of Dynamic Properties of Elastomers

During the course of the last half-century, elastomer properties have been studied in more and more detail. A thorough understanding of the properties of elastomers is essential due to wide application of elastomers in industry. The use of support damping as a means of controling rotating machinery vibrations is seeing increasingly wide application in advanced turbo-machinery. However, there is a surprising lack of literature about elastomer dampers apart from a series of NASA reports.

The earlier literature on elastomer dampers is reported by NASA between 1972 and 1980 [12,13]. In those early years, a program had been pursued at MTI (Mechanical Technology Incorporated), the intention was to quantify dynamic performance of elastomer dampers, to provide the capability, to design for desired characteristics, to evaluate the effects of environment, to demonstrate the effectiveness of elastomer in vibration control for high-speed rotating machinery, and to evaluate any problems which may be encountered in their application to rotating machinery vibration control [12]. The thrust of this work was continued by Tecza et al [12, 13] under this program.

Within this program, a powerful test method for determining elastomer component properties has been developed entitled "The Base Excitation Resonant Mass Method" by Tecza et al in NASA Report Part V [12]. The investigation of the effects of strain, ambient temperature and frequency on elastomer component properties was executed using the Base Excitation Resonant Mass Test Method. This test method employed a large electromagnetic shaker to apply base excitation to a one-degree-of-freedom spring-mass-damper system [12].

The elastomer test specimens form the spring and damper upon which a rigid mass is supported whose magnitude can be varied over a wide range. The transmissibility and phase angle across the elastomer spring were measured in the region of resonance which allows accurate determination of both stiffness and damping [12]. It has been tentatively concluded, for an elastomer in the rubbery region such as polybutadiene, that the dynamic characteristic of an elastomer shows a more consistent dependence on strain than on frequency. Additionally, in all cases, the elastomer was effective in controlling system vibrations [12].

A test rig designed to measure the stiffness and damping of elastomer cartridges under rotating load excitation was described by Darlow and Smalley [13] in NASA Report Part IV. This method of

generating test data for calculating dynamic elastomer properties was essentially the same as the Base Excitation Resonant Mass Technique, except in this case the elastomer specimen was subjected to rotation rather than a reciprocating load. An elastomer cartridge rotating load test rig employs rotating unbalance in a rotor, which runs up to 60000 rpm as the excitation mechanism was used to test the dynamic properties of the elastomer. A variable resonant mass is supported on elastomer elements and the dynamic characteristics are determined from the measurements of input and output acceleration. Different shapes and sizes of elastomer cartridge were considered in the testing. It was found that the stiffness reduces when increasing the thickness of the elastomer, which is in good agreement with the findings in this work.

Dynamic stiffness and damping were measured for each elastomer cartridge and compared with predictions at different frequencies and strains. In this case, the dynamic properties of elastomer were predicted from Beam Column and Gőbel equations [13]. The properties for the ring cartridges were predicted as the arithmetic average of the values obtained from the Beam Column and Gőbel equations. The difference between the Beam Column and Gőbel equations is the inclusion of the radius effect. In the Beam Column equation, the radius effect was considered. It was reported in NASA Report Part III that the prediction from these two equations generally bracketed the ring cartridge test results and that an average of the two predictions usually presented a reasonably good estimate of the actual dynamic properties of the ring cartridge [13].

However, the prediction of the dynamic properties was conducted both including and neglecting the effects of shear loading on the elastomer cartridge, for comparison purposes. It was found that the measured stiffness agreed quite favourably with the predictions that include the effect of shear. However, the measured damping agrees with the predictions only for low frequency test results. The test results

compare well with the predicted values, particularly those from the Gőbel equation [13].

Dynamic systems suffering from instability or resonance problems often lack sufficient damping to reduce vibrations to an acceptable level. Bormann and Gasch [14] developed a simplified approach for the proper selection of elastomers and an optimised design of ring geometry. Both the non-linear static behaviour and the contact problem as well as the temperature and frequency dependent thermo-viscoelastic behaviour are represented by equations derived from the theory of elasticity and these were proven by experiments [14]. In this case, the relationship of the parameters was presented in the format master curves. Here, the master curve is so called a data sheet or design chart giving the loss factor and frequency dependent on the modulus and bearing stiffness. The master curve can be present in different way; for example master curves can appear as the time and temperature dependent modulus of stress relaxation. Based on the material's Master-curve, design charts for simple rotor systems were developed as a graphical approach in order to reveal the complicated interrelationship between elastomer stiffness and damping properties, the bearing to shaft stiffness ratio and the achievable system damping at resonance. The numeric solution can be simplified with the help of Master-curves, since the relevant model-parameters in terms of internal degrees of freedom eliminate the frequency dependence from the damping and stiffness matrices. It was concluded that the presented design-charts, based on the material Master-curves, are well suited for the design of simple rotor systems and for the proper selection of the elastomer rings and their geometry [14].

Torsional vibration in the crankshaft of an internal combustion engine is an inherent problem in its mechanical design [15]. There are several devices that can be used to dampen these undesirable torsional vibrations which are known as vibration absorbers or dampers. The effect of quadratic and cubic non-linearities in elastomeric material dampers

used to reduce torsional oscillations of internal-combustion engines shafts was investigated by El-Bassiouny [15]. In this work, a non-linear elastomeric damper or absorber is used to control the torsional vibrations of the crankshaft in internal combustion engines, when subjected to an external excitation torque.

Recently, a paper by *Petrone et al.* [16] identified a methodology of study, valid for elastomers in general, in order to experimentally characterize their dynamic behaviour and simulate this behaviour by means of a structured mathematical model. An elastomer was chosen and its equivalent viscous damping coefficient was experimentally determined using a specifically designed test rig.

The responses to several sinusoidal excitations, characterized by different amplitude and frequency values were analyzed to determine the stiffness and equivalent viscous damping coefficient. It was found that the dynamic stiffness increased on increasing the excitation frequency and the static load to which the elastomer element was subjected, and decreased on increasing the amplitude of excitation itself. Furthermore, the coefficient of equivalent viscous damping decreased on increasing the excitation frequency and increased on increasing the acceleration amplitude and the static preload applied. The experimental and simulated stiffness and damping were compared; maximum discrepancies of less than 5% were obtained over the entire frequency range, except for frequencies under 40 Hz due to the experimental system being less accurate at low frequencies [16]. In this paper, it had been reported that stiffness tends to increase and damping tends to decrease on increasing the excitation frequency, which is also in good agreement with the findings in this work.

This chapter has provided a broad view of the development and literature about elastomer properties. It has been seen that research in to the dynamic properties is being developed in order to meet the demand of

the increasing application of elastomers in industrial communities. However, there is a lack of information about the dynamic properties of elastomers. The dynamic properties of elastomers need to be studied in order to identify the influence of dynamic characterization on machines due to the wide application of elastomers as dampers/isolators. This area still requires much research to be carried out.

In this project, the influence of the dynamic properties of elastomers on machine behaviour is studied using experimental and data analysis techniques. The results obtained are discussed later in Chapters 4, 5 and 6.

CHAPTER 3

THEORETICAL METHOD FOR SYSTEM IDENTIFICATION

The background literature and developments in the field of elastomer properties has been discussed in the previous chapter. The main aim of this project has been brought out in Chapter 2 and which is to describe and quantify the effect of the dynamic properties of elastomers on machine behaviour by using a combination of experimental and theoretical techniques. This chapter is concerned with the theoretical method of identifying the dynamic properties of elastomers from hammer and shaker tests.

In the early stages of the project, run-down tests were carried out to identify the dynamic properties of elastomers. From the run-down test results obtained, it was found that the experimental results were mainly influenced by the flexibility of the shaft rather than the elastomers. Therefore, later on in the project, hammer tests and shaker tests are carried out in order to verify the influence of elastomers on machine behaviour more precisely.

The bearing pedestal vibration was measured using an accelerometer connected to a charge amplifier and mounted in the horizontal direction. The position of the accelerometer is shown in Figure 3 – 1. Additionally, the force applied to the bearing housing is measured during the experiment. It is assumed that the applied force is known as the excitation force, which is produced by either hammer or shaker. The

relevant forces in the elastomers such as shear and tensile/compressive stresses are neglected in order to simplify the model of this work.

In this case, the bearing housing is forced in the horizontal transverse direction and motion arising is clearly a summation of the horizontal motion of the centre of mass and rotation about this point. However, in the interests of simplicity, rotation is assumed to dominate over the centre of gravity translation allowing the representation of the system as a single-degree of freedom.

3.1 Equation of Motion for Hammer/Shaker Test

A schematic of the hammer test and shaker test is shown in Figure 3 - 1. The accelerometer was mounted in the horizontal direction on the bearing housing in order to measure the vibration of the bearing housing when an excitation force was applied. There are two recesses on the bearing housing specially designed for rubber and steel plates in order to provide variable stiffness and damping properties to the system. The details of the experimental technique and rubber and steel arrangement are discussed in Chapter 4.

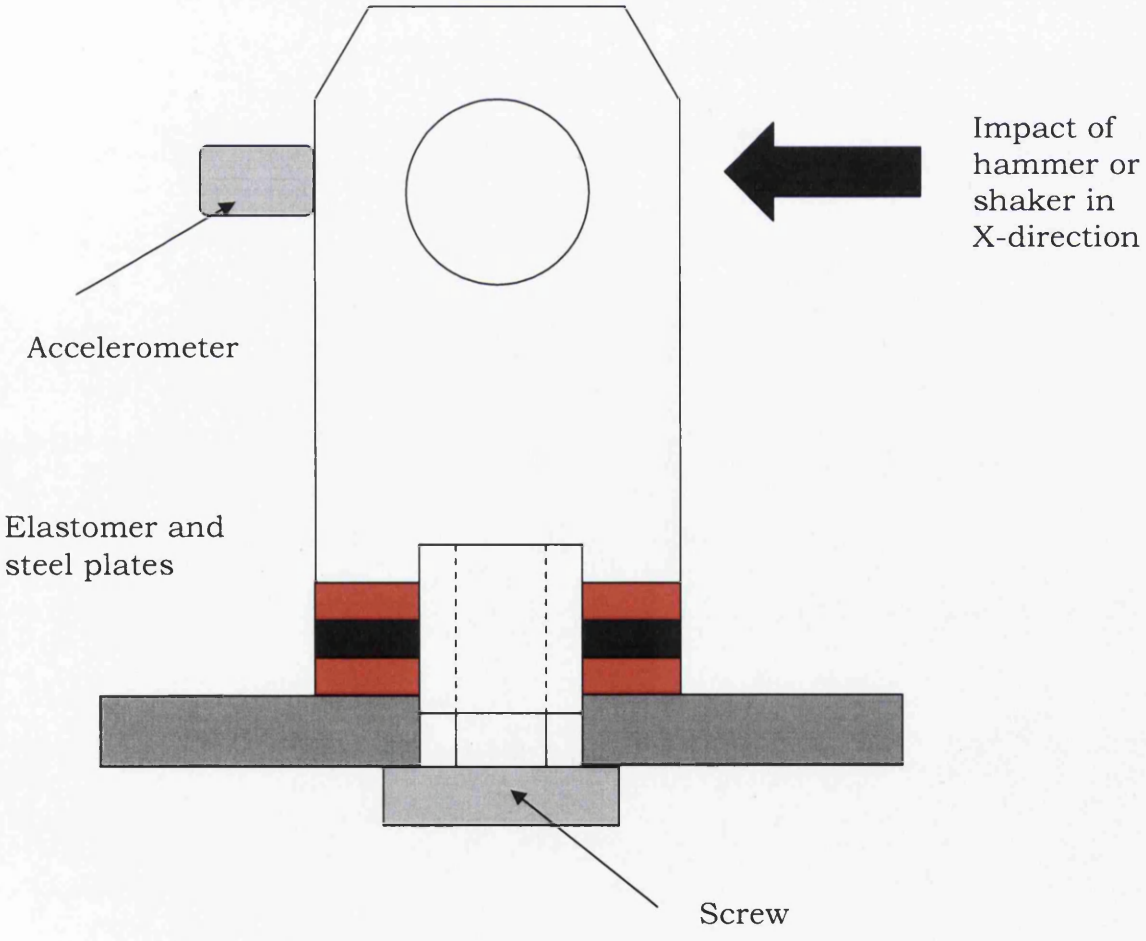

Figure 3 - 1 Schematic of hammer and shaker test model

Rotational motion is involved in both the hammer and shaker tests, as the generalised co-ordinate could be represent in angular displacement.

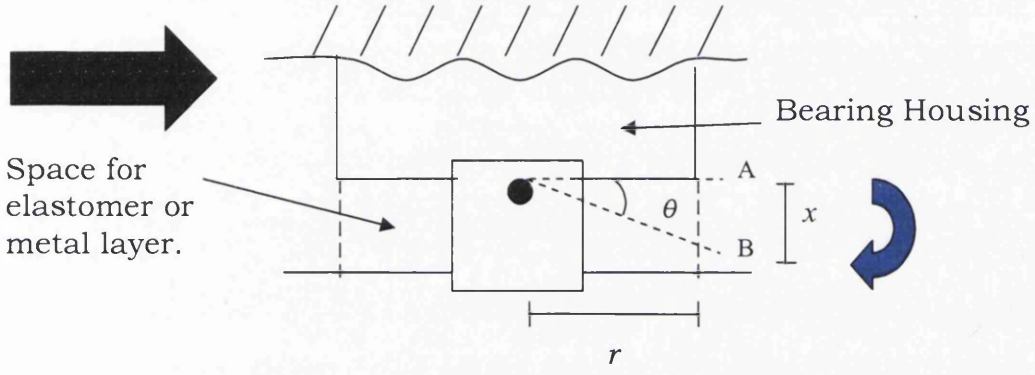

Figure 3 – 2 Schematic of the motion of the bearing housing

The body diagram in Figure 3 - 2 is showing the rotation motion of the centre of mass about this point. Here it is assumed that the bearing housing is moving round the circle from A to B which experienced an angular displacement of θ radians. The relationship between the circular distance moved, x, of the body and the *angular displacement*, θ, is given by

$$x=r\theta$$ *Equation 3 - 1*

When the angle is small, x is very nearly equal to the magnitude of the linear displacement of the body.

The general equation of motion for a linear multi-degree of freedom (MDOF) system can be expressed as [17]

$$M\ddot{r} + C_t\dot{r} + Kr = f \qquad \textit{Equation 3 - 2}$$
$$C_t = C_i + C_e$$

The mass, damping and stiffness are represented by M, C and K. C_t is the total damping acting on the system, due to various external and internal sources, C_e and C_i respectively. r is the vector of measured displacement. f is the force acting on the system in the x-direction

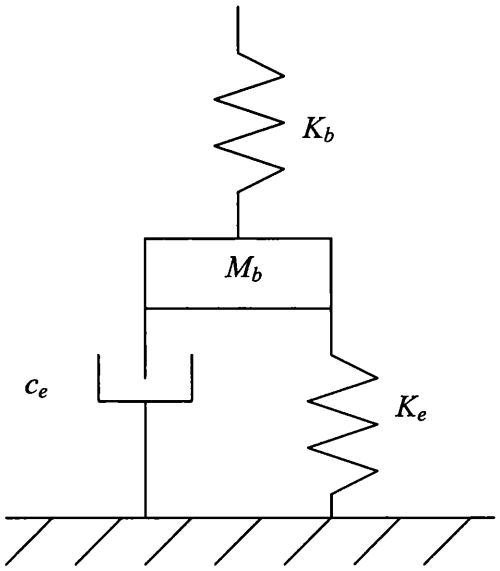

Figure 3 – 3 Schematic of bearing with elastomer model

The schematic of the bearing and elastomer system model for the hammer and shaker test is illustrated in Figure 3 – 3. The bearings are represented by direct stiffness terms, K_b. No damping due to the bearing

housing is included. Stiffness and damping containing K_e and c_e terms show in Figure 3 – 3 are used to represent the elastomer dynamic properties. M_b represents the mass of bearing and housing.

In this case, the gyroscopic terms are neglected, as the rotating disc placed in between the bearings has very small inertia which is not significantly influencing the dynamic behaviour of the system. The gyroscopic effects are not significant when dealing with the type of turbogenerators found in power stations and this is also the case with the models considered here [17]. The external damping dominates the internal damping, hence, the internal damping is neglected and has not been included in this case. Additionally, gravity loads are neglected. Therefore, *equation 3 – 2* reduces to:

$$M\ddot{r} + C_e\dot{r} + Kr = f \qquad \textit{Equation 3 - 3}$$

The general equation of motion of a linear system is expressed in *equation 3 – 3*. Nevertheless, as mentioned previously, the motion involved in the hammer and shaker test is rotational. Therefore, the equation of motion for the entire rotor-bearing system may be expressed in form as

$$I\ddot{\theta} + \Gamma\dot{\theta} + \chi\theta = M \qquad \textit{Equation 3 - 4}$$

I = Moment of inertia (kgm^2)

Γ = Torsional Damping (Nms/rad)

χ = Torsional Stiffness (Nm/rad)

M = Moment (Nm)

θ = Angular displacement (rad)

3.2 Identification of both dynamic stiffness and damping of the elastomer from hammer/shaker test

The general equation of motion of the system is shown in *Equation 3 - 4*. Here we assume that the angular displacement of the system is θ. The solution of this homogenous differential equation associated to the general equation of motion of the system with a single of degree freedom is of the type

$$\theta = \bar{\theta} e^{i\omega t}$$
$$\dot{\theta} = i\omega \bar{\theta} e^{i\omega t}$$
$$\ddot{\theta} = -\omega^2 \bar{\theta} e^{i\omega t}$$

Equation 3 - 5

By substituting *Equation 3 - 5* into *Equation 3 - 4*, it follows that

$$-\omega^2 I\bar{\theta} + i\omega\Gamma\bar{\theta} + \chi\bar{\theta} = M$$

Equation 3 - 6

By rearranging *Equation 3 - 6*, the general solution of the equation becomes

$$\bar{\theta} = \frac{M}{\chi + i\omega\Gamma - I\omega^2}$$

Equation 3 - 7

The response equation is in the form of a frequency response function (FRF). For an elastomer, stiffness and damping are frequency-

dependent parameters. By introducing $\frac{\chi - i\omega\Gamma - I\omega^2}{\chi - i\omega\Gamma - I\omega^2}$ into *Equation 3 – 7,* the i term in the denomination is eliminated. Hence, the response equation can be written as

$$\bar{\theta} = \frac{M}{\chi + i\omega\Gamma - I\omega^2} \times \frac{\chi - i\omega\Gamma - I\omega^2}{\chi - i\omega\Gamma - I\omega^2}$$

$$= \frac{M(\chi - i\omega\Gamma - I\omega^2)}{(\chi - I\omega^2)^2 + \omega^2\Gamma^2} \qquad \textit{Equation 3 - 8}$$

Equation 3 - 8 can also be written as

$$\frac{\bar{\theta}}{M} = \frac{\chi - i\omega\Gamma - I\omega^2}{(\chi - I\omega^2)^2 + \omega^2\Gamma^2} \qquad \textit{Equation 3 - 9}$$

In this case, the general equation of motion of the system (*Equation 3 - 8)* can be put in the complex form of $\bar{\theta} = a + ib$. By separating the real and imaginary parts, the following equations are achieved.

$$a = \frac{M(\chi - I\omega^2)}{(\chi - I\omega^2)^2 + \omega^2\Gamma^2} \qquad \textit{Equation 3 - 10}$$

$$b = \frac{M(-\Gamma\omega)}{(\chi - I\omega^2)^2 + \omega^2\Gamma^2} \qquad \textit{Equation 3 - 11}$$

Assuming that $Z = (\chi - I\omega^2)^2 + \omega^2\Gamma^2$

equation 3 - 10 and *3 - 11* can be written as

$$a = \frac{M(\chi - I\omega^2)}{Z}$$ *Equation 3 - 12*

$$b = -\frac{M(\Gamma\omega)}{Z}$$ *Equation 3 - 13*

The following method is used to achieve two separate individual equations for both stiffness and damping.

$$a^2 + b^2 = \frac{M^2[(\chi - I\omega^2)^2 + \Gamma\omega^2]}{Z^2}$$

$$= \frac{M^2(Z)}{Z^2}$$

$$= \frac{M^2}{Z}$$ *Equation 3 – 14*

Rearrange *Equation 3 - 14*, the following equation is obtained

$$Z = \frac{M^2}{a^2 + b^2}$$ *Equation 3 - 15*

By substituting *Equation 3 – 15* into *Equation 3 – 12*, the stiffness of the system becomes

$$a = \frac{M(\chi - I\omega^2)}{\frac{M^2}{a^2 + b^2}}$$

$$= \frac{(\chi - I\omega^2)(a^2 + b^2)}{M}$$

$$\chi - I\omega^2 = \frac{Ma}{a^2 + b^2}$$

$$\chi = \frac{Ma}{a^2 + b^2} + I\omega^2 \qquad \textit{Equation 3 - 16}$$

Substituting *Equation 3 - 15* into *Equation 3 - 13* provides an equation for the estimation of the damping of the system.

$$b = -\frac{M(\omega\Gamma)}{\frac{M^2}{a^2 + b^2}}$$

$$= -\frac{(\omega\Gamma)(a^2 + b^2)}{M}$$

$$Mb = (-\omega\Gamma)(a^2 + b^2)$$

$$\Gamma = -\frac{Mb}{\omega(a^2 + b^2)} \qquad \textit{Equation 3 - 17}$$

Equations 3 - 16 and *3 - 17* are used to determine the stiffness and damping of the elastomers in Chapters 5 & 6.

A method has been presented here which, along with the response data from hammer or shaker test, will allow the dynamic stiffness and damping of elastomers to be identified. The experimental technique and rig for achieving the experimental results will be discussed in Chapter 4.

CHAPTER 4

RUN DOWN TEST

This chapter details the experimental equipment and results obtained from a run-down test using the identification theory given in Chapter 3. The hardware of the machine itself, as well as the associated measurement, instrumentation and data acquisition systems are described. A small rotor rig, which already existed in School of Engineering at the University of Wales Swansea, was significantly modified for this research study.

This rig was modified to suit the present purpose of elastomers dynamic properties identification. A set of bearing supports, which is able to withstand the excitation forces produced by the rotor, were machined with slots to allow elastomer layers to be added. The elastomer used in this project was *fluorosilicone.*

There are three different experiments in this project. These are run down tests, shaker tests and hammer tests. Figure 4 – 1 illustrates the relationship between these three series of tests. Each kind of experiment is done to verify the dynamic properties of the elastomer and study the influence of the dynamic properties of the elastomer on machine behaviour. The difference between three type of test is the frequency range beside the experimental equipment. The maximum frequency of run down test is 50 Hz. Hence, hammer and shaker tests are carried out in order to verify the dynamic properties of elastomer at higher frequency range.

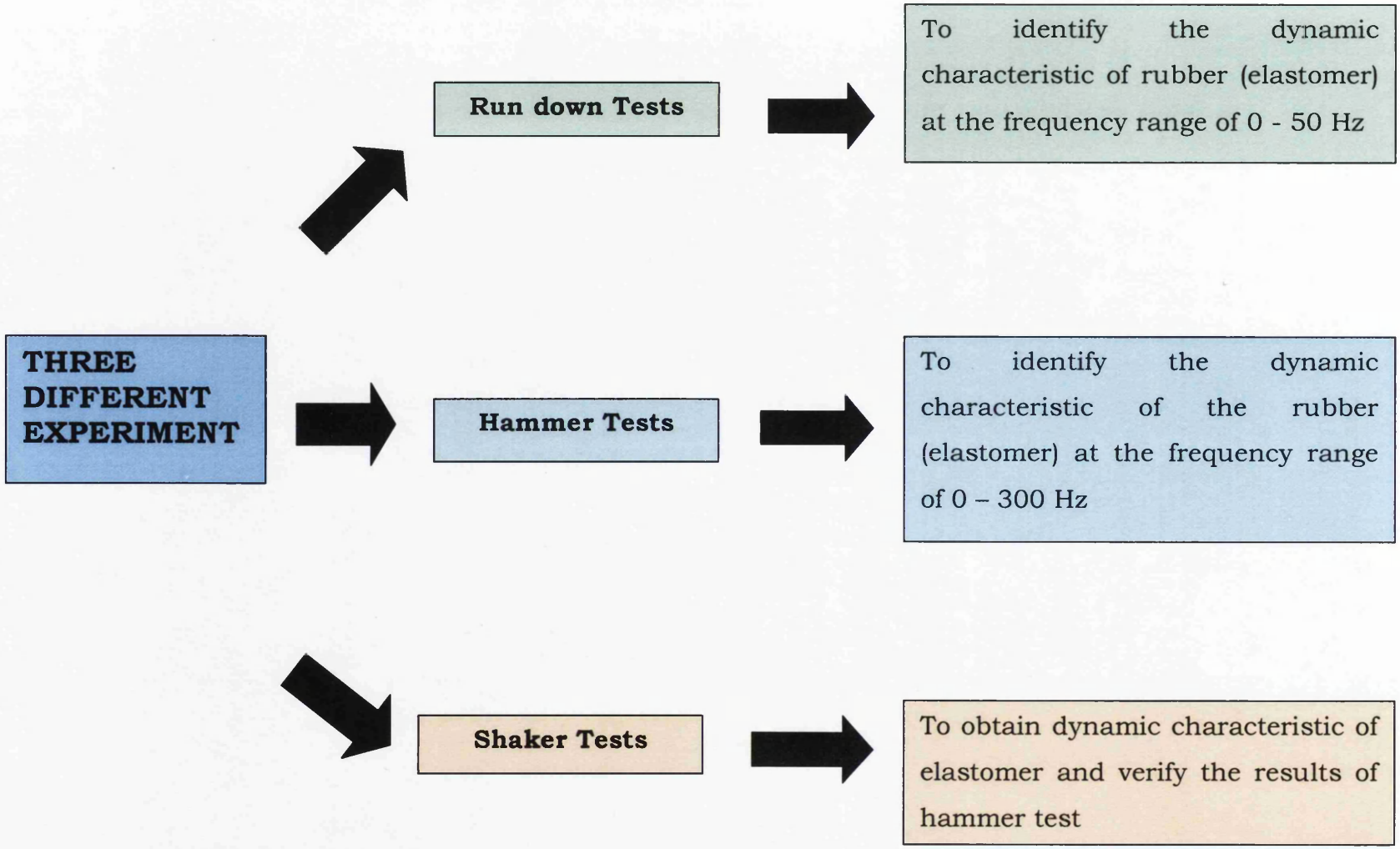

Figure 4 – 1 Experimental tests

4.1 The Experimental Rig for the Run-down Test

A general view of the experimental rig for the run down test is shown in Figure 4 - 2. The equipment was mounted on a large rigid steel table. The rig consists of a steel shaft approximately 750 mm long with nominal diameter 12mm and one balancing disk.

Figure 4 - 2 General view of run-down experiment rig

A schematic view of the rig is shown in Figure 4 – 3. The rig consists of a rotor having a balance disk, which is supported on the base plate through two bearings. The rotor is coupled to the motor through a flexible coupling. The vibrations measured at the bearing pedestals in both the vertical and horizontal directions during machine run-down were used for the present study. Here, the bearing housing nearer to the motor is referred to bearing housing A and the other is referred to bearing housing B. The results obtained from the experiment will be discussed later in this chapter.

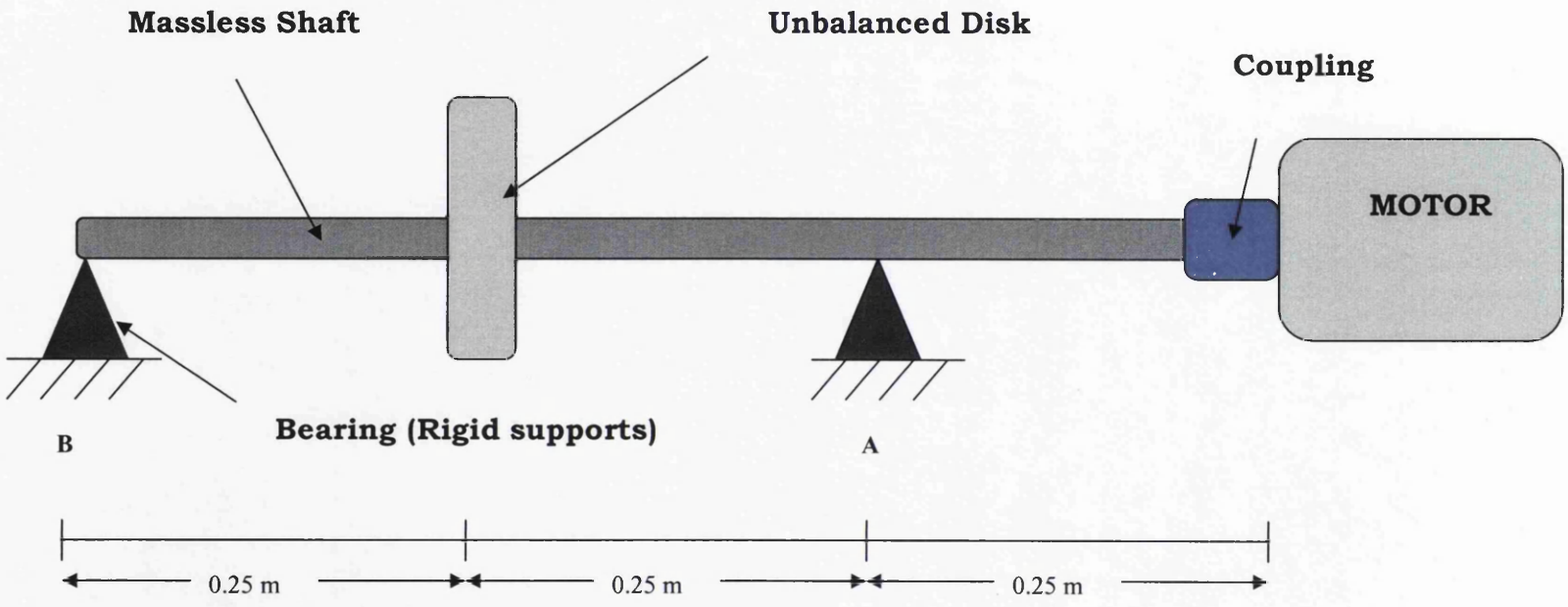

Figure 4 - 3 Schematic of rotor-bearing-foundation model

4.1.1 Bearings

The bearing housing is one of the key features of the experimental apparatus in this project. It was used in run down tests, hammer tests and shaker tests. Figure 4 - 4 shows a general view of the bearing housing used in this project. In this work, the type of bearing chosen to be used was ball bearings. Ball bearings, as shown below in Figure 4 – 5, are probably the most common type of bearings for small machines. These bearings can handle both radial and thrust load, and are suitable for applications where the load is relatively small.

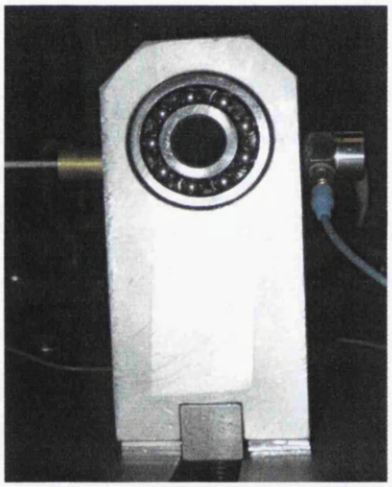

Figure 4 - 4 Bearing Housing

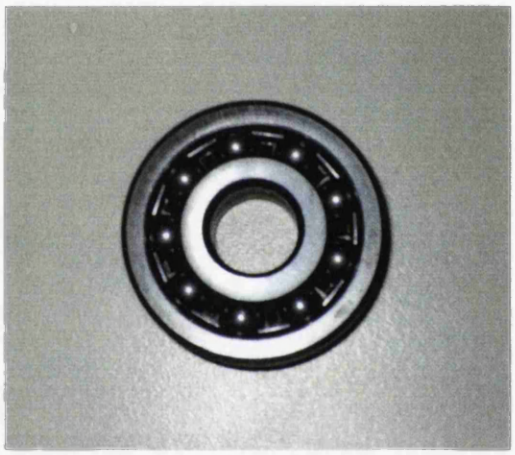

Figure 4 - 5 Ball bearings

4.1.1.1 Design of Bearing Housing

The bearing housing dimensions are 114 mm x 49 mm x 36 mm (length x width x depth). A schematic of the bearing housing is shown in Figure 4 - 6.

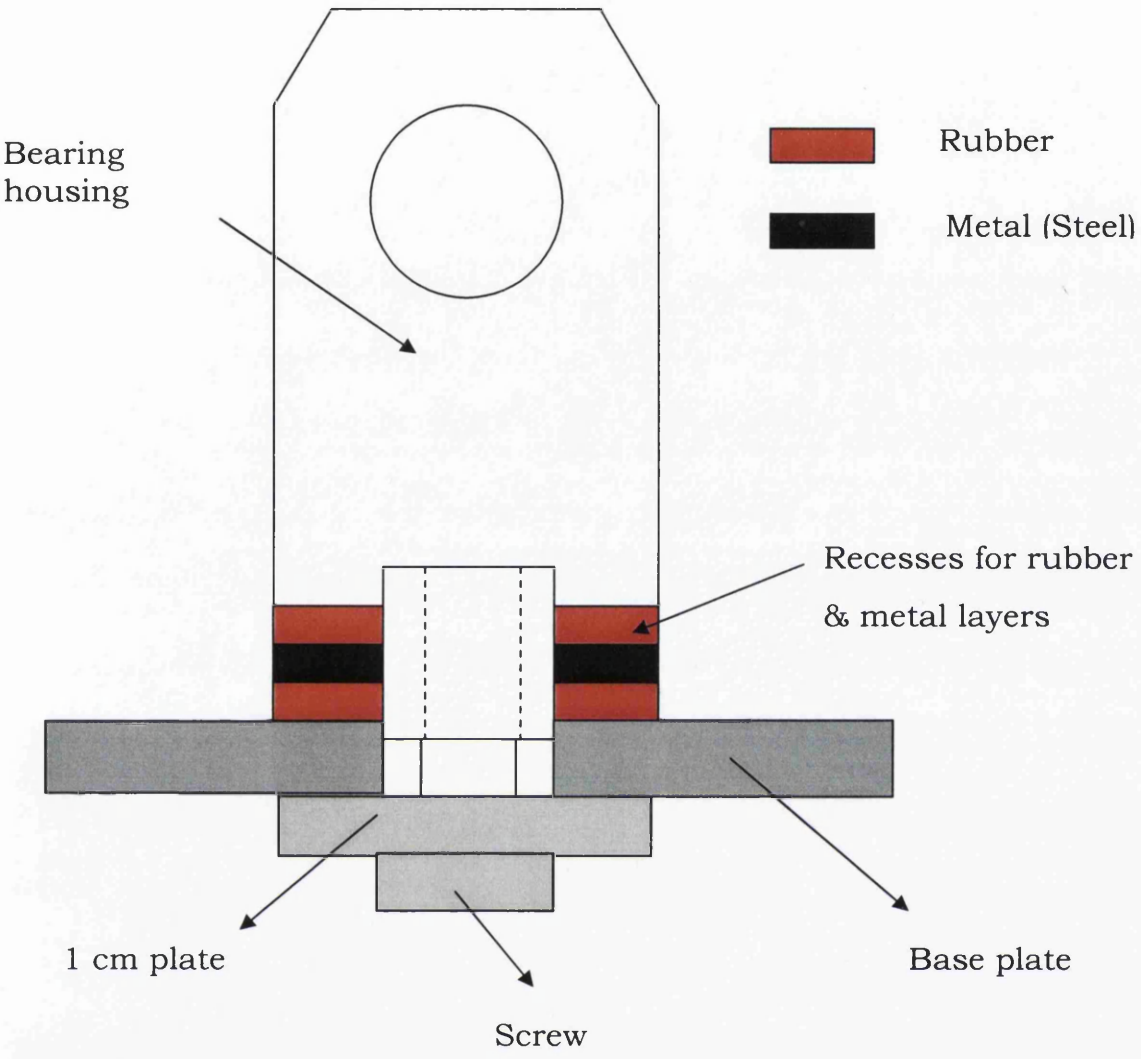

Figure 4 - 6 Schematic of Bearing housing (not to scale)

The bottom of the bearing housing incorporates two recesses with a dimension of 11 x 36 x 6 mm to allow for 3-layers of 2 mm thick elastomer or steel plate to be used. Different layers of elastomer were used in the run down tests to supply various stiffness and damping properties to the test rig, in order to study the influence of the dynamic properties of elastomers on machine behaviour.

4.1.1.2 Arrangement of elastomer and steel layers

The bearing housings contain two recesses to allow accommodate 3 layers of elastomer or steel plate. The different elastomer and metal layers arrangements used during the experiments are shown in Figure 4 – 7.

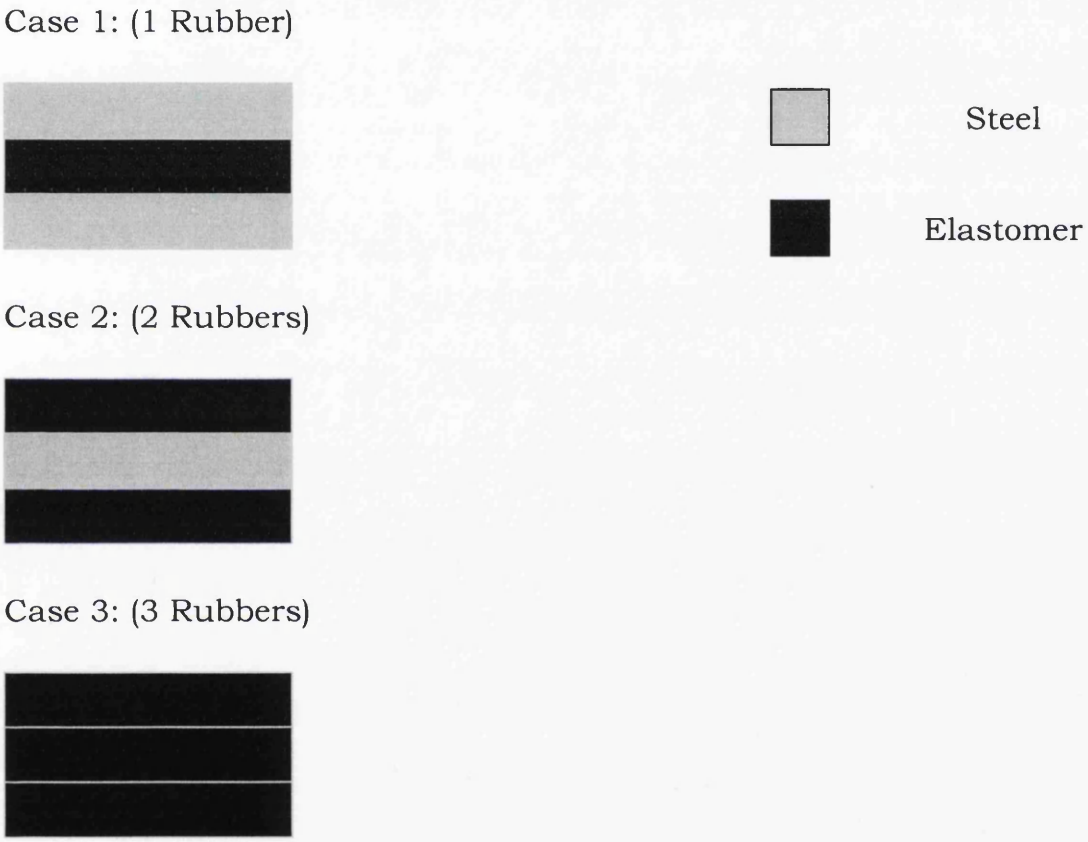

Figure 4 - 7 Combinations of steel and elastomer layers

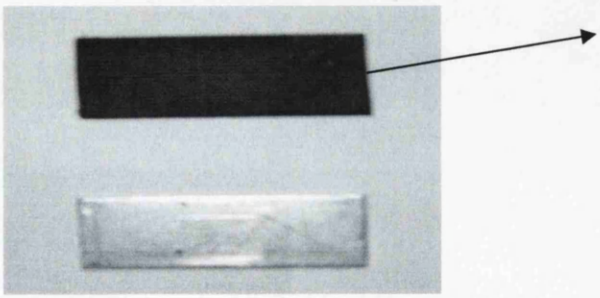

Figure 4 – 8 Elastomer and steel layers

4.1.2 Baseplate and clamps

The steel baseplate (1100 x 300 x 11 mm) seen in Figure 4 - 2 was supported by 3 steel blocks of size 50 x 300 x 100 mm to ensure the baseplate remained rigid during the experiment. The plate consists of a 16mm wide slot to allow for the fixing of the bearing housing. These 3 steel blocks were tightened down at both ends and middle of the base plate. The rigidity of the baseplate and clamps was checked by performing an impact hammer test on the plate and observing no resonance within or near the rotor running speed range.

4.1.3 Motor and controller

The rotor was driven by a 0.55 kW permanent magnet D.C. motor (Figure 4 - 9). The main rotor shaft is connected to the motor by a flexible coupling. The maximum operating speed of the motor is 3000 rpm.

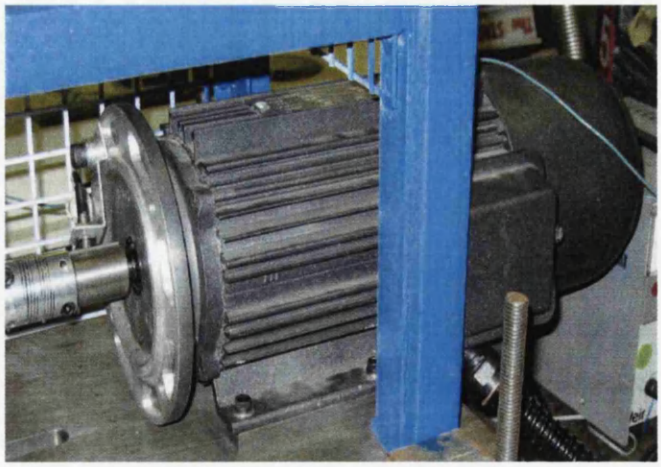

Figure 4 - 9 0.55 kW Permanent Magnet D. C. Motor

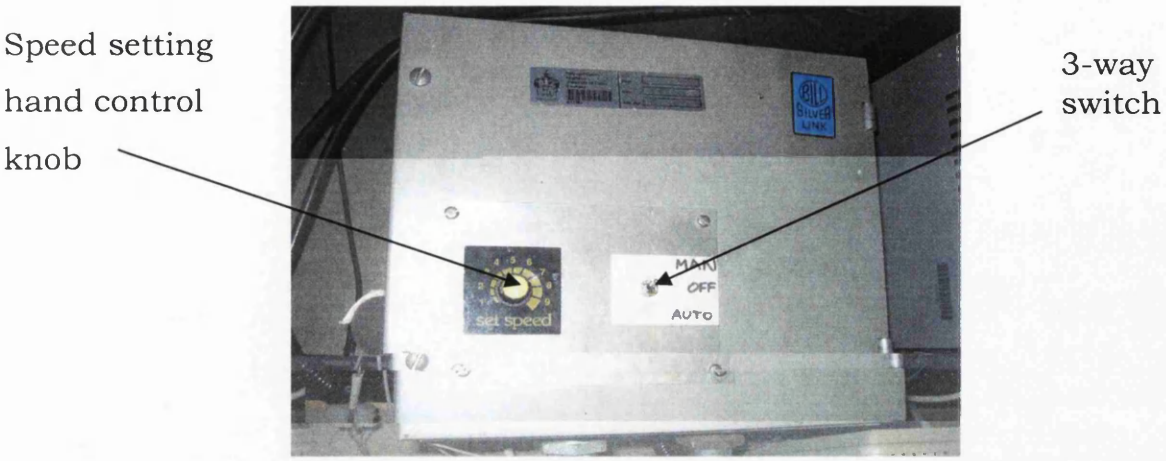

Figure 4 – 10 LYNX-08 Thyristor Motor Controller

A LYNX-08 thyristor motor controller shown in Figure 4 – 10 was used to provide the necessary voltage supply to the motor. The LYNX 08 thyristor motor controller can be used to set the running speeds, ramping and reversing of the experiment. It also had overload protection. There is a hand controlled potentiometer knob on the controller box to set the minimum and maximum running speed from 0 to 3000 rpm.

The controller could receive its input from an external source (potentiometer knob) of 0 to 10 V, where 0 V and 10 V corresponded to the minimum and maximum of the running speeds respectively. This was the main purpose of the controller. The motor controller can also allow manual control and automatic control from an external data acquisition system. Manual control was normally used during commissioning or testing a new configuration of the rotor. Automatic control was used when it was desired to collect data for analysis.

The external data acquisition system provides an output voltage in the range 0 to 10 V, which is ideally suited for the motor controller. There is a 3-way switch on the controller box to allow selection of *manual* or

automatic. When the controller box is set to *automatic* mode, the computer will control the running speed of the motor by follow the setting on the program. More details of the program will be discussed later in Section 4.1.6.2.

4.1.4 Shaft

A solid steel shaft of diameter 12 mm and length 750 mm was used in this project. The steel shaft was used to connect bearings, disk and coupling. The schematic of the test rig is shown below.

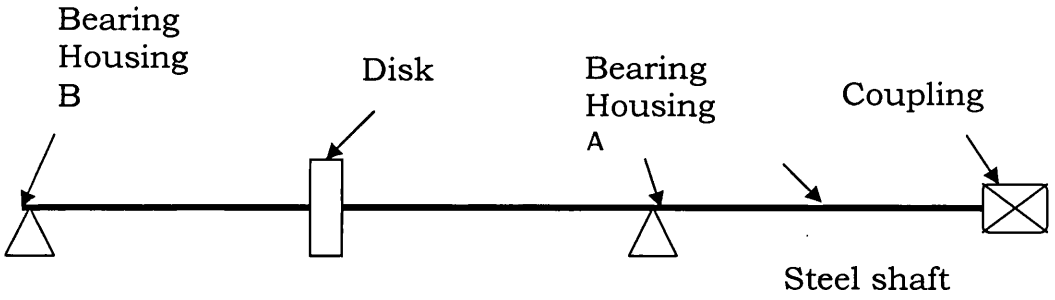

Figure 4 – 11 Schematic of the rig

4.1.5 Balancing disk

A balance disk of inside diameter 12 mm, outside diameter 74 mm and thickness 15 mm was used in the run down test. The disk can be fixed at any desired point along the shaft by using small grub screws. The original disk containing 2-grub screw was modified to 4-grub screw in this project work to prevent unequal mass distribution. The grub screws are located in holes drilled through the radius and at every 90° of the disk as shown in figure 4 - 12.

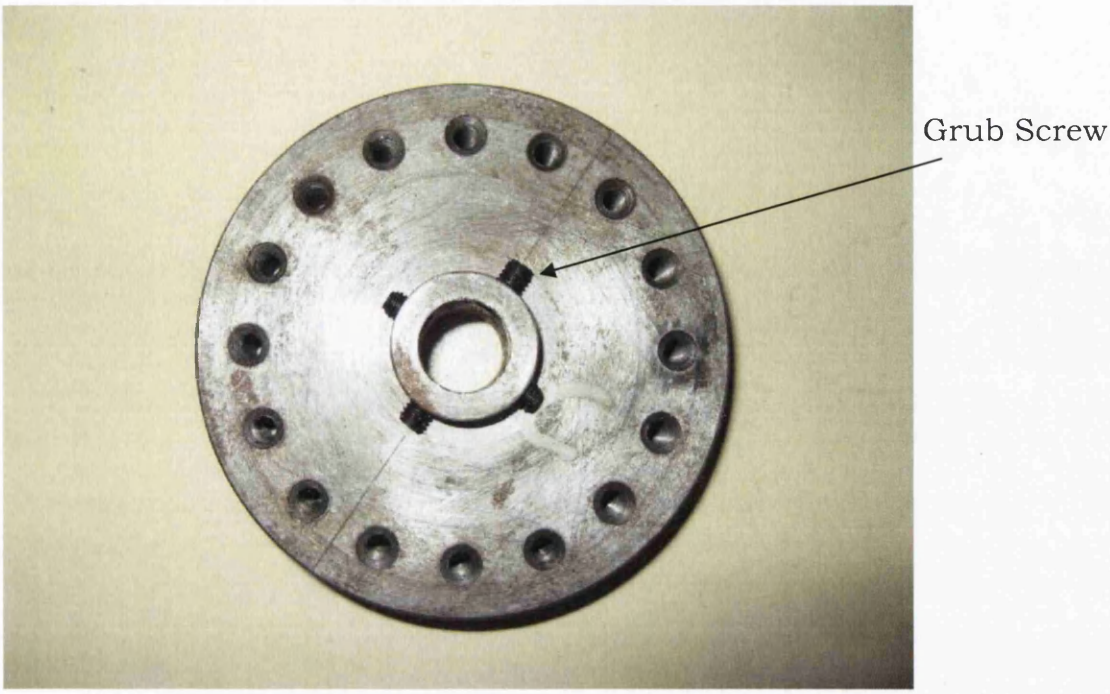

Figure 4 - 12 Balancing Disk

The balancing disk contains 16 equally spaced M4-threaded holes at radii of 30 mm to allow for additional balance weights. An assortment of bolts, nuts and grub screws can be used as balance weights. These have various masses between 0.5g to 3g. The mass of the disk is 0.482 kg.

4.1.6 Measurement Devices, Instrumentation, Data Acquisition and Order Tracking

The identification method to be investigated requires frequency-based measurements of the rotor response measured at the bearing housings, during a run-down of the machine. The objective of the measurement system was therefore to record the synchronous response of the rotor over the run-down period.

This section is divided into three sub-sections. Firstly, the measurement devices and instrumentation used to provide the measured signal will be described; secondly, the data acquisition system used to collect data is discussed; and finally, the order tracking carried out on the data is outlined. The information is discussed in more detail in the thesis by Edwards [17].

4.1.6.1 Accelerations and Reference Signal

4.1.6.1.1 ACCELERATIONS

The bearing pedestal vibration was measured using four DJB Type A/20 accelerometers which are mounted on each bearing in both horizontal and vertical directions. The position of the accelerometers is shown in Figure 4 - 13. These general-purpose piezoelectric accelerometers were advantageous for the present study due to their small size and low mass. The performance of the accelerometers was good in capturing vibrations produced by this application. The accelerometers are mounted on the bearing housing using wax. The wax was found to be an ideal solution as it provided a rigid mounting and allowed the accelerometers to be removed when necessary.

A four channel D. J. Birchall CA/04 charge amplifier was used to convert the piezoelectric charge produced by the accelerometer into a low impedance voltage. The amplifier was set to the calibration constant of the particular accelerometer and a variable gain setting allowed the desired voltage range to be achieved. In this case, the gain was set so that the maximum reading did not exceed 10V, which was the upper limit of the input voltage into the data acquisition system.

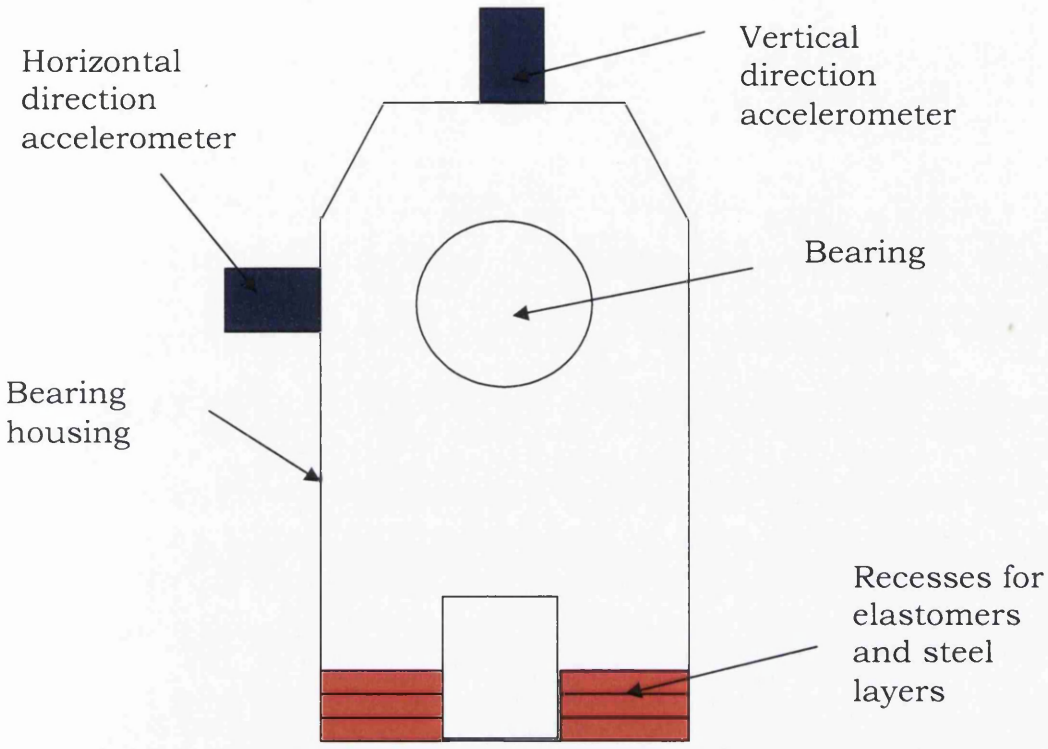

Figure 4 - 13 Position of accelerometers

4.1.6.1.2 TACHOMETER SIGNAL

In order to perform the signal processing required for these experiments, a reference signal was necessary. This reference signal was a tachometer signal to allow the angular position of the rotor to be known relative to a constant location on the shaft. There are several methods of producing this signal. In this project, a more simplistic and cheap approach was used, where the rotation of a single keyway cut into the rotor was detected by a proximity sensor. This arrangement is shown in Figure 4 - 14.

The Keyence EZ-8M on/off proximity sensor was powered by a 9V supply, which provided an output pulse of almost 9V when passing

through the edge of the keyway, and returning to 0V once the keyway passed the sensor. In this way, the tachometer sensor provides a once-per-revolution pulse. The sensor has a detecting distance within 1.5 mm and works in a target area of 10 x 10 mm for all ferrous metals.

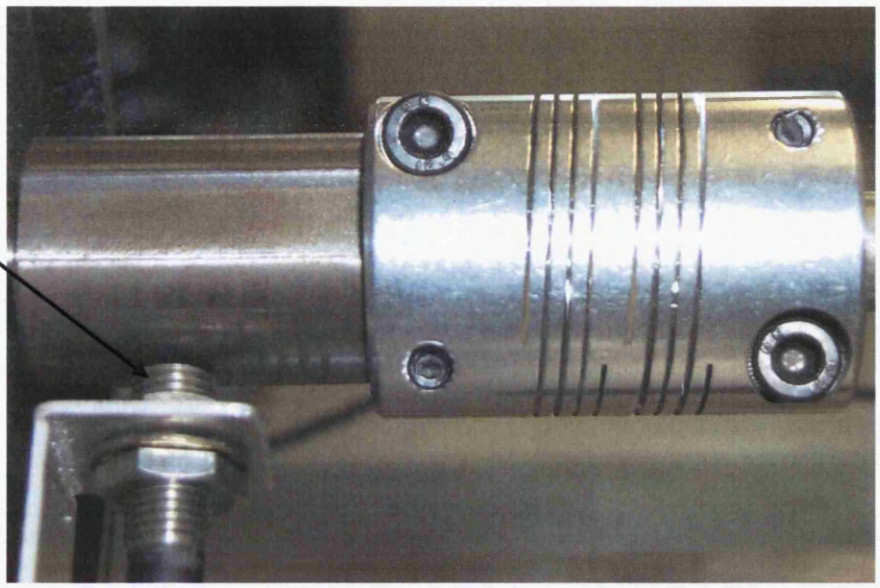

Figure 4 – 14 Views of tachometer/keyway arrangement (left) and flexible coupling (right)

4.1.6.1.3 STROBOSCOPE

A Brüel and Kjaer Type 4912 hand-held stroboscope was used. The stroboscope can give an effect of freezing the motion of the rotor. This is useful for monitoring the parts of the rotor during operation. The *Internal Trigger* mode allowed the frequency of the stroboscope to be set manually. Setting the frequency slightly above the frequency of the rotor will allow a slow motion view of the motion of the rotor at a particular speed. Setting the frequency at the frequency of the rotor will freeze the motion of the rotor at a particular speed. This function was very useful for the purpose of viewing the rotor motion at the critical speed.

4.1.6.2 Data Acquisition

PC-based data acquisition (DAQ) systems are commonly used in many applications due to the rapid increase in PC performance. The advantages of PC-based data acquisition systems (DAQ) are the cost and simple installation process. Only minor hardware is required for the application. There are 2 main principal functions of the DAQ systems: (i) to send an output signal to the motor in order to achieve either a run down or a run up test over a user defined operating period, (ii) to collect and store the tachometer and accelerometers feedback signals produced during the experiment at a user defined sample rate.

A National Instruments PCI-MIO-16E-4 PC Based DAQ card was used together with the corresponding SCB-68 signal connection board to meet the specification mentioned above. This DAQ card had 16 single-ended or 8 differential analogue input channels with 12-bit resolution and a maximum collective sample rate of 500 kHz, which is more than enough for this application.

The software selectable gain permitted input voltage was in the range ± 50 mV and ± 10 V. The 10 V range of gain, which permits the input voltage, was used in this application to match the magnitude of the signal produced by the accelerometers and tachometer. There are two 12-bit analogue output channels with a maximum update rate of 1 MHz on the National Instrument PC Based DAQ card. One of these output channels was used for the voltage output to the motor controller. 12-bit resolution was sufficient for both input and output channels.

The DAQ system was integrated into a Pentium 223 PC with 64 RAM and 426 MB of hard disk space. The performance of the computer is sufficient for the application. The data acquisition card was completely software programmable. A DAQ driver software (NI-DAQ) supplied together with the DAQ card was used. All the functions required to

operate the DAQ card were contained in NI-DAQ which includes the routines for analogue input, analogue output, buffered data acquisition, waveform generation etc. A choice of programming language could be used to create the operation using the NI-DAQ function in order to operate the DAQ card. In this case, Microsoft Visual Basic 3.0 was chosen as the programming language. The software programme *FlexiDaq*, developed by Edwards [17] during his PhD study, controls the motor run-down speed, data acquisition hardware and stores the accelerometer and tacho signals in the PC.

The NI-DAQ functions were called via the Microsoft Visual Basic program. The accelerometer and tachometer data was stored on the computer hard disk. Double-buffered data acquisition was used for the experiment. Half of the buffer was constantly streamed to the PC hard disk at the same time as the other half was constantly being filled with the fresh data. The end result of the custom written program was the Graphical User Interface (GUI) shown below and was written by Edwards [17].

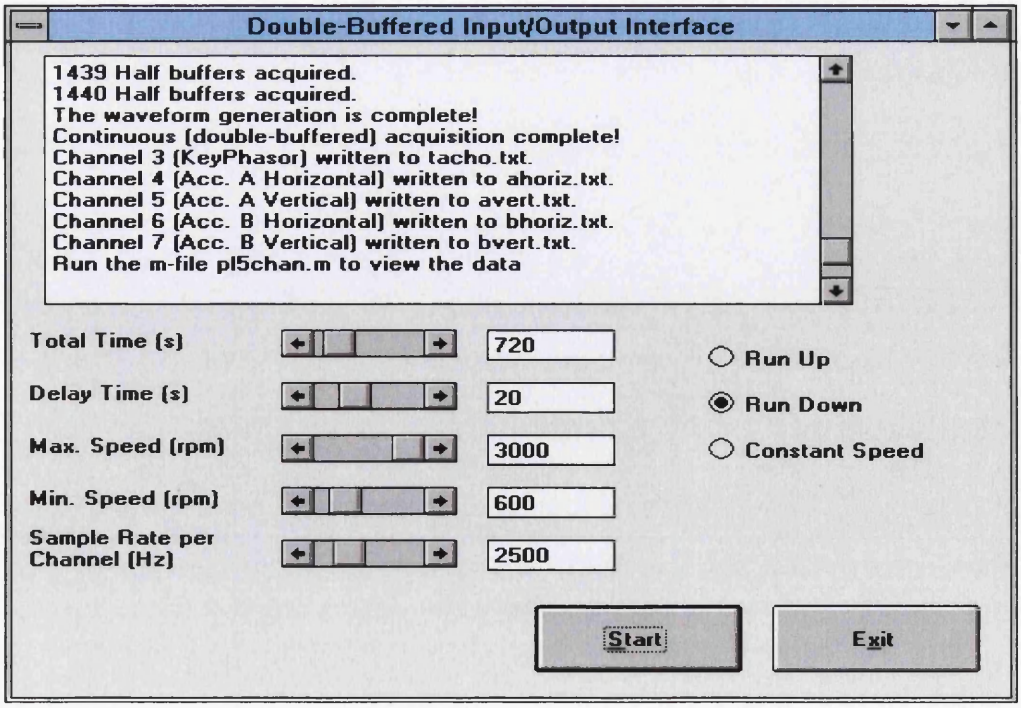

Figure 4 - 15 Graphical User Interface developed for data acquisition

The measured signal for each sensor was collected at a rate of 2500 samples per second. This high acquisition rate was used because no anti-aliasing filters were in place. The constant sample rate of 2500 Hz was set at the *Sample Rate Per Channel.* The duration of the experiment can be varied using *Total Time (s).* The speed of the experiment is in the range 0 to 3000 rpm. This can be set in the section *Min. Speed* and *Max. Speed* in the Graphical User Interface (GUI) developed for the data acquisition. The period of *Delay Time* allowed the rotor to settle down before the data acquisition process started. The data collection starts after the period of delay time.

In the graphical user interface shown in Figure 4 - 15, it can be seen that the channel connected to a particular accelerometer and also the data file in which the data is stored are clearly identified. For example, the data from the horizontal accelerometer at Bearing A, which is connected to Channel 4 of the DAQ card, was stored in the file with the file name of *ahoriz.txt.* The upper window of the GUI supplied all the information about the acquisition process to the user.

4.1.6.3 Order Tracking of Run-down Data

The extracting of order-domain data from time domain data is known as order tracking. The 1X component of the run-down data in the frequency domain has been used for the dynamic properties of elastomer identification. Given the four channels of time-domain response data and the tachometer signal stored, order tracking was performed on this data in order to obtain the 1X data. *Fyle* and *Munck* [18] (1997) and *Bossley et al.* [19] (1999) present the theory of order tracking. Either a computational program can be written for order tracking or any commercial software code or hardware can be used for this purpose.

Here, the software code *VSI Rotate 2.0* [20] from Vold Solutions (2000) has been used for data order tracking. VSI Rotate is a powerful software package for analyzing noise and vibration in mechanical equipment. It includes a set of analytical functions which process machine speed (tachometer) and time waveform (data) signals from the sensor for robust analysis of rotating and reciprocating machinery. VSI Rotate takes raw time domain response data as the input and analyses the data in many different ways to support the clearest diagnosis.

4.2 Run-down Test Experimental Results

Figure 4 – 16 shows the tachometer signal from the run-down tests. The rotor speed was ramped down in a linear fashion from 50 Hz to rest over 180 seconds.

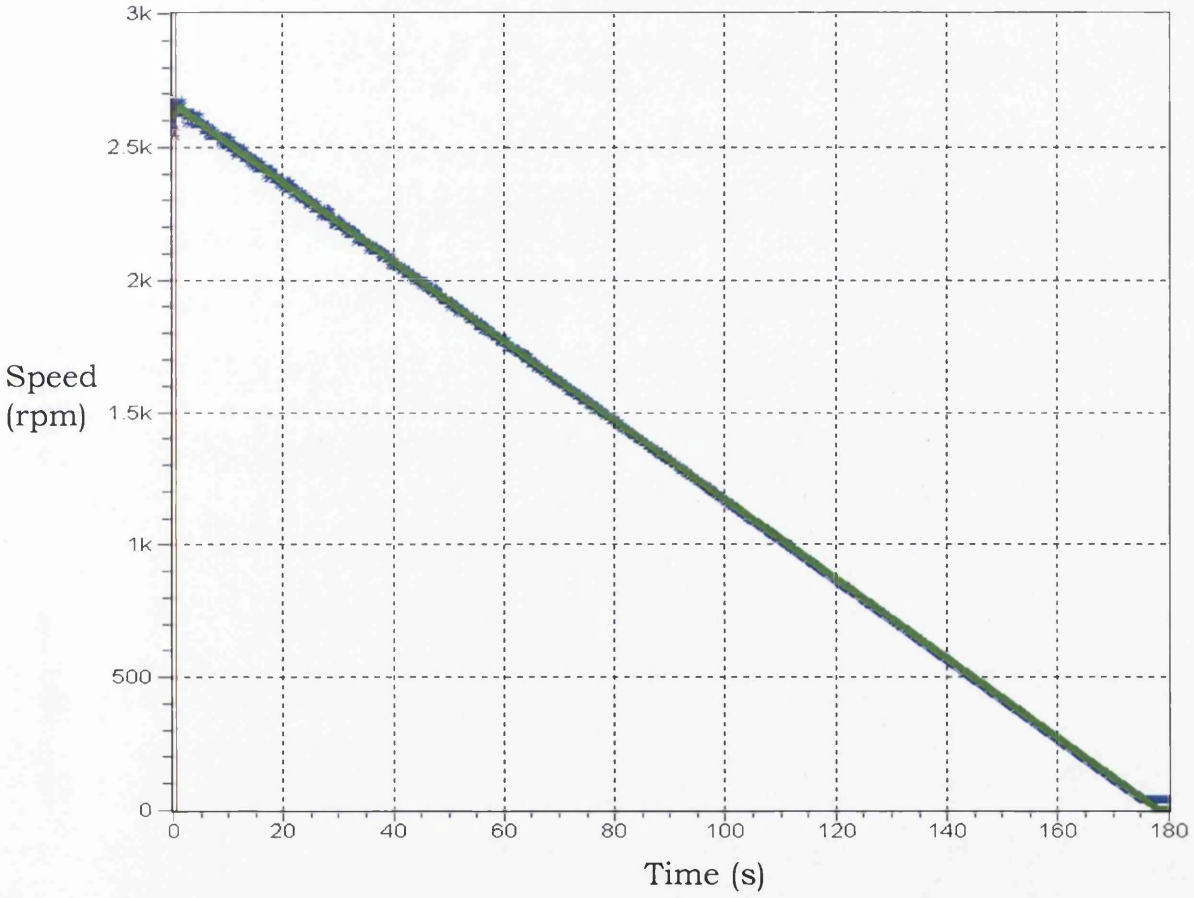

Figure 4 - 16 Tachometer Signal

The response data collected on the both bearing housings (A and B) during the run-down tests are now presented. Bearing A is located nearer to the motor. In this case, two accelerometers are mounted on each bearing housing in the vertical and horizontal direction.

The run-down tests are performed for three different cases, all with a different elastomer arrangement, which has been discussed previously in this chapter. Here, the run-down tests are categorized as 1-rubber, 2-rubbers and 3-rubbers tests. In this case, the run-down test results are plotted using the VSI rotate; unfortunately, the disadvantage of this program is that the obtained phase and displacement graphs do not have directly corresponding frequency axes.

4.2.1 1–Rubber Run-down Test Results

Figures 4 – 17 to 4 - 20 show all the response data from the accelerometers locate at bearing A and B. From Figure 4 – 17, it can be seen clearly that the accelerometer mounted on the bearing in the vertical direction is not collecting any signal except noise. This is due to a fault in the accelerometer.

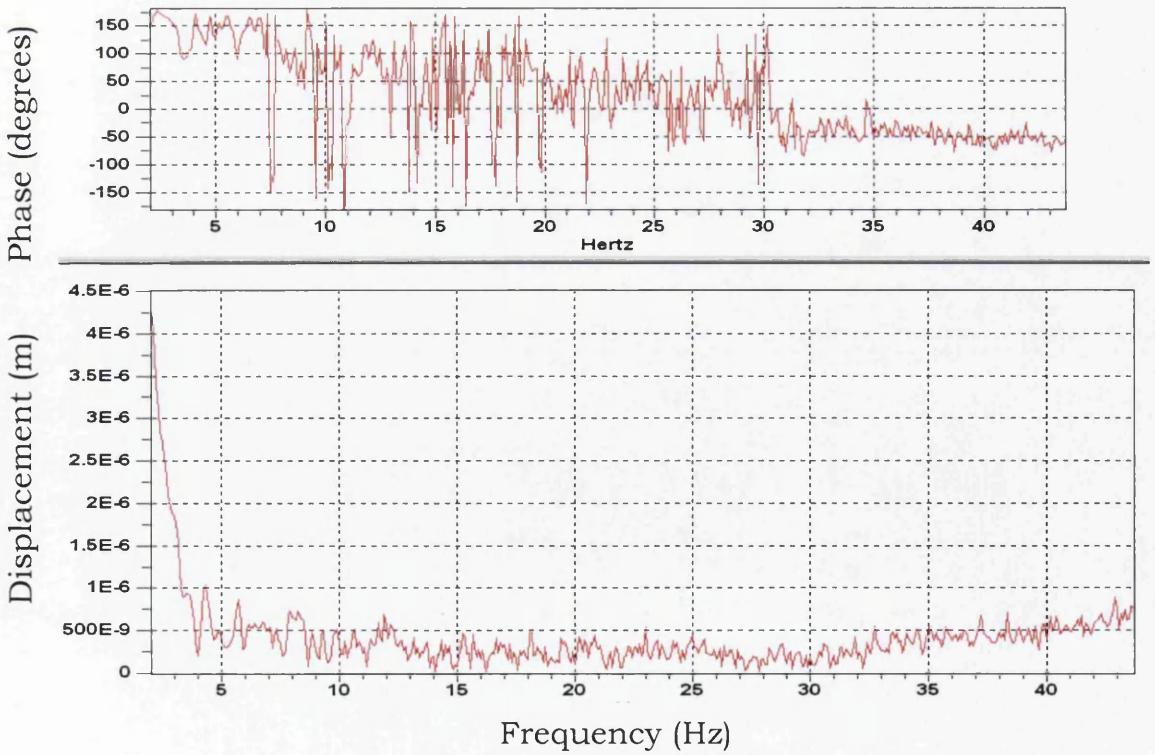

Figure 4 - 17 Responses at Bearing A (Vertical) – 1 rubber test

From Figures 4 - 18, 4 - 19 & 4 - 20, it is shown that the system processed a critical speed within the 50 Hz running range of the rotor.

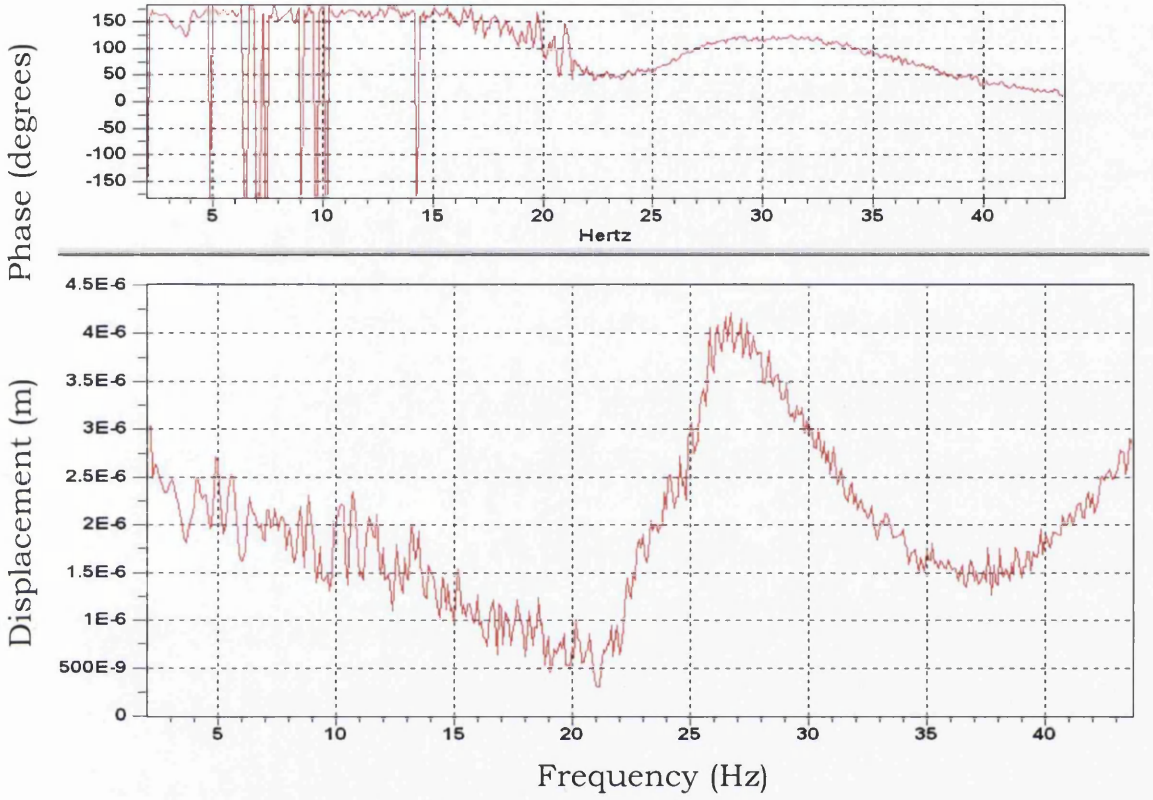

Figure 4 – 18 Responses at Bearing A (Horizontal) – 1 rubber test

From the results showing in Figure 4 - 18, the decreasing amplitude at low frequency is mainly due to the low signal to noise ratio. The results collected from the experiment are actually the combination of measured signal and noise. Hence, in this case, the result is not accurate in the low frequency range.

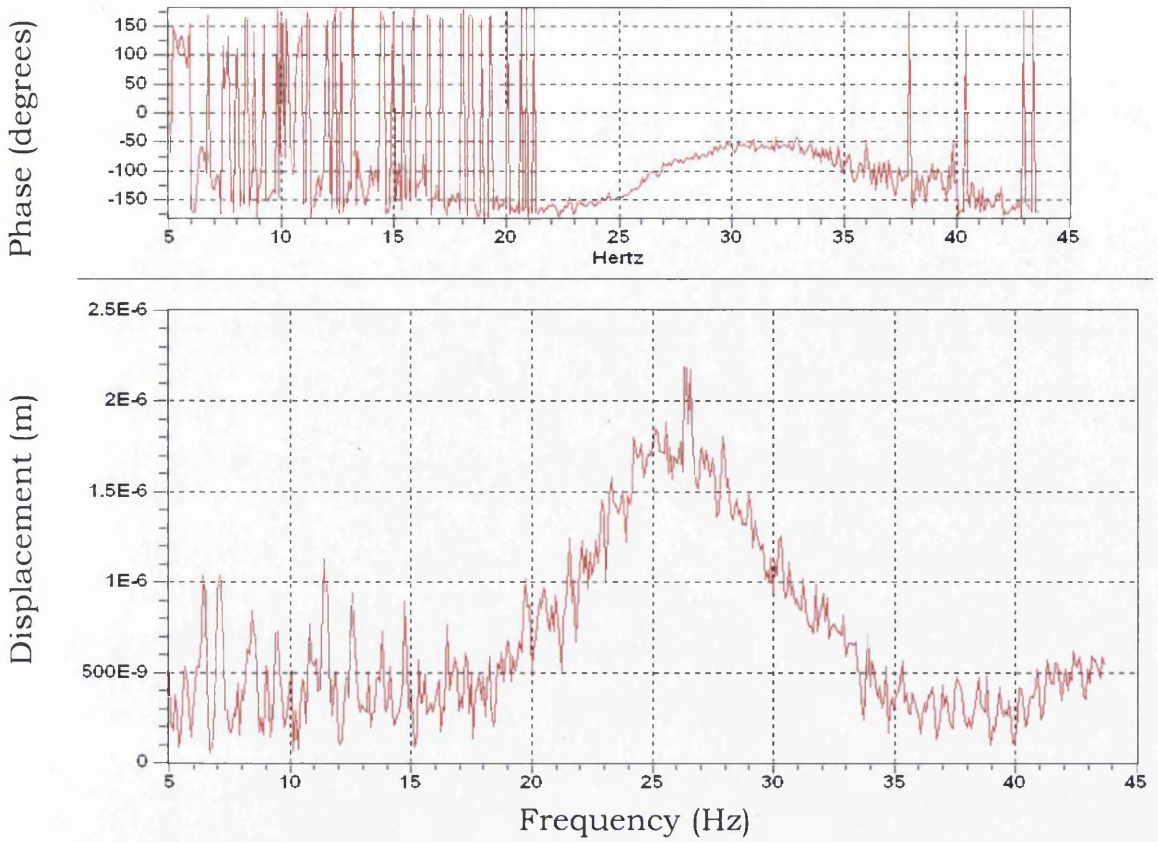

Figure 4 - 19 Responses at Bearing B (Vertical) – 1 rubber test

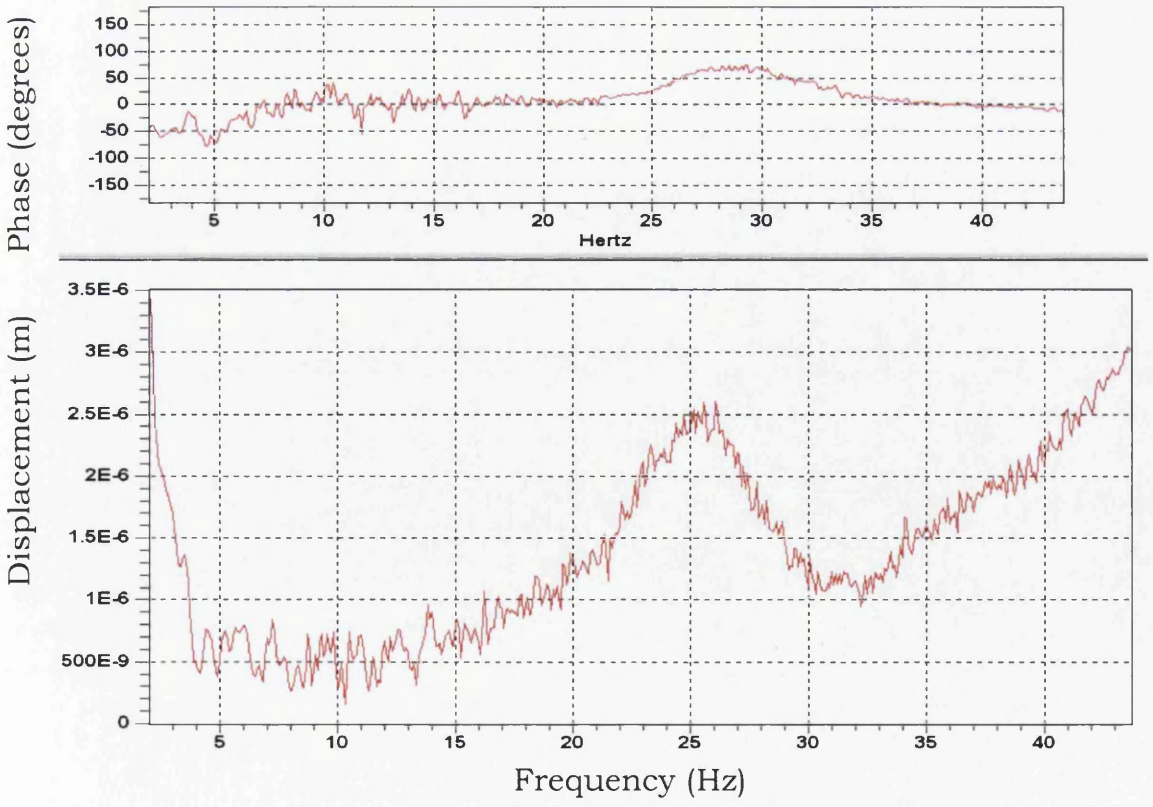

Figure 4 - 20 Responses at Bearing B (Horizontal) – 1 rubber test

Figure 4 - 21 shows that the amplitude of vibration at bearing A (nearer to motor) is higher than the amplitude of vibration at bearing B. Moreover, the natural frequency at bearing A is higher than bearing B due to the different location of bearing housing mounted on the baseplate.

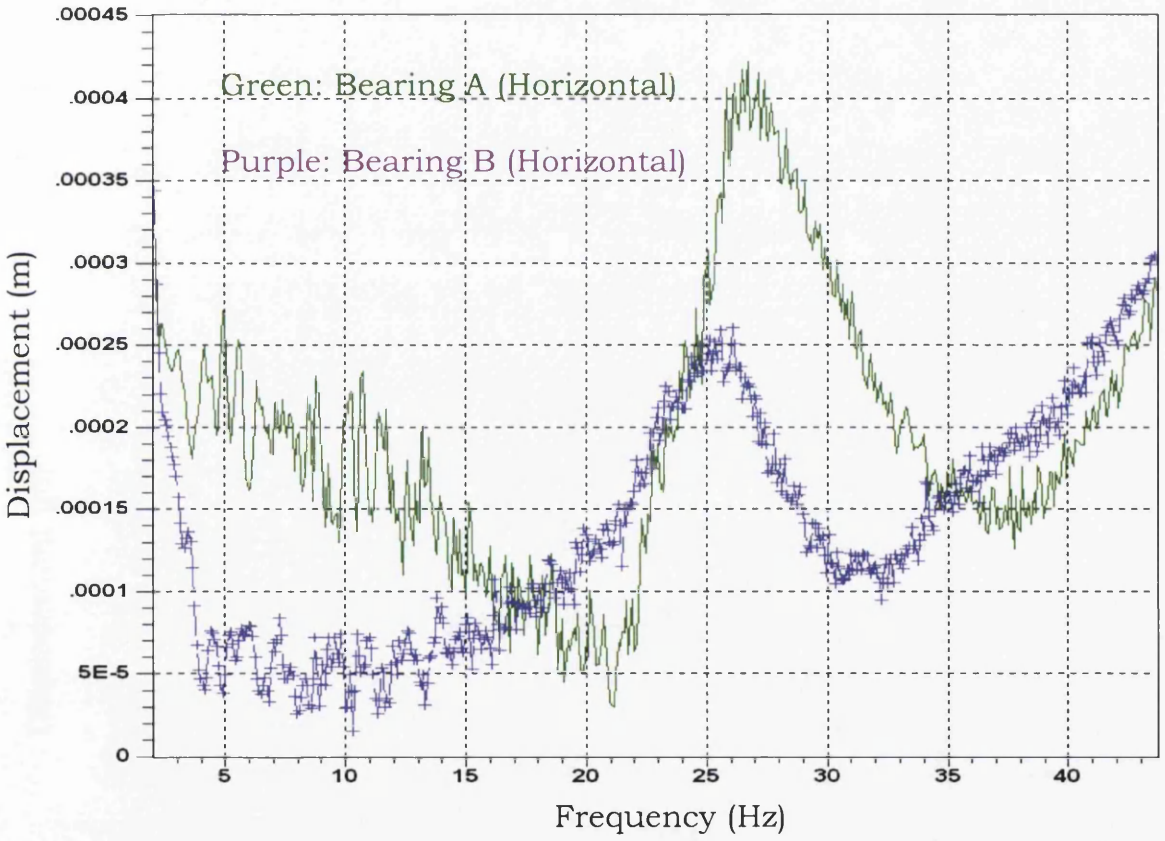

Figure 4 - 21 Comparison of horizontal responses at bearing A & B – 1 rubber test

Figure 4 - 22 compares the horizontal and vertical accelerometer responses at bearing housing B; the amplitude in the horizontal direction is higher than the amplitude in the vertical direction. The unbalance of the disc generates an ellipse type of rotation motion; as a result the vibration of the bearing housing is higher in the horizontal directions.

Figure 4 - 22 shows that the natural frequency of the system in the vertical and horizontal direction is the same.

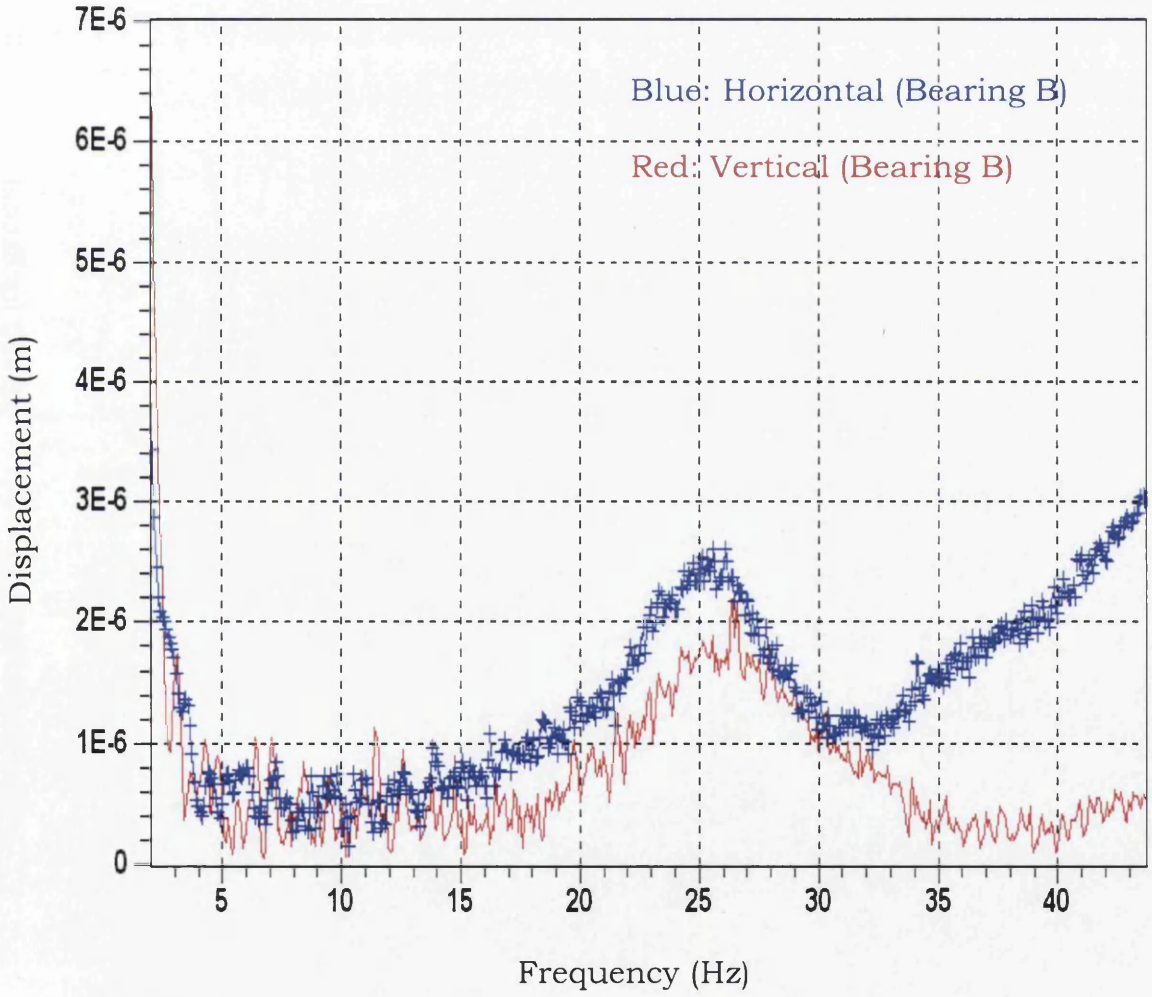

Figure 4 – 22 Comparison of Horizontal & Vertical responses at bearing B – 1 Rubber test

4.2.2 2–Rubbers Run-down Test Results

Figures 4 – 23 to 4 – 26 show the response results of the accelerometers located at bearing A and B. From Figure 4 - 23, it is seen that the accelerometer mounted on bearing housing A in the vertical direction was not collecting any signal except noise due to a fault. This also happened in the 1-rubber run-down test. Figure 4 – 24, 4 - 25 & 4 - 26 show that the system possessed critical speeds within the 50 Hz running range of the rotor. From the results obtained, it is seen that significant noise is occurring during the experiments. Hence, it is difficult to achieve an accurate response from the accelerometer at low frequency due to the low signal to noise ratio.

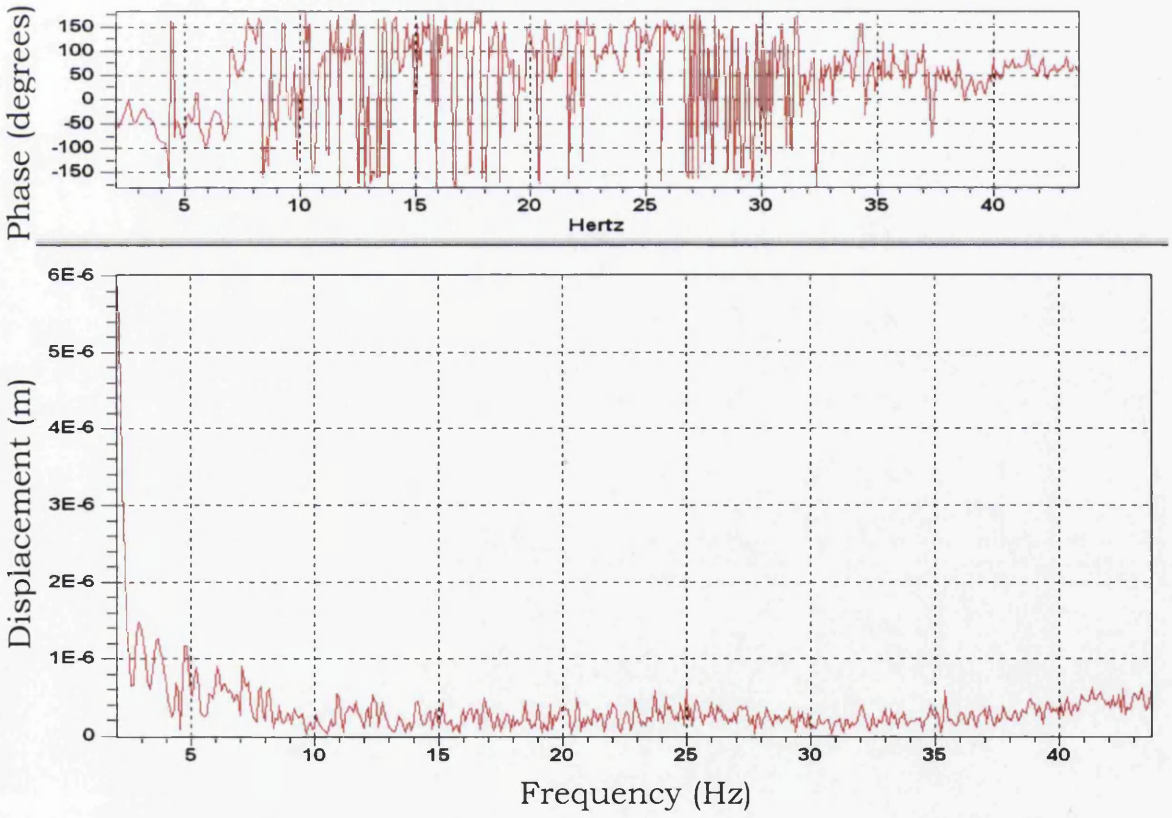

Figure 4 - 23 Responses at bearing A (Vertical) – 2 rubbers test

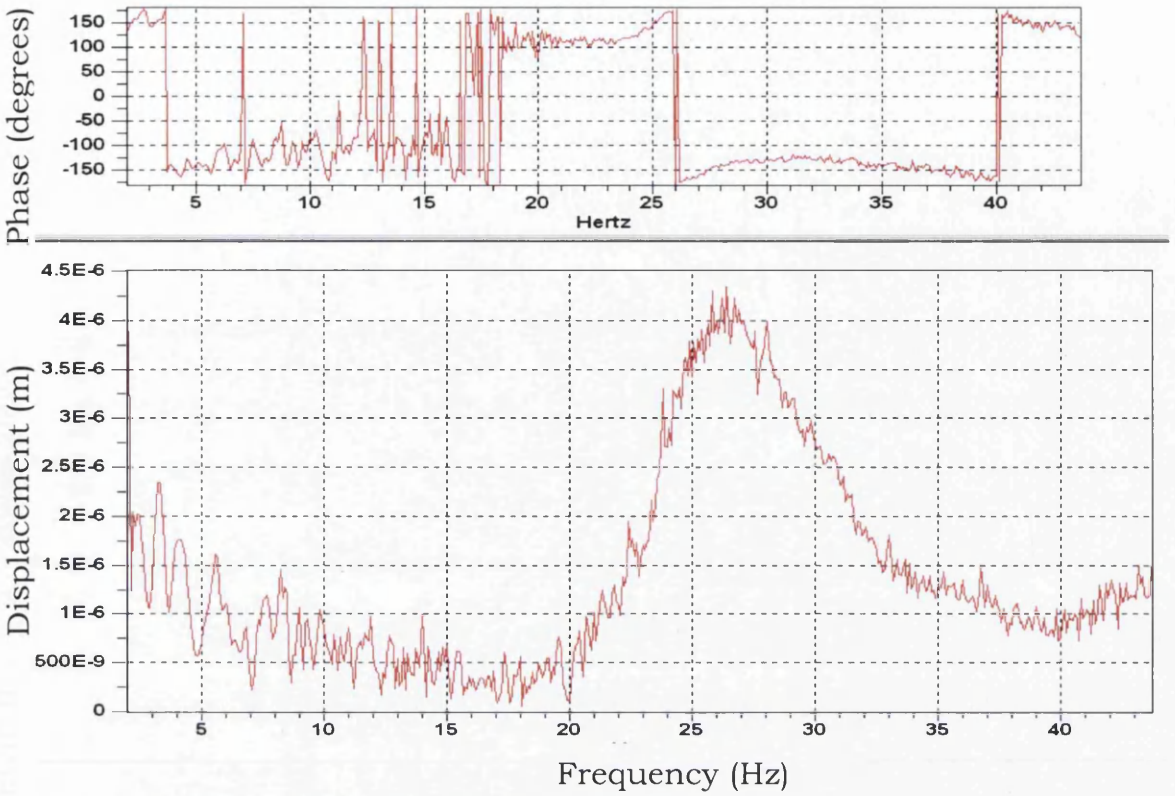

Figure 4 – 24 Responses at bearing A (Horizontal) – 2 rubbers test

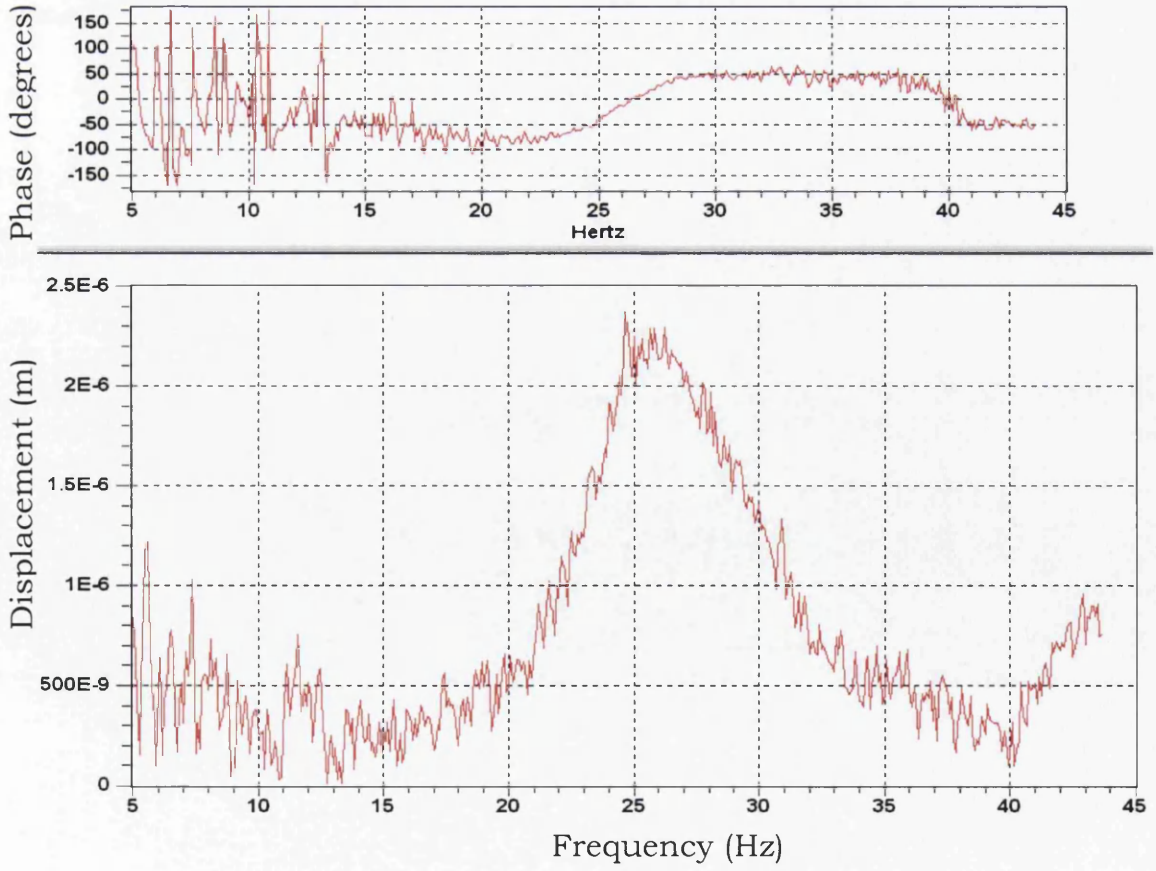

Figure 4 – 25 Responses at bearing B (Vertical) – 2 rubbers test

From the horizontal response at bearing A (Figure 4 - 24), the decreasing response amplitude is mainly due to the low signal to noise ratio.

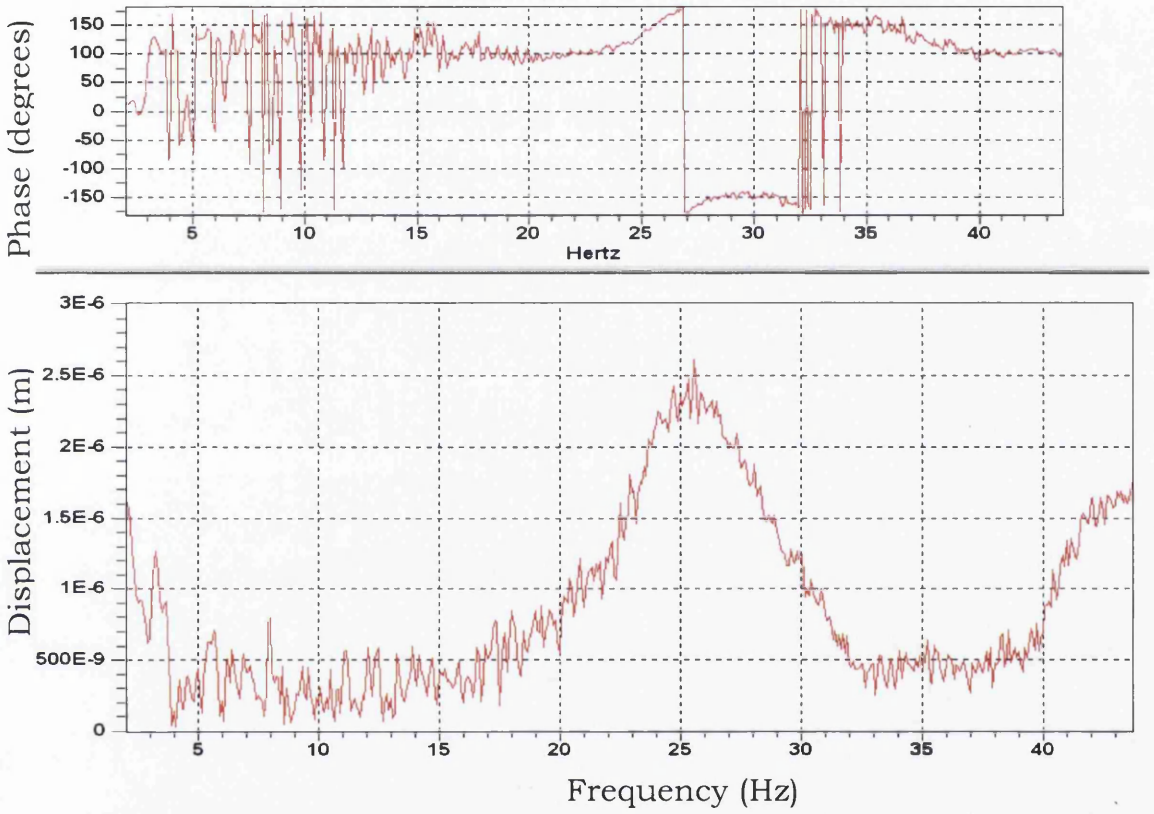

Figure 4 – 26 Responses at bearing B (Horizontal) – 2 rubbers test

Figure 4 - 27 shows the response of the accelerometer mounted in the horizontal direction at both bearing A and B. The results show that the vibration at bearing A is higher than at bearing B. The natural frequency is slightly different at bearing A and B due to the different location of bearing housings mounted on the baseplate as in the earlier case.

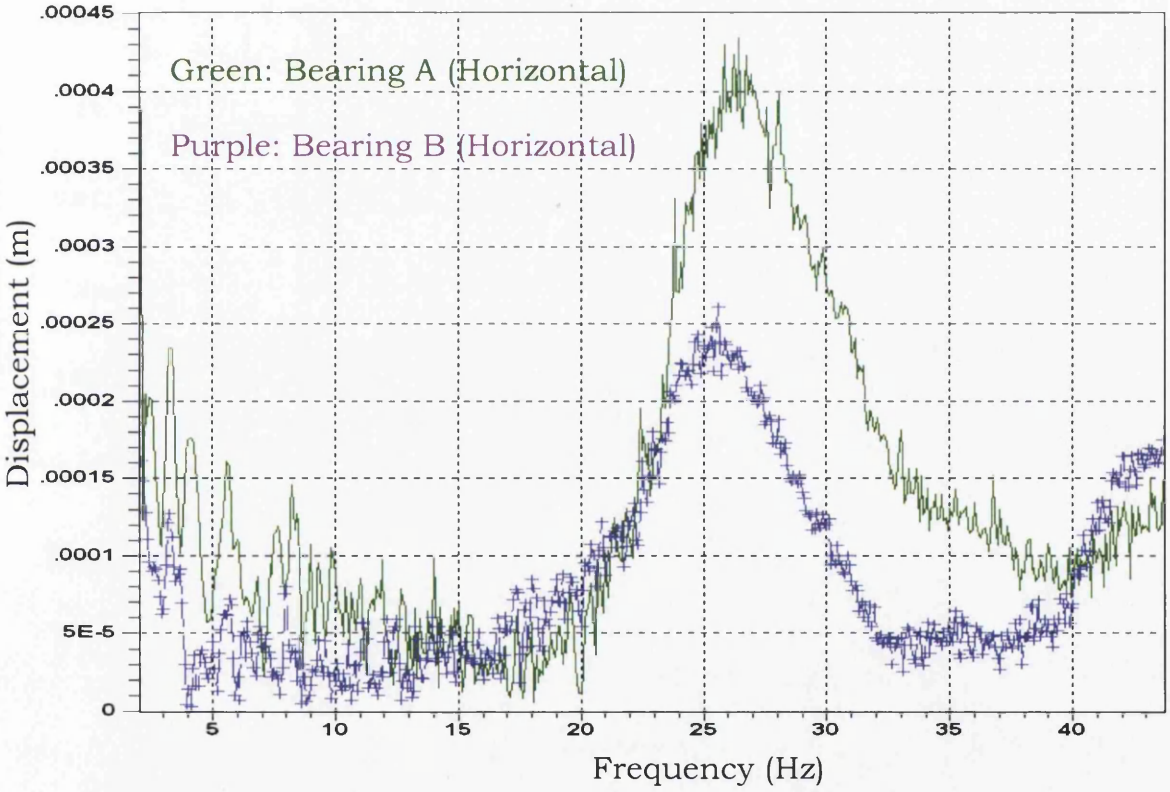

Figure 4 - 27 Comparison of horizontal responses at bearing A & B

Figures 4 – 28 & 4 – 29 show that the horizontal vibration at bearing B is slightly higher than in the vertical direction. However, the natural frequencies for bearing B in the vertical and horizontal direction are the same.

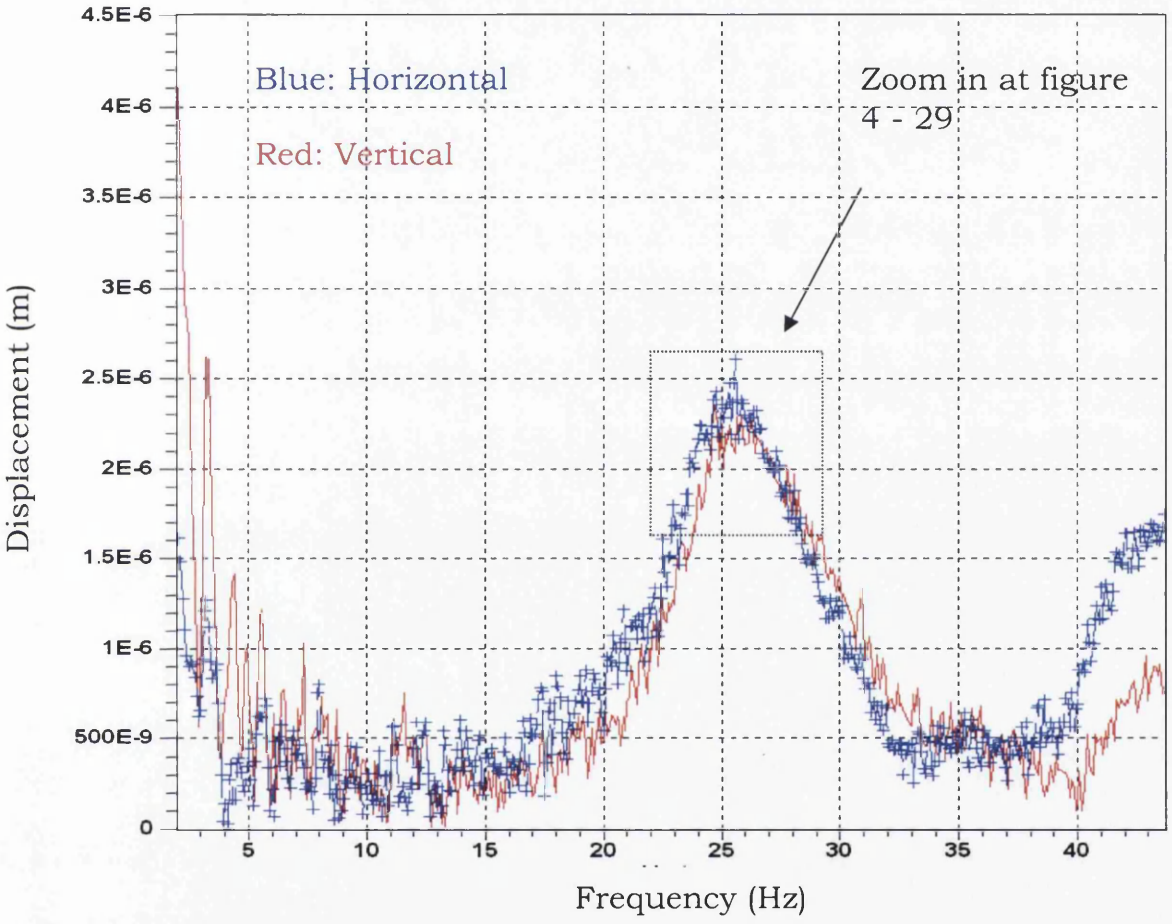

Figure 4 – 28 Comparison of horizontal and vertical direction responses at bearing B – 2 rubbers test

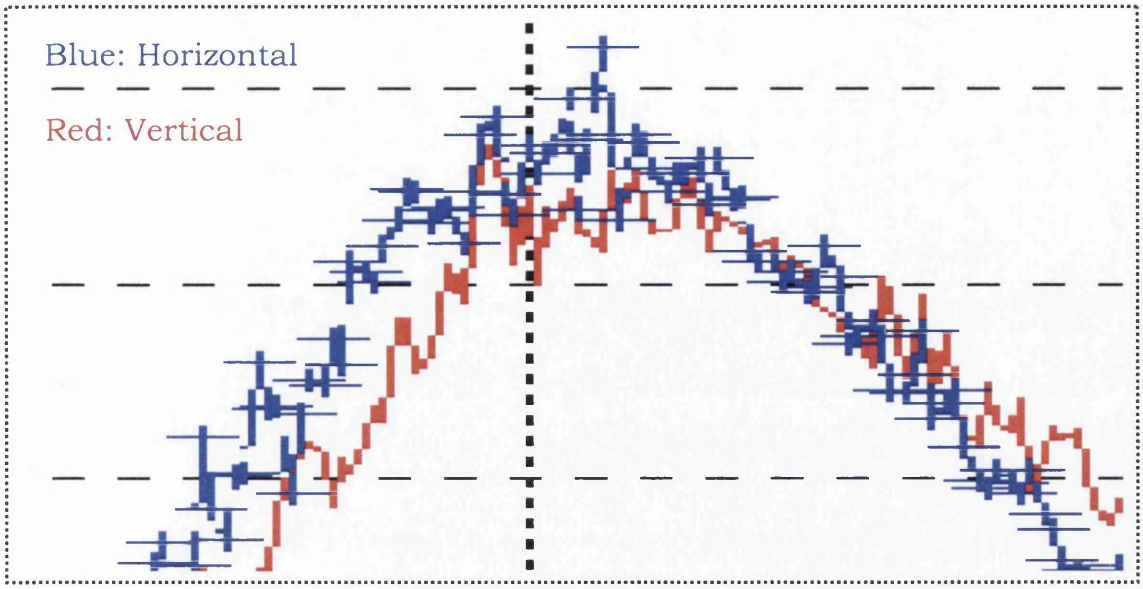

Figure 4 - 29 A zoom in of the natural frequency peak of figure 4 - 28

4.2.2 3–Rubbers Run-down Test Results

Figures 4 – 30 to 4 – 33 shows the accelerometer results for the 3 - rubbers run down tests. The accelerometer at bearing A in the vertical direction is not collecting any result other than noise. This happened during 1-rubber run-down and 2-rubbers run-down tests. In this case, the vertical response results at bearing A are not taken into consideration.

Figures 4 – 31, 4 - 32 & 4 - 33 show that the system has a critical speeds within the 50 Hz running range of the rotor. From the response data obtained, it again shows that significant noise existed during the experiments.

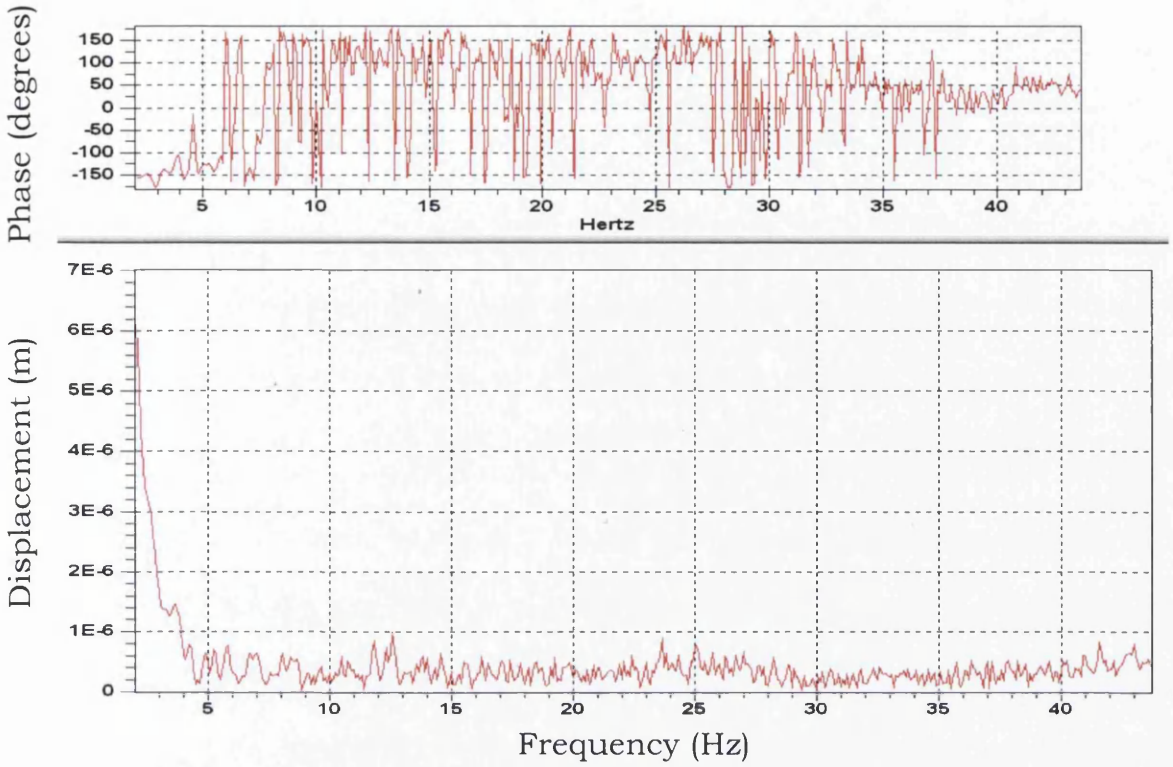

Figure 4 – 30 Responses at bearing A (Vertical) – 3 rubbers test

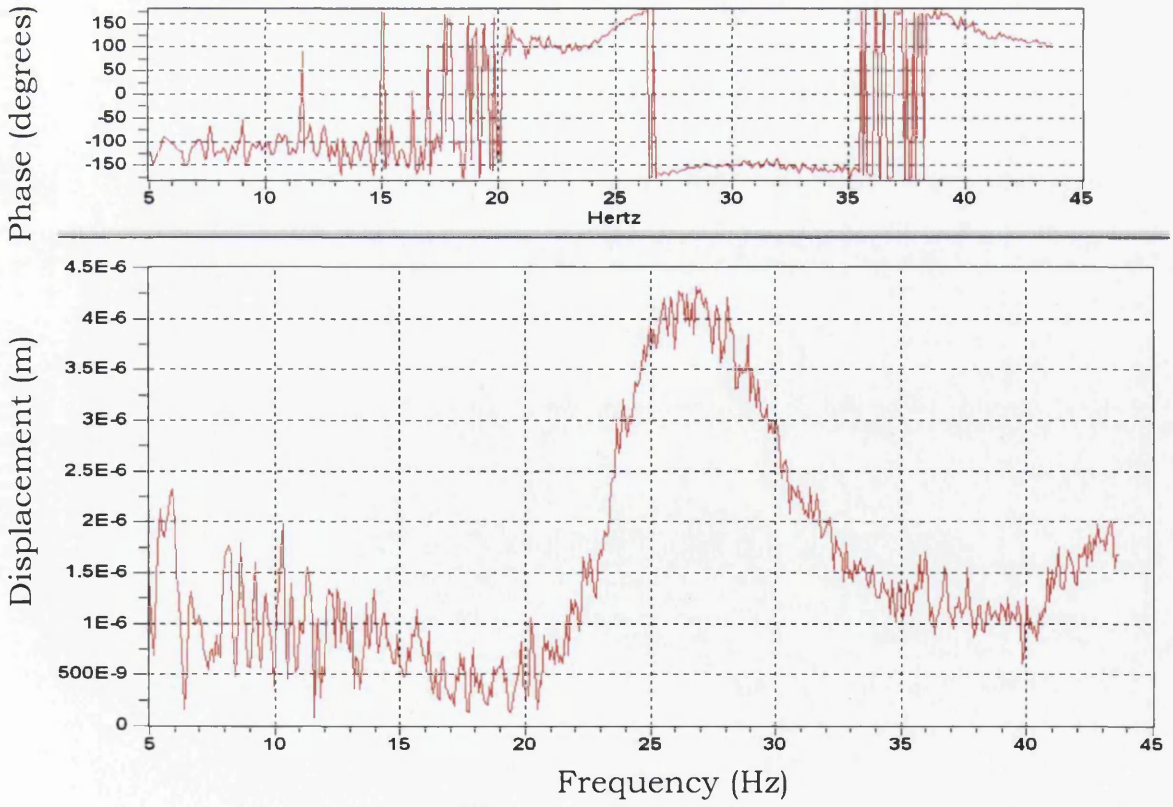

Figure 4 – 31 Responses at bearing A (Horizontal) – 3 rubbers test

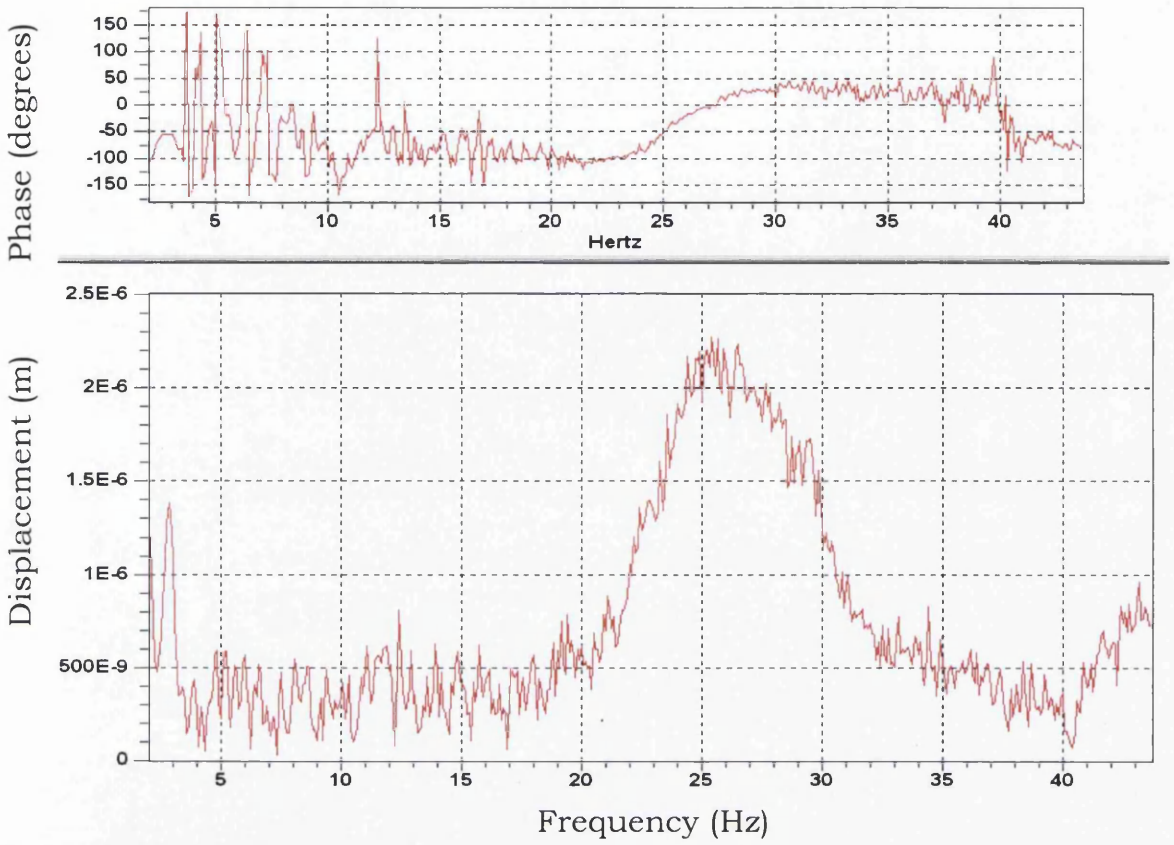

Figure 4 – 32 Responses at bearing B (Vertical) – 3 rubbers test

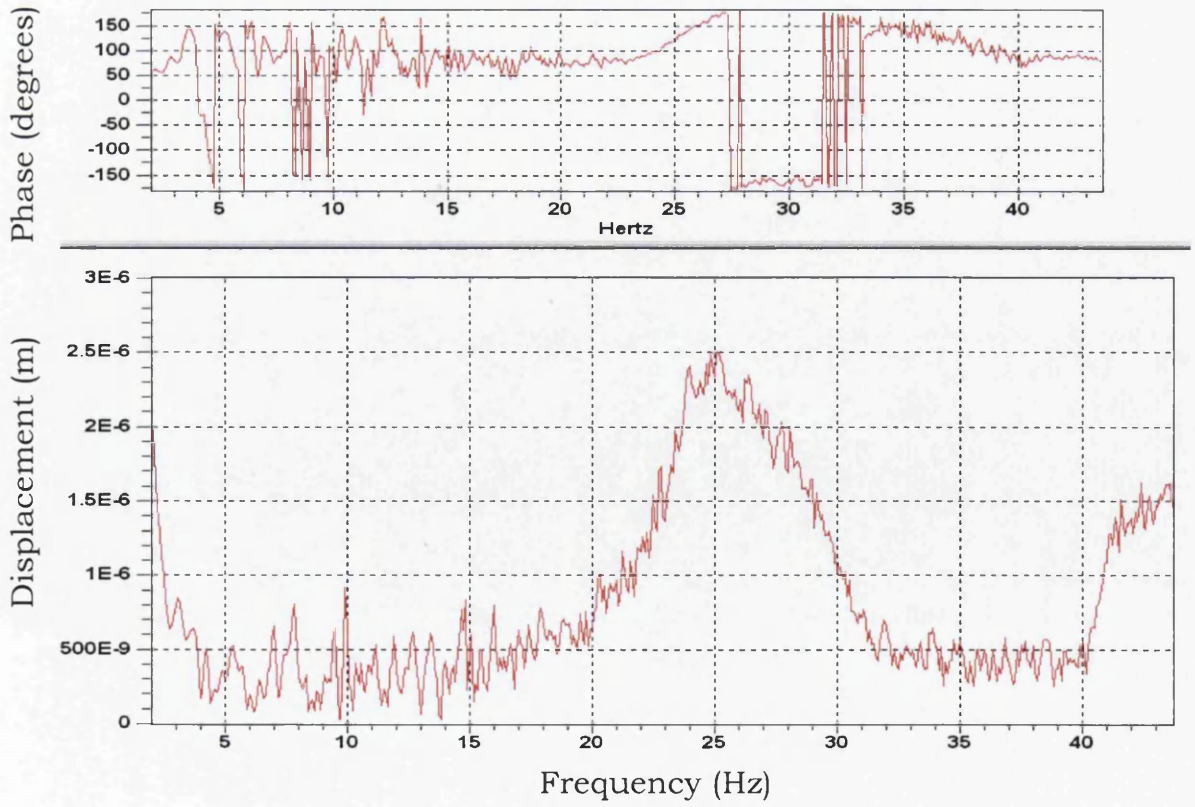

Figure 4 – 33 Responses at bearing B (Horizontal) – 3 rubbers test

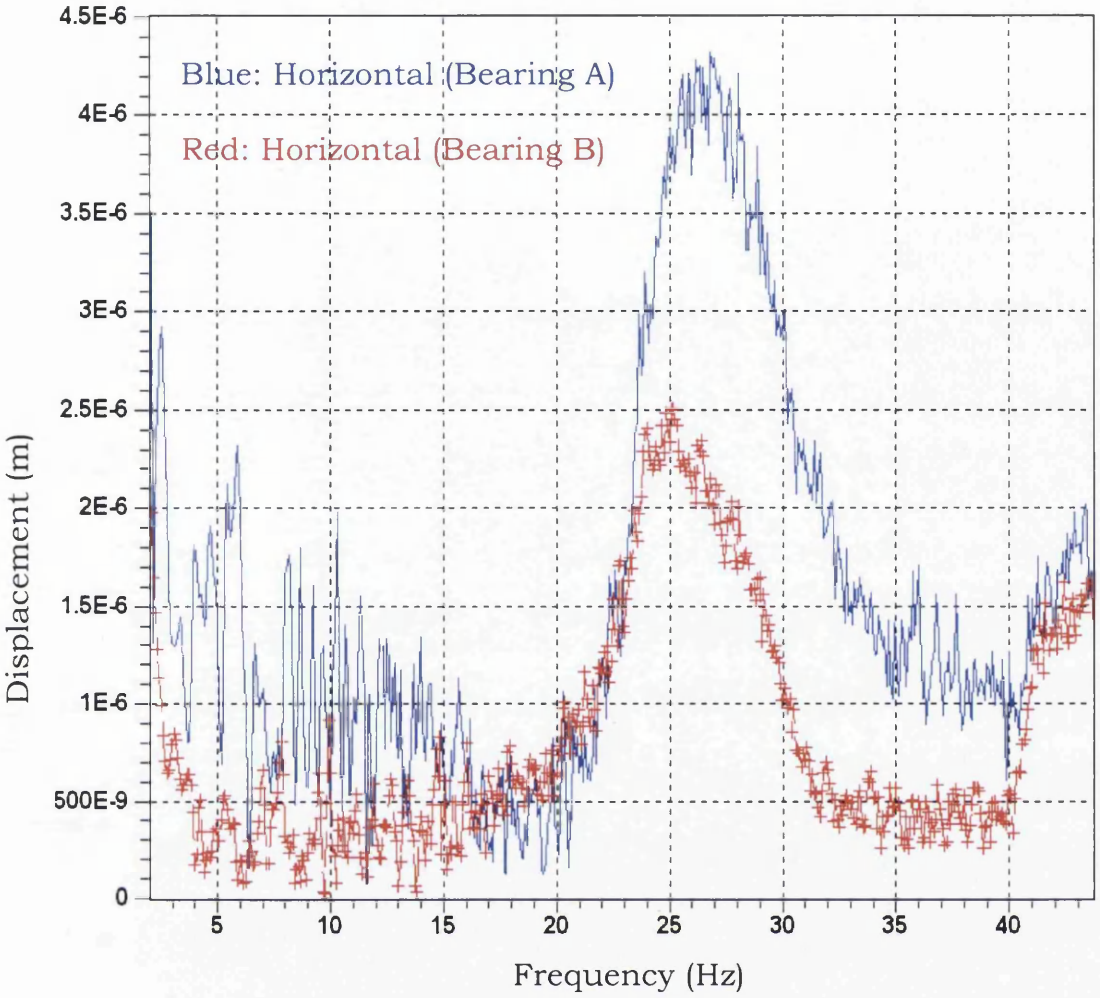

Figure 4 – 34 Comparison of the horizontal responses at bearing A & B – 3 rubbers test

Figure 4 - 34 compares the horizontal response results at bearings A and B. The horizontal responses at bearing A are higher than at bearing B. Since bearing A is located nearer to the operating motor, the vibration at bearing A is higher than at bearing B. This shows good agreement with the 1-rubber and 2-rubbers run-down tests

The natural frequency of bearing A is slightly higher than bearing B, which is due the different location of the bearings on the baseplate. This was also observed in the 1-rubber and 2-rubbers run-down tests. Hence, there is good agreement between the 1-rubber, 2-rubbers and 3-rubbers

run-down tests that the location of the bearings will affect the natural frequency of the system.

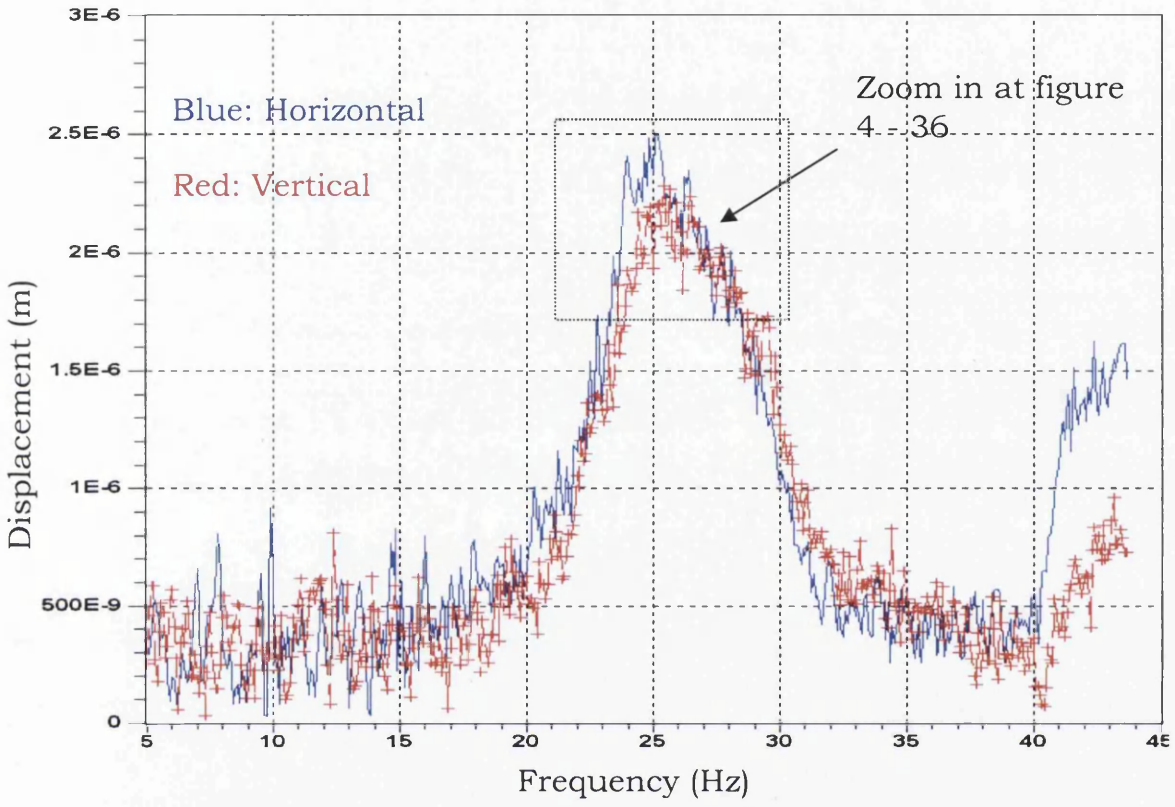

Figure 4 – 35 Comparison of horizontal and vertical direction responses at bearing B – 3 rubbers test

Figure 4 - 35 shows the responses data for the accelerometers mounted on bearing B in the horizontal and vertical direction. From Figure 4 - 35, the difference of responses is not significant. A closer view of the figure is presented below in order to clarify the results obtained.

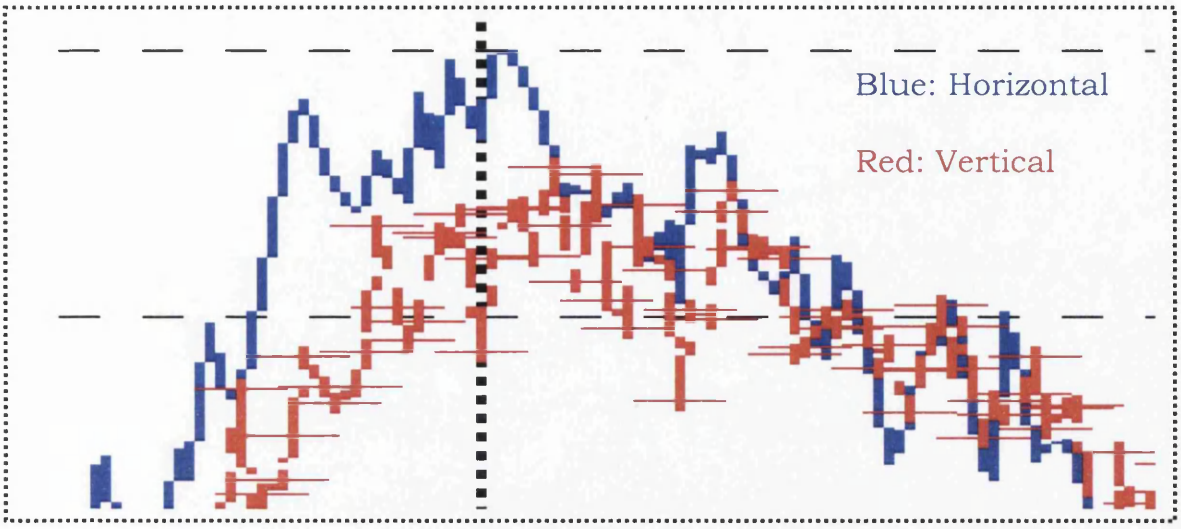

Figure 4 - 36 A zoom in of the natural frequency peak of Figure 4 - 35

Figure 4 – 36 shows that the amplitude response in the horizontal direction is slightly higher than the vertical direction amplitude response at bearing B. Additionally, the result in Figure 4 - 35 show that the natural frequency of the system in vertical and horizontal directions is the same.

There is good agreement between the 1-rubber, 2-rubbers and 3-rubbers run-down tests in that the vibration in the horizontal direction is larger than the vibration in the vertical direction. From the response data obtained, the natural frequency is the same in the vertical and horizontal direction. The natural frequency of the system is the same in any direction (vertical or horizontal) but does vary at different locations.

4.2.4 Comparison of the results from 1-Rubber, 2-Rubbers and 3–Rubbers Run-down Tests

The experimental run-down test results for 1-rubber, 2-rubbers and 3-rubbers are compared in Figures 4 – 37, 4 – 38 & 4 – 39.

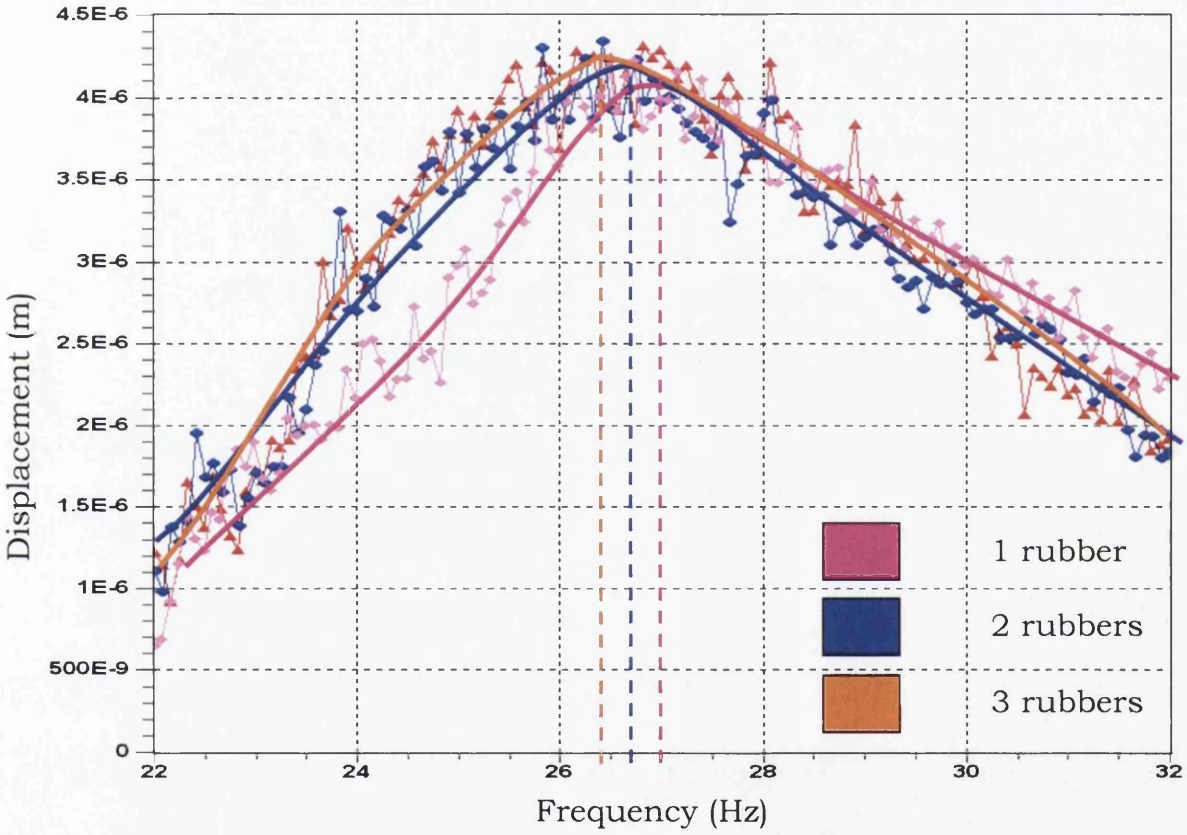

Figure 4 – 37 Comparison of the horizontal response results at bearing A with different elastomer layers

Figure 4 – 37 shows the horizontal response at bearing A for 1-rubber, 2-rubbers and 3-rubbers tests. It was found that the 3-rubbers run-down test has the highest amplitude followed by 2-rubbers and 1-rubber tests.

Additionally, Figure 4 - 37 shows that the natural frequency for the 3-rubbers run-down test is lower than the natural frequency for the 1-

rubber run-down test. Here, the natural frequencies for the 1-rubber, 2-rubbers and 3-rubbers tests are approximately 27 Hz, 26.7 Hz and 26.4 Hz respectively. Similar, the maximum displacements are 4.1E-6, 4.2E-6 and 4.25E-6 metres respectively.

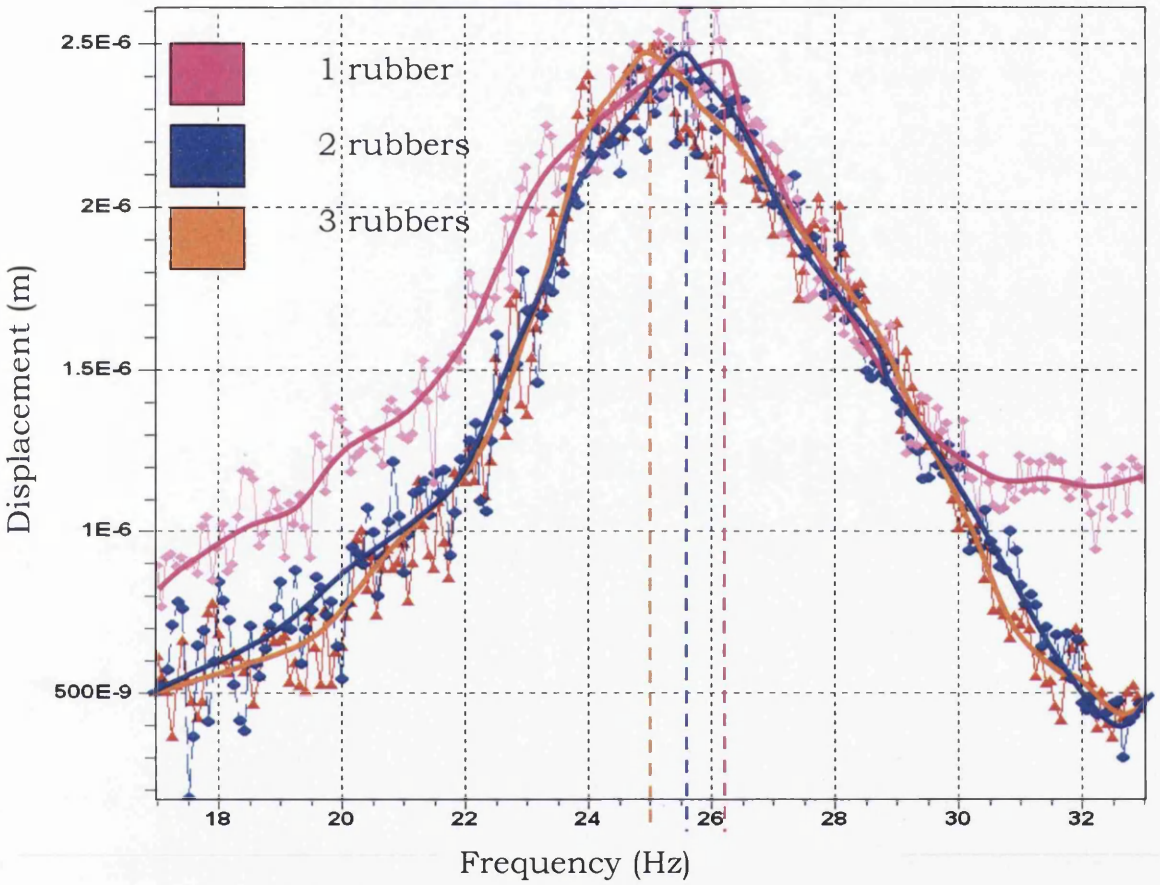

Figure 4 – 38 Comparison of horizontal response results at bearing B with different elastomer layers

Figure 4 - 38 represents the response result for the accelerometers mounted in the horizontal direction at bearing B. Here, it was found that the 3-rubbers achieved the highest response amplitude. Furthermore, the use of 1-rubber to the system causes the least vibration.

From Figure 4 – 38, it is seen that the natural frequency of the system is decreased when increasing the number of the elastomer layers.

It was observed that the 1-rubbers test has the highest natural frequency followed by 2-rubbers and 3-rubbers test. Here, the natural frequencies of 1-rubber, 2-rubbers and 3-rubbers run-down test at bearing B (accelerometer mounted in horizontal direction) are approximately 26.2, 25.5 and 25 Hz respectively. Similar the maximum displacement is 2.45E-6, 2.47E-6 and 2.5E-6 metres respectively.

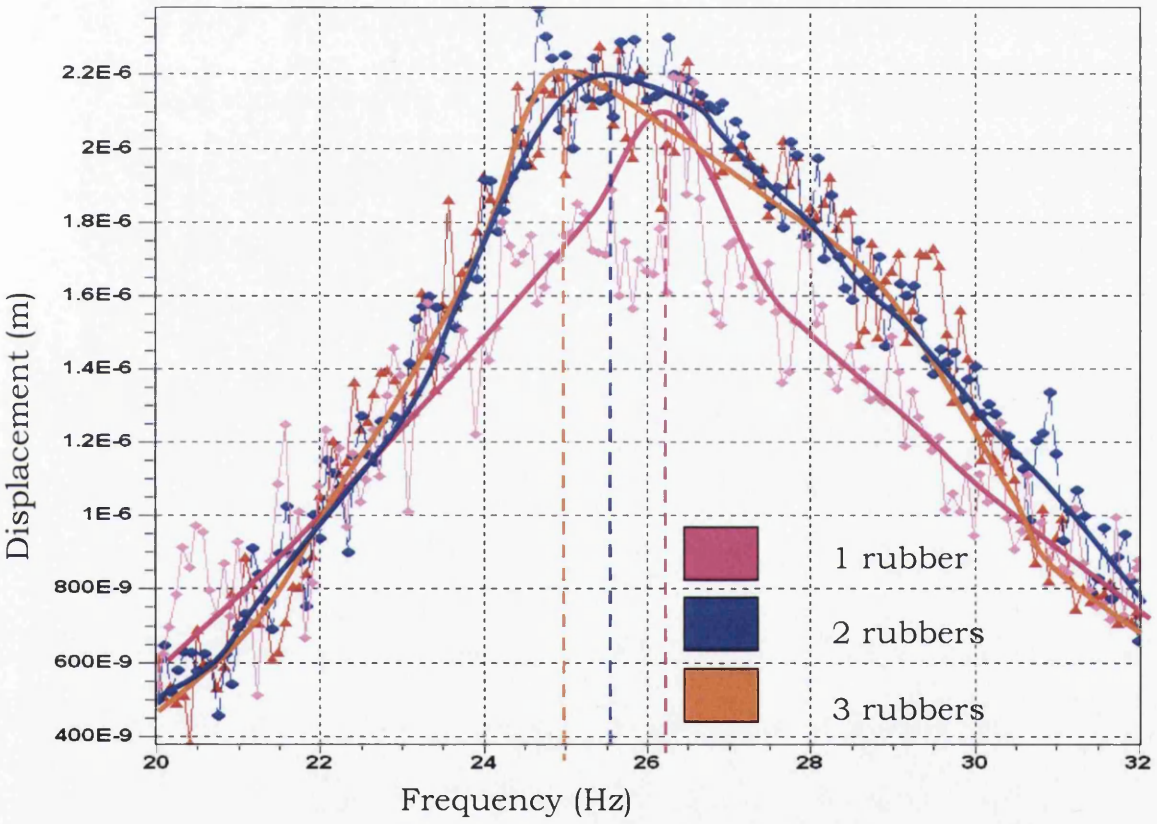

Figure 4 - 39 Comparison of the vertical response results at bearing B with different elastomer layers

Figure 4 - 39 above shows the response from the accelerometer mounted on bearing B in the vertical direction. The response amplitude of the 3-rubbers run-down test is the highest followed by 2-rubbers and 1-rubber. The maximum displacements are 2.1E-6, 2.19E-6 and 2.23E-6 metres respectively.

Additionally, it was found that the natural frequency of the 1-rubber run-down test is the highest followed by 2-rubbers and 3-rubbers test. The natural frequencies of the system decrease when increasing the number of the elastomer layers. Here, the natural frequencies of 1-rubber, 2-rubbers and 3-rubbers run-down tests are approximately 26.2, 25.5 and 25 Hz respectively. It was observed in all run-down tests that the difference of the natural frequencies results is not significant.

4.2.5 Discussion of the results from the run-down tests

This section compares and discusses all the run-down test results obtained from the experiment when different layers of elastomer are applied to the system. Good agreement is found between the results of 1-rubber, 2-rubbers and 3–rubbers tests. The results confirm that the response amplitude and natural frequency is dependent on the flexibility of the support system. The number of elastomers affects the vibration and natural frequency of the system. It was found that when more rubbers are used, the flexibility of the system is greater, as expected.

From the run-down results presented in the last section, it is seen that the vibration of the system increases with the increment of the elastomer layers (thickness) due to increases in the flexibility of the system. Therefore, higher response amplitude is achieved in the 3-rubber run-down test. During the test, the elastomer layers were added in series which is shown in Figure 4 – 40. In this case, the damping reduces when the thickness of elastomer increases.

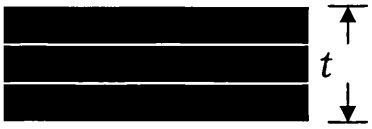

Thickness of elastomer, t = Number layer of elastomers

Figure 4 – 40 Schematic of elastomer layers added in series

The use of elastomers as support damping to control the vibrations of machinery is seeing increasingly wider application in industry. According to the previous research on the dynamic properties of elastomers, which has been discussed in Chapter 2, the application of an elastomer is an effective method of reducing the vibration of the system. However, the key point in the design of an effective damper is to understand the elastomer characteristics.

According to the literature regarding the dynamic properties of elastomers from NASA [13], it was found that the size and shape of the elastomers affect the dynamic and damping properties of the system. It was also found that damping increased with the area of elastomer [13]. It was concluded that larger areas of elastomer provide higher damping to the system.

In the work, it has been shown that an increase in the thickness of the elastomer resulted in an increase in the amplitude of vibration and a decrease in the natural frequency in all cases.

From standard dynamics theory, the natural frequency is proportional to the square root of the stiffness of the system. In this case, 1-rubber test achieved the highest natural frequency due to highest stiffness. Additionally, the result showed that the natural frequency is different at different locations on the machine.

Here, the run-down test results indicate that the influence of the elastomers on the behaviour of this particular machine is small. The results obtained at 1-rubber, 2-rubbers and 3-rubbers tests are not significant. It was observed that the shaft is more flexible if compare to the bearing housing. Therefore, the results are partly influenced by the flexibility of the shaft. Therefore, hammer and shaker tests are carried out in this research project in order to study more about the influence of dynamic properties of elastomers on the machine behaviour and also to verify the run-down test results.

The advantage of hammer and shaker tests is that a higher operating frequency range can be achieved during the experiment. There is a limitation on the maximum frequency range for run-down test up to 50 Hz. Therefore, hammer and shaker tests are performed in this project to investigate the influence of the elastomer thickness on the behaviour of the machine at higher frequency. The results and experimental details are presented in the next chapters.

CHAPTER 5

HAMMER TEST

This chapter discusses the experimental method of hammer testing. The results obtained from the hammer test are also discussed.

Impact excitation is one of the most common methods used for experimental modal testing. Hammer impacts produce a broad-banded excitation signal ideal for modal testing with a minimum amount of equipment and set up.

Impact testing is a form of transient testing, where the structure is tapped gently with a specially designed hammer, and the resulting impulse response is measure. This is the quickest and most convenient type of excitation. Here, an *Impulse-force hammer* (PCB 086C03) was used in the hammer test. *Impulse-force hammers* are widely used in vibration testing to produce short duration (i.e. impulse) forces to measure the impulse response produced. A force transducer is attached to the hammer to measure the impulse force. A schematic of the experimental set-up is shown in Figure 5 – 1.

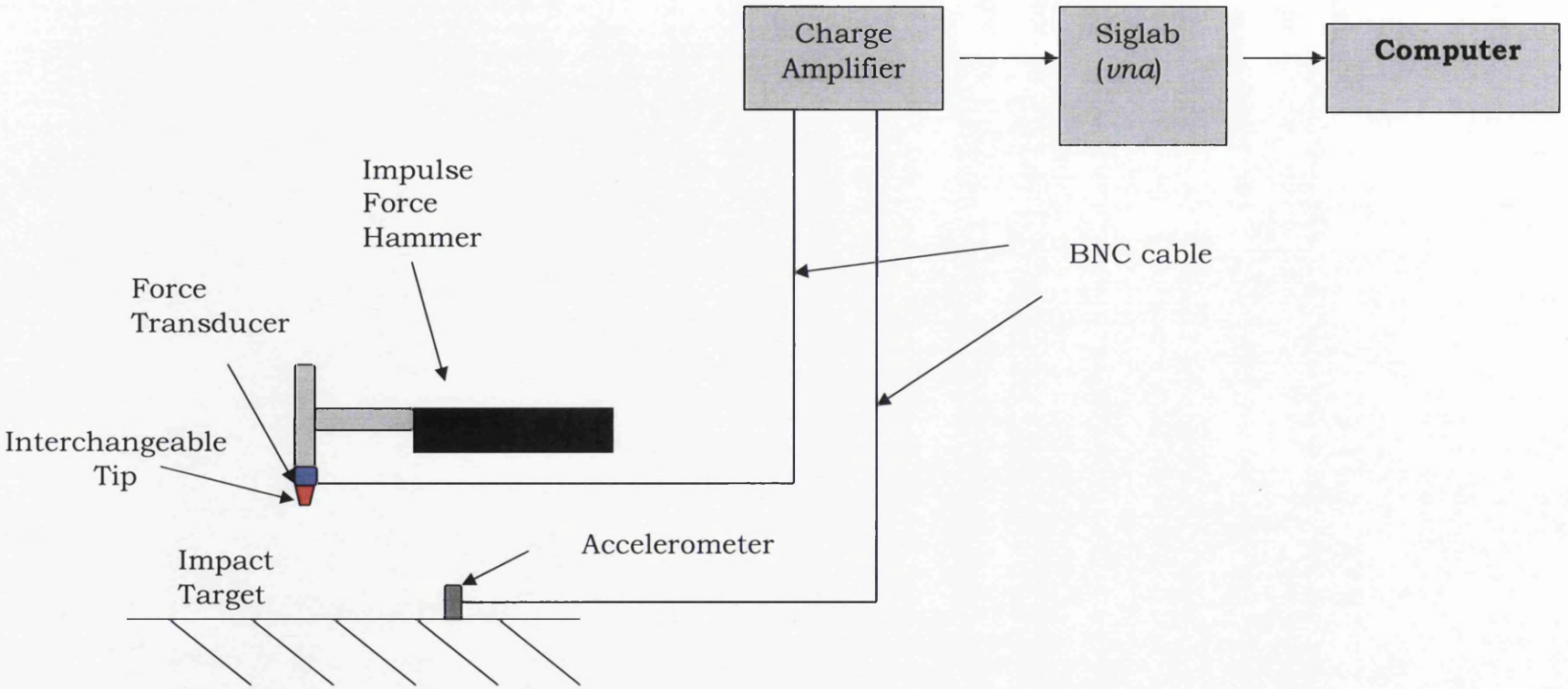

Figure 5 – 1 Schematic of Hammer Test Experimental Set-up

5.1 Hammer Test Experimental Equipment

A DJB Type A/20 accelerometer was used in the Hammer Test. The accelerometer and impulse-force hammer are both connected to a DJB Type CA/04 charge amplifier by BNC cables. Channel 1 was used for the accelerometer and channel 2 was used for the force transducer. The charge amplifier converts the piezoelectric charge produced by the accelerometer and force-impulse transducer into low impedance voltage. The gain setting and the calibration constant of the particular transducers (accelerometer and impulse-force transducer) were set on the charge amplifier to allow the desired voltage range to be achieved.

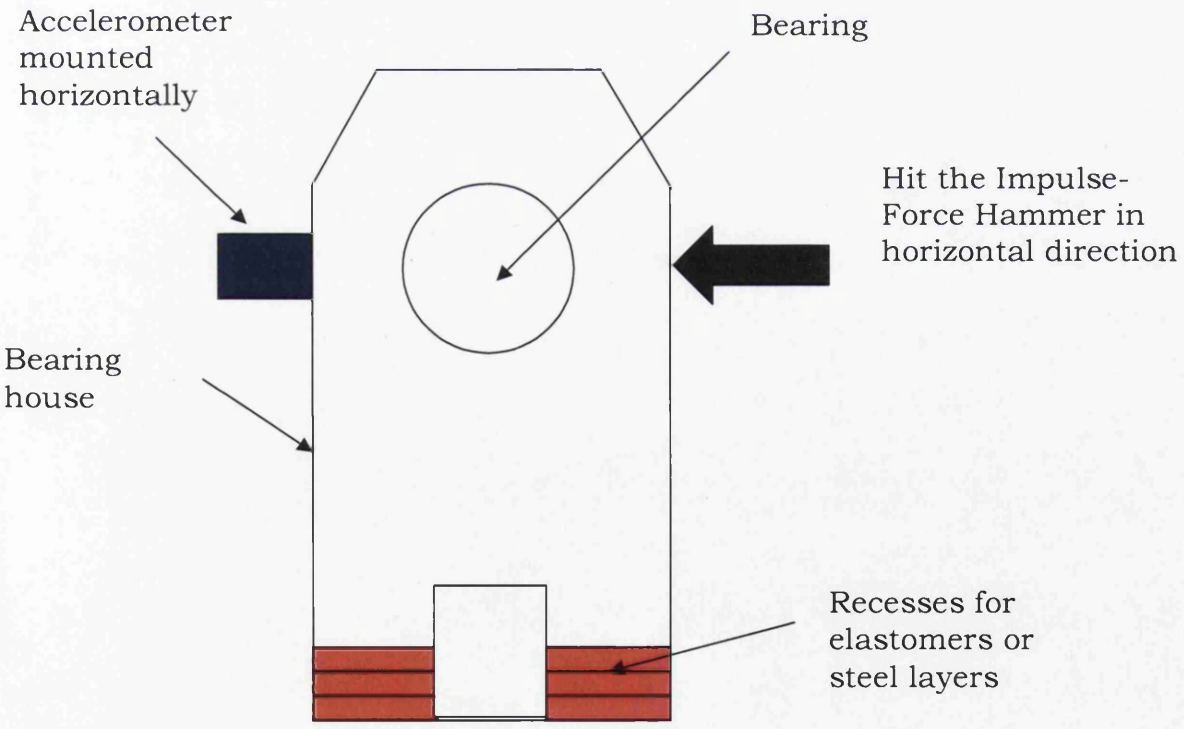

Figure 5 – 2 Hammer tests on bearing housing

The bearing housing used in the hammer test is exactly the same as that used in the run-down test, which is specially designed to provide variable stiffness and damping properties of the system. During the hammer test, the impulse-force hammer is gently tapped or hit on the bearing housing to create impact forces. The Siglab program is then used to conduct a spectral analysis of the acquired signals.

5.2 Signal Processing (*vna* - virtual network analyzer)

The signal-processing program for the Hammer Test is discussed in this section. The *vna* (virtual network analyzer) in the *Siglab* [21] program was used as a dynamic signal analyzer to process the data from the Hammer Test. One of the functions of dynamic signal analyzers is the collection of data for use in modal analysis. Modal analysis can be generally defined as the determination of an optimal set of parameters that can be used to describe the dynamic response of a mechanical system. DSPT Siglab is a multi-channel dynamic signal analyzer for characterizing signals and systems. It is a combination of function generator, spectrum analyzer and network analyzer.

For the Hammer Test, *vna* (virtual network analyzer) in Siglab program was used to collect and process the signals from the accelerometer and impulse-force transducer. The signals from both accelerometer and force transducer go to the charge amplifier which is shown in Figure 5 – 1. The charge amplifier has a normalised gain compensation function to allow the piezoelectric accelerometer or force transducer within the range 1-100 pC/g (psi, kPa, Newton etc.) to be used with the indicated scaling.

With the correct charge sensitivity for both accelerometer and force transducer set on the charge amplifier, Siglab receives the signals in Volts (V). In order to convert the accelerometer signals to g (m/s^2) and force transducer to Newtons (N), the output setting of the charge amplifier was set in the *vna* program. In this case, 1 N/V was set in channel 1 (force transducer) and 0.316 g/V was set in channel 2 (accelerometer).

The output of the charge amplifier depends on the gain setting. In this case, 0.3 was set on the gain control section of the accelerometer channel and 1 was set on the gain control of the force transducer channel. Therefore, the output of channel 1 (accelerometer) was 0.316 g/V and the output of channel 2 (force transducer) was 1 N/V.

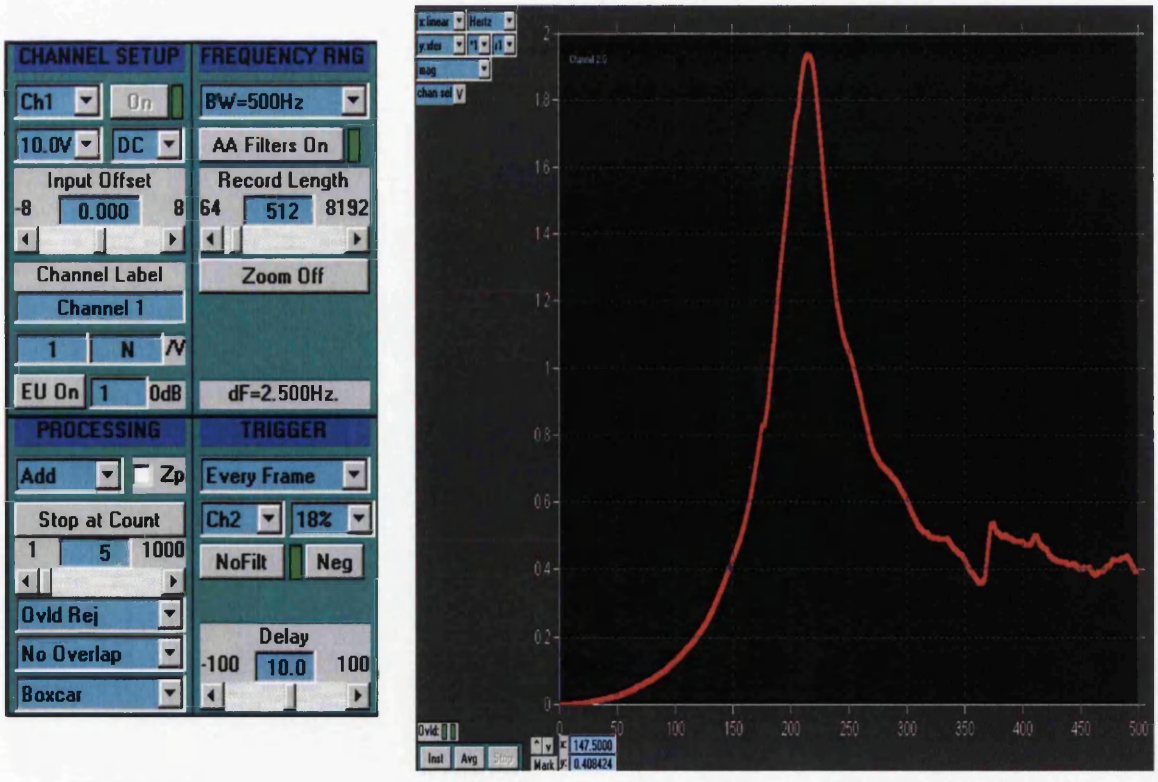

Figure 5 – 3 *vna* (virtual network analyzer) program settings

The *vna* (virtual network analyzer) program settings for the hammer test is shown in Figure 5 - 3. A bandwidth (BW) of 500 Hz is set. Only frequencies below 500 Hz are of interest in this experiment. In the *stop at count* section, the number of averages of the test was set as 5 to increase the accuracy of the measurements. The measurement stops when the selected number of averages is completed. In this case, the program will stop automatically when the hammer has been hit 5 times on the test specimen and an average measurement of the 5 hits is produced.

A computational program for both hammer and shaker tests, for elastomers dynamic properties identification using the theory given in Chapter 3, has been developed in Matlab [22]. The results obtained from hammer test will be discussed in the next section.

5.3 Hammer Test Results

The bearing housing and one accelerometer used in the run down tests were used in the hammer tests. The accelerometer was mounted horizontally on the bearing housing. The hammer was tapped gently on the bearing housing horizontally to create an impact force to the system. The set-up of the hammer test has been discussed previously in this chapter. The accelerometer response amplitude is presented in Figure 5 – 4. The response motion in this case is rotation; therefore, the response amplitude is represented as angular displacement. The definition of angular displacement is the motion of the object rotating in a common axis in a circular path.

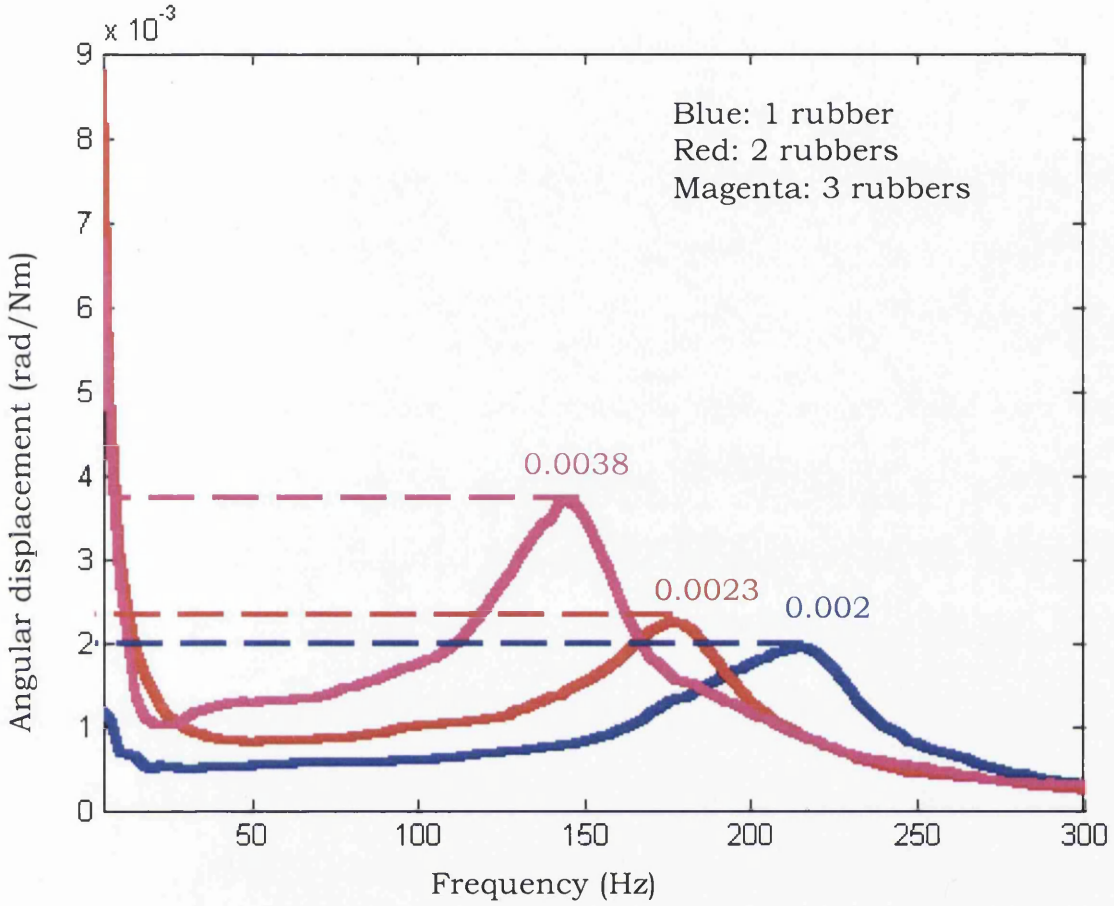

Figure 5 – 4 Hammer Tests (Displacement results)

Figure 5 - 4 shows the response (rad/Nm) results from 1, 2 and 3 rubbers hammer tests. At low frequency, the signal to noise ratio was low as mentioned previously in Chapter 4. In this case, the signal obtained from the hammer test was actually a mixture of signal and noise, therefore, the experimental results at low frequency is not accurate.

Figure 5 - 4 shows that the 1-rubber hammer test achieved the highest natural frequency followed by 2-rubbers and 3-rubbers test.

Furthermore, the results show that the 3-rubbers hammer test has the highest response amplitude followed by 2-rubbers and 1-rubbers test. The 3-rubbers hammer test experiences the highest vibration response but lowest natural frequency. The 1-rubber hammer test experiences the least vibration response but the highest natural frequency.

The output data from the hammer test was used to define the stiffness and damping as discussed previously in Chapter 3. The stiffness and damping results are shown in Figure 5 - 5.

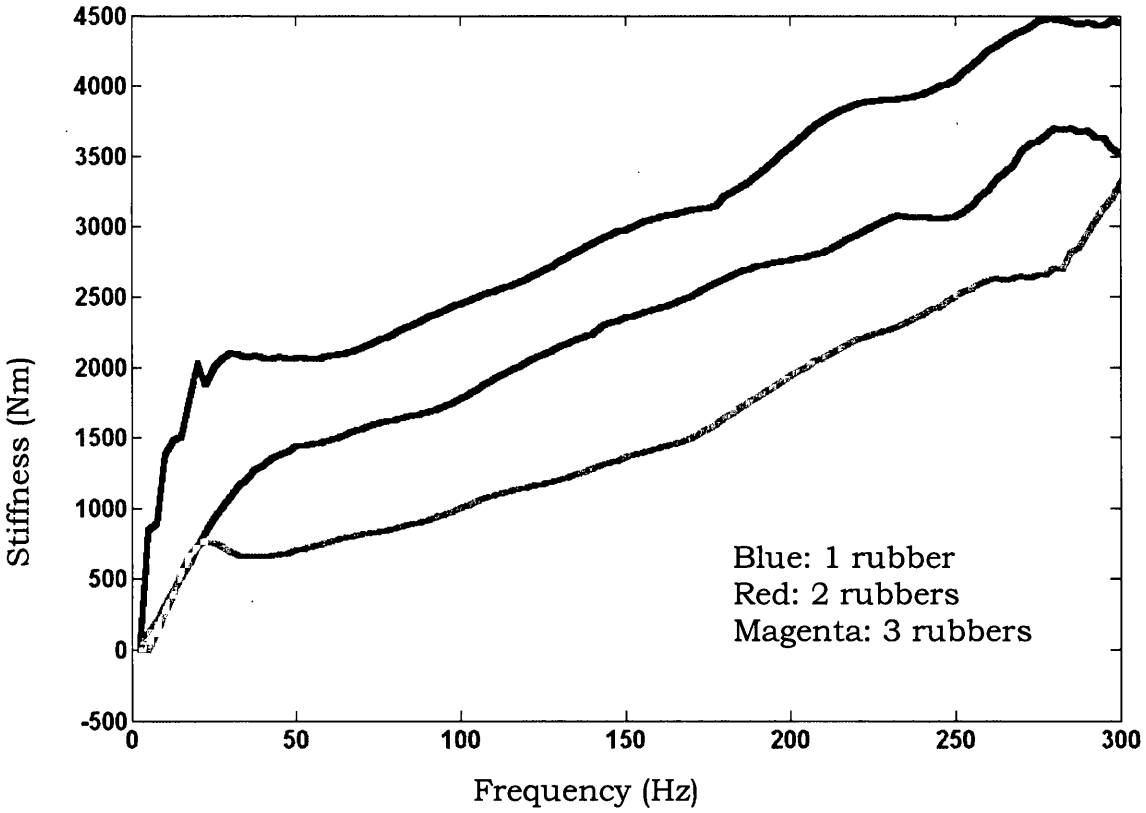

Figure 5 – 5 Hammer Tests (Stiffness results)

The stiffness tends to increase on increasing the excitation frequency. Here, the stiffness of 1-rubber test is the highest followed by 2-rubbers and 3-rubbers test.

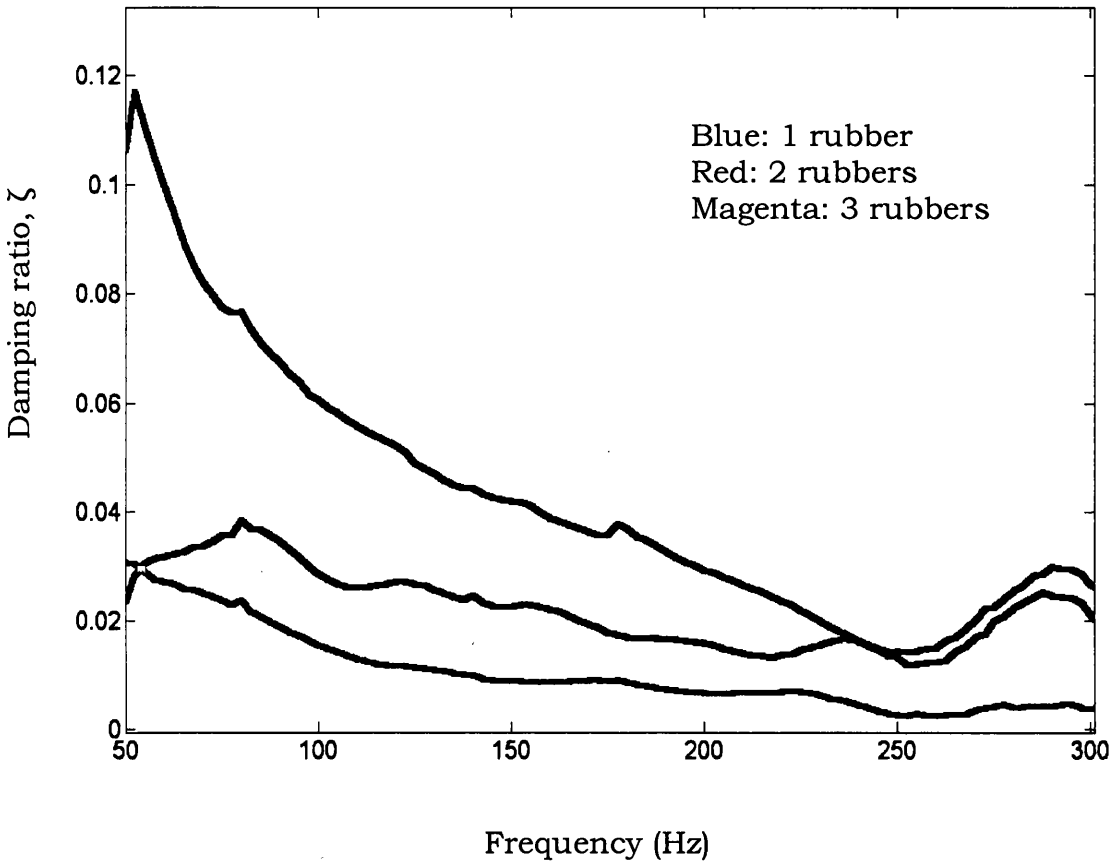

Figure 5 – 6 Hammer Tests (Damping results)

Figure 5 – 6 shows the damping results for the hammer test. The damping results obtained under 50 Hz are not sensible. Again, this is due to the low signal to noise ratio which been discussed previously. In particular, the damping tends to decrease on increasing the excitation

frequency. 1-rubber test achieved the highest damping followed by the 2-rubbers and the 3-rubbers test.

5.4 Discussion

The overall results show that stiffness tends to increase on increasing the excitation frequency and the damping tends to decrease with increasing of excitation frequency.

The hammer test signals obtained below 50 Hz are not accurate. This is due to the low signal to noise ratio. Therefore, the system is less accurate at low frequencies when the accelerations are low.

Applying different layers of elastomer to the experimental apparatus tends to produce variable stiffness and damping properties to the system. This work aims to study the influences of dynamic properties of elastomers on machine behaviour. From the hammer test results, it was found that the vibrations increase with the number of layers of elastomers applied on the system. In this project, the elastomer layers were added in series as shown in Figure 4 – 41. Increasing the thickness of the elastomer layers caused more flexibility of the system. Therefore, the 3-rubbers test experienced the highest vibration and 1-rubbers test experienced the least vibration.

The response amplitude results (Figure 5 – 4) indicate that the system is non-linear, i.e. the response amplitude of the 2-rubbers test was not 2/3 of 3-rubbers test and the response amplitude of 1-rubbers test was not 1/3 of 3-rubbers test. Several tests have been carried out

with different voltage inputs using the shaker to verify the non-linearity of the system. These results will be discussed later in the next chapter.

Both stiffness and damping results show that the 1-rubber test had the highest stiffness and damping followed by 2-rubbers and 3-rubbers test. The stiffness results reflect the flexibility of the system. Furthermore, the damping of the system reduced due to the increase of the thickness of the elastomers.

When more layers of elastomer are added in series to the system, the system becomes more flexible, thus, the damping of the system reduces. The damping produced will be proportional to the rate of change of stress. However, damping increases with the area of the elastomer [12].

It was found that the natural frequency reduced with the number of layer of elastomers applied to the system. Here, the results showed that the 3-rubbers test achieved the lowest natural frequency followed by 2-rubbers and 1-rubbers test. The natural frequency is proportional to the stiffness of the system. The same outcome was seen in the run-down test results.

The shaker test experimental details and results obtained are discussed in the next chapter.

CHAPTER 6

SHAKER TEST

The experimental results from hammer testing in Chapter 5 have been verified by a shaker test. A photograph of the shaker test rig is shown in Figure 6 – 1. Shaker tests produce excitation signals which are ideal for modal testing with a minimum amount of equipment and set up. The shaker test rig consists of a vibration generator (shaker), bearing housing with recesses for elastomers and transducers. The type of transducers used in the shaker test is a force sensor and accelerometer in order to measure the force and acceleration of the system respectively.

Hammer tests and shaker tests are similar but with some important differences. One difference is the excitation force produced to the test rig. For a hammer test, the hammer is used to create an impact force to the system. However, a vibration generator (shaker) is used in shaker tests to supply an excitation force to the system. In this case, the excitation supplied from the shaker may be a swept sine excitation. Swept sine measurements are among the most commonly used tools for the characterisation of the dynamic behaviour of mechanical systems. Two types of sweeps are well known, firstly the linear sweep and secondly the exponential (or logarithmic) sweep. In this work, a linear sweep is chosen to perform the shaker test. The response amplitude and force is recorded as the excitation frequency is swept across the range of interest.

The instrument described herein is presented as a simple alternative that can be used for both field and laboratory measurements with high accuracy.

6.1 Shaker Test Experimental Apparatus

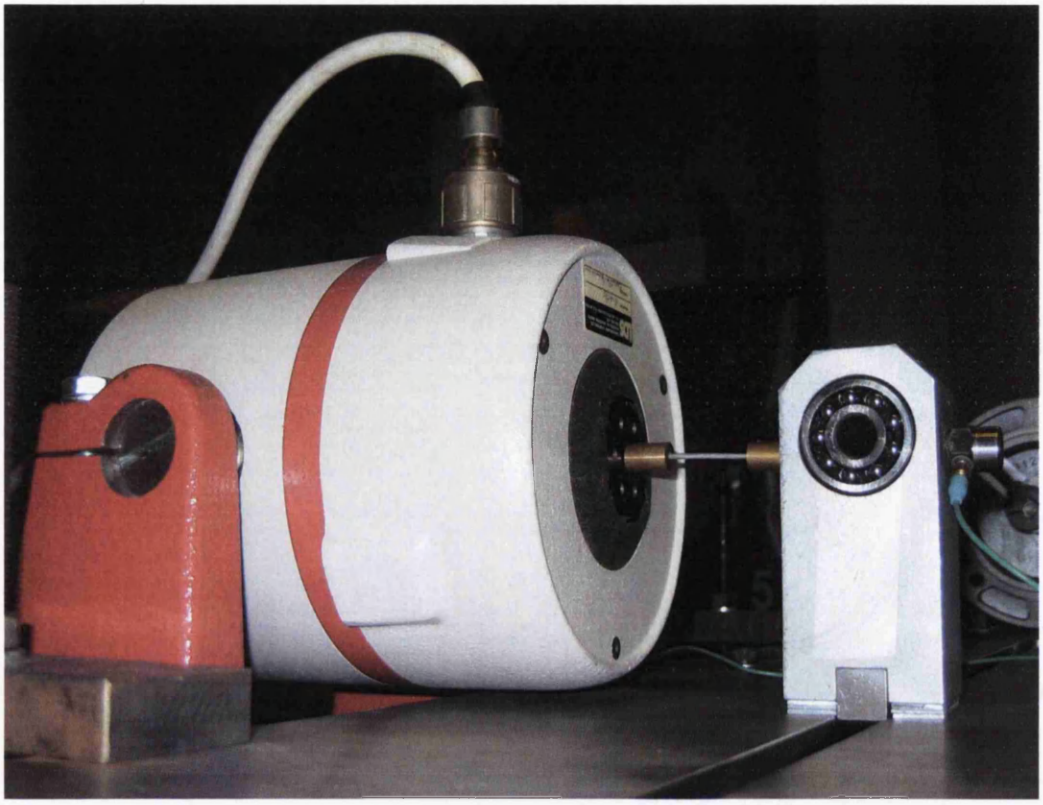

Figure 6 – 1 Picture of shaker test

Figure 6 - 1 shows a bearing housing mounted on the base plate attached to a shaker, which is the vibration generator. The shaker applied different forces to the bearing. An accelerometer is mounted on the bearing housing vertically to measure the angular acceleration of the bearing housing during the test. During the experiment, the bearing was excited under the swept-sine excitation supplied by the shaker starting at 1 Hz and going up to 300 Hz.

Figure 6 – 2 Power Amplifier used to drive the shaker

A *Ling Dynamic Systems* (LDS) shaker system model V406 (Figure 6 – 1) was used as a vibrator to produce force to the bearing housing. The LDS PA100E power amplifier which was used to drive the LDS 400 series Vibration Generator is shown in Figure 6 - 2. There is a rotary master gain control on the power amplifier, which is able to set the level of the amplifier output signals.

The swept-sine excitation signal is supplied by a sine wave generator via a power amplifier to the exciter, which harmonically drives the bearing housing. The use of swept-sine excitation provides a high excitation level compared to random excitation and a short testing compared to stepped-sine excitation. In this case, a frequency value ranging from 5 – 300 Hz was selected to test the dynamic behaviour of the elastomers. By varying the frequency and amplitude of the exciting signal, the corresponding force and acceleration signals are measured and stored in the computer. The signal is then observed using the Siglab program. The details of signal processing will be discussed later in this chapter.

Figure 6 – 3 Siglab hardware (DSPT Siglab 20-22)

SigLab is a lab-quality measurement system with outstanding front-end signal conditioning, including programmable gain, offset, coupling, overload detection. DSPT Siglab was chosen as the dynamic signal analysis system for the hammer and shaker test in this project. The Siglab hardware (DSPT Siglab 20-22) is shown in Figure 6 – 3.

As mentioned previously in Chapter 5, DSPT Siglab is a multi-channel dynamic signal analyzer for characterizing signals and systems in the lab. It is a combination of function generator, spectrum analyzer and network analyzer. One of the advantages of the Siglab/Matlab integration is the ability to address unique application requirements by programming Siglab within the Matlab environment. Siglab is routinely used to estimate transfer functions associated with dynamic systems including control systems. To make a transfer function on a dynamic system, an excitation is supplied to the system and the system's response to this excitation is measured.

Siglab comes with two software applications for transfer function estimation: swept-sine and broad-band random FFT based network analyzer. In this case, the swept sine technique is used. The advantage of the swept-sine estimation technique is its rejection of noise and non-linear system behaviour.

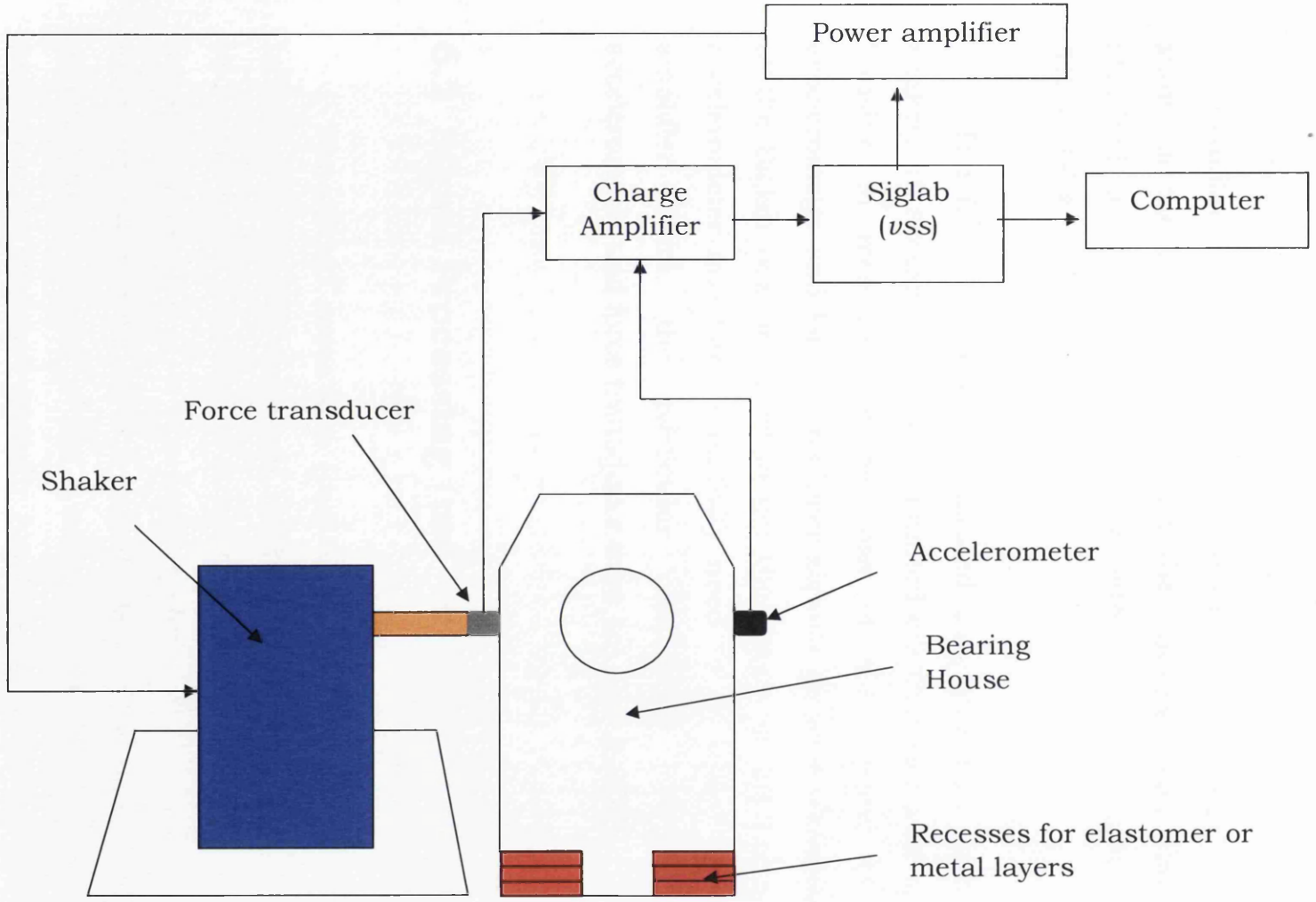

Figure 6 – 4 Schematic diagram of experimental set-up of shaker test

A schematic of the shaker test experimental set-up, including the general arrangement of the experiment instruments, is shown in Figure 6 – 4. The whole apparatus was mounted on a massive rigid steel table. The bearing housing was mounted on the steel baseplate seen in Figure 6 – 1. The installation of the bearing housing on the baseplate was exactly the same as the run-down test and the hammer test. The shaker was attached to the bearing housing with a force transducer mounted horizontally.

The force transducer measured the excitation produced by the shaker. An accelerometer was mounted on the other side of the bearing housing to measure the response of the bearing housing. Both accelerometer and force transducer signals go pass the charge amplifier to the Siglab box. In order to get the result in the correct scale, the accelerometer and force sensitivity need to be scaled with the charge amplifier. Here, the particular calibration constants for both accelerometer and force transducer were set on the charge amplifier.

6.2 Signal Processing (*vss* – virtual swept-sine)

The virtual swept sine (*vss*) which is a swept sine measurement technique in Siglab was used in the shaker test. Swept stepped sine (more precise) is a method of measuring the frequency response function (transfer function) of a dynamic system. It is the oldest network measurement technique but is still the best for a system with high noise or one which is linear within a narrow range. In the absence of these problems, the fft-based transfer function technique used by *vss* is the best choice because it is faster.

A sine wave is used in the swept sine tests, as the system excitation will step through the frequency range of interest. The reference

channel (channel 1) measures the excitation signals while the response channel (channel 2) measure the output of the system. In this case, the force transducer was connected to channel 1 and the accelerometer was connected to channel 2. The ratio of the sine wave amplitudes (response channel / reference channel) is displayed as the transfer function magnitude.

As mentioned previously, the advantage of a swept-sine estimation technique is that it is the least affected by noise and non-linear system behaviour, since there is a tracking filter function in the *vss* program that is able to reduce the noise in the system.

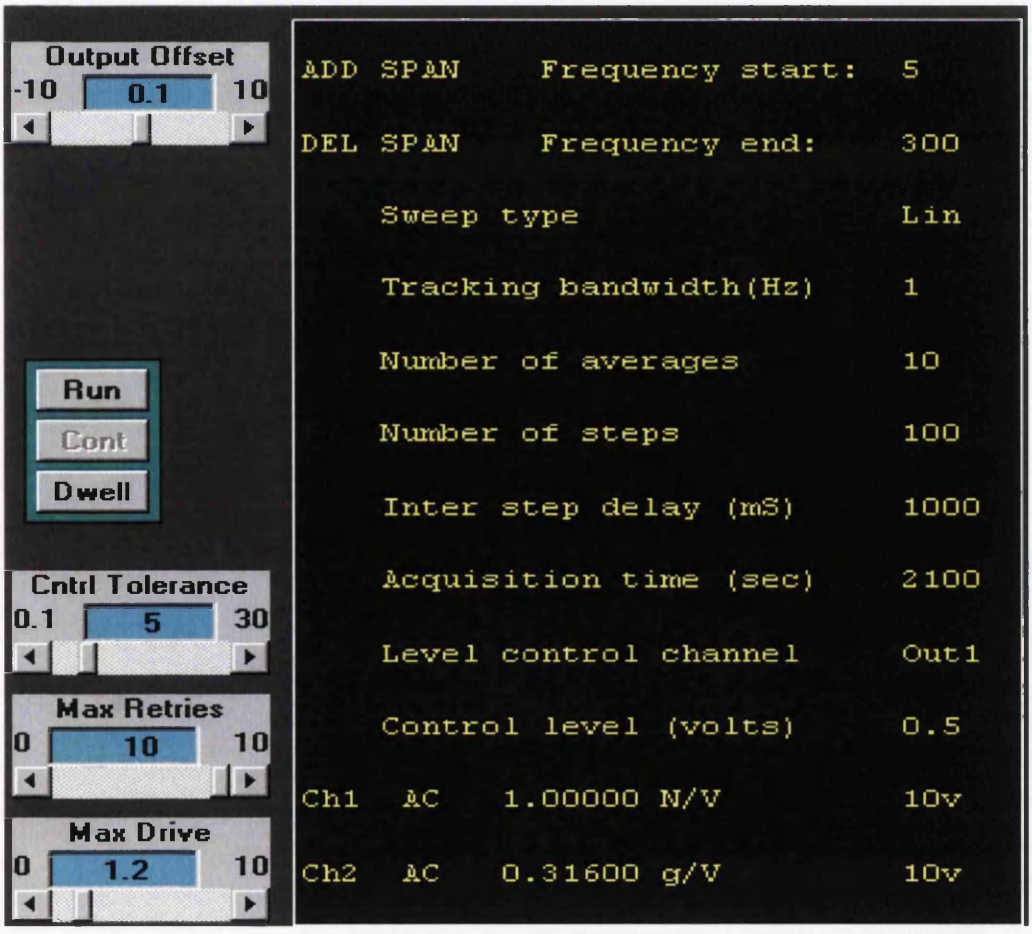

Figure 6 – 5 *vss* (virtual swept-sine) program – *setup display mode*

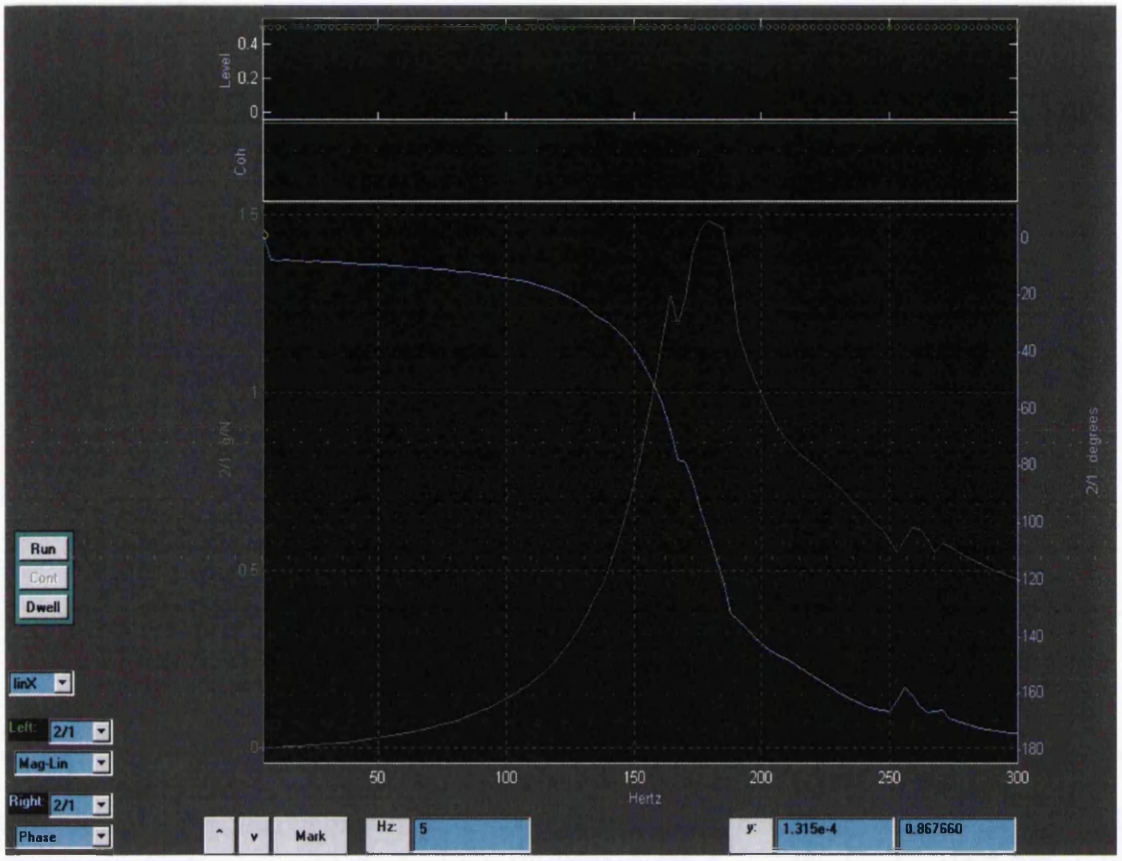

Figure 6 – 6 *vss* (virtual swept-sine) program – *graphs display mode*

In the *vss* program, test variables for example upper and lower limits, number of frequency steps, excitation amplitude, input gain setting, tracking filter bandwidth and number of averages need to be specified in the *setup display mode* (see Figure 6 – 5). In this case, a frequency range of 1-300 Hz was specified in the *vss* program. Linear sweep type of *vss* program was chosen during the test. The *Number of averages* was specified as 10, which can improve the accuracy of the measurement. Increasing this number of averages also reduces the effects of the system noise at the expense of increased measurement time. *vss* has a graphs display mode, as shown in Figure 6 – 6.

The transfer function data, coherence data and also the frequency data are all saved under a file/save operation. Their Matlab variable names are XferDat, CohDat and Fvec. There are several methods to access the data. In this case, a Matlab program was used to retrieve and plot the result data produced by the shaker and hammer tests.

6.3 Shaker Tests Results

From Figure 6 – 7, it can be seen that the 3-rubbers test encounters the highest vibration followed by 2-rubbers and 1-rubber test. The response amplitude is dependent on the flexibility of the rig structure arrangement. More rubbers will introduce higher flexibility to the rig. Therefore, higher response amplitude is obtained from the 3-rubbers test due to its higher flexibility.

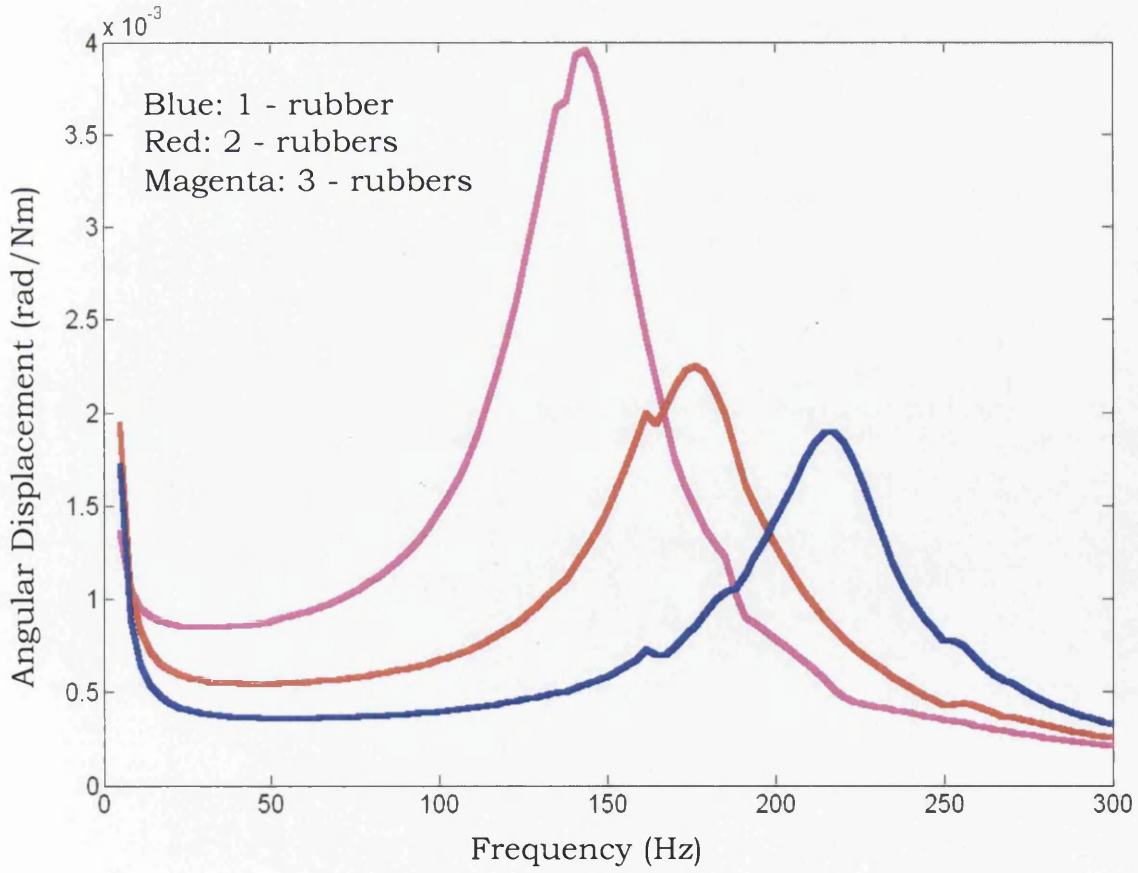

Figure 6 – 7 Shaker test (displacement results)

It was also found that the 1-rubber test achieved the highest natural frequency followed by 2-rubbers and 3-rubbers test. It is also due to the flexibility of the rig. Higher stiffness will induce higher natural frequency.

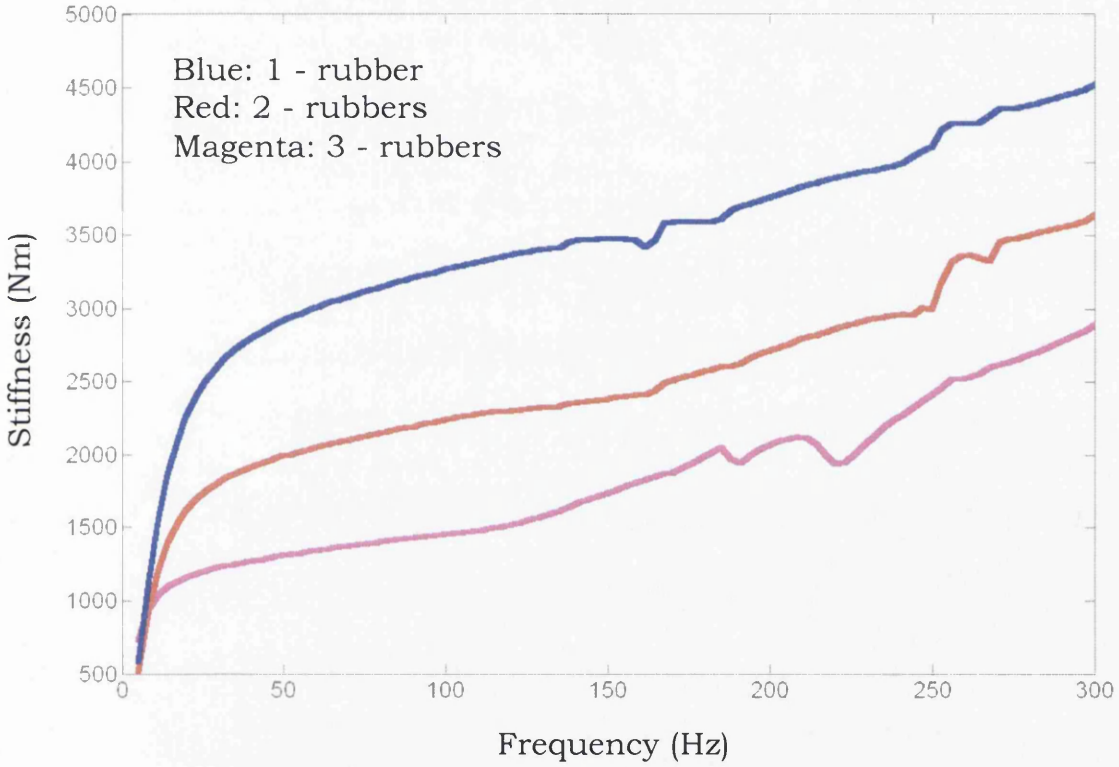

Figure 6 – 8 Shaker tests (stiffness result)

Figure 6 – 8 shows the stiffness results from the shaker test. The stiffness tends to increase on increasing the excitation frequency. From the above figure, the1-rubber test has the highest stiffness result follow by 2-rubbers and 3-rubbers test.

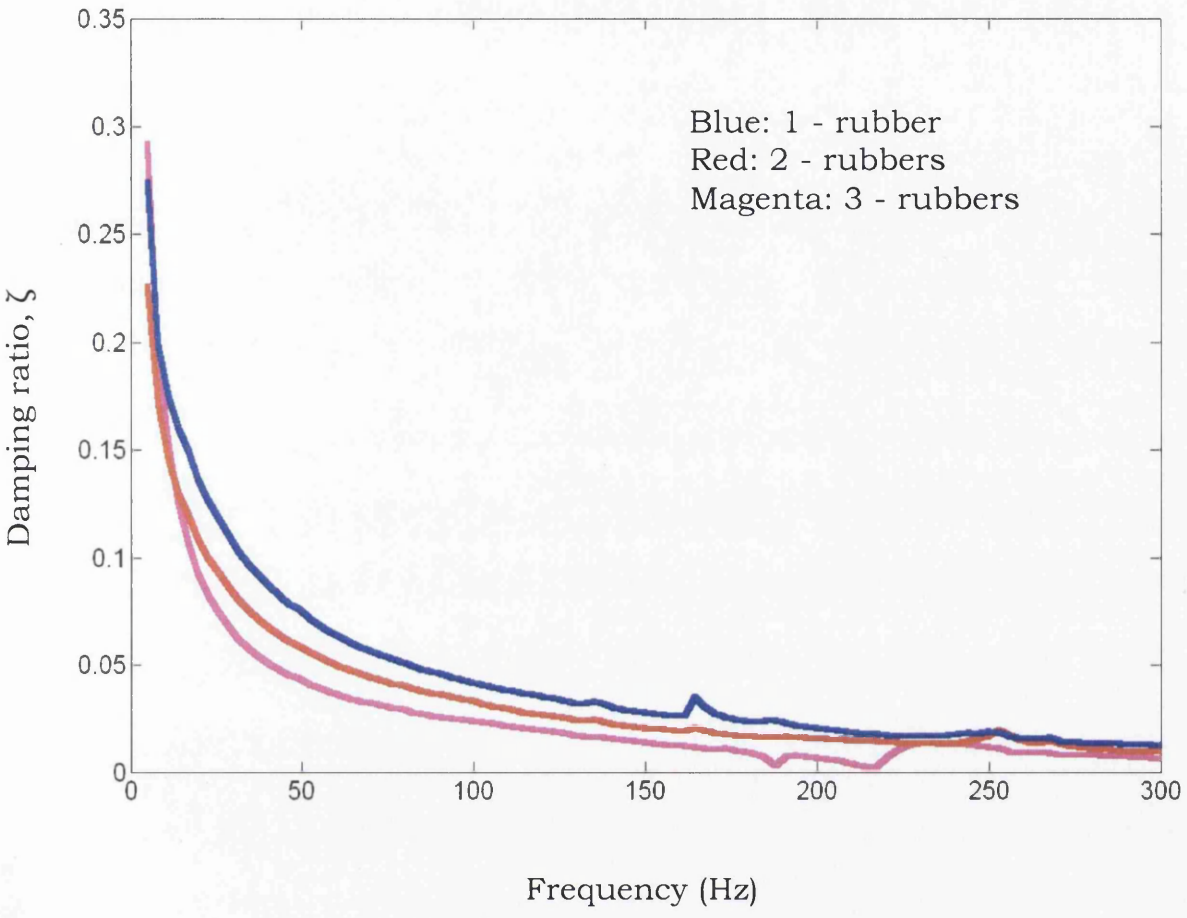

Figure 6 – 9 Shaker tests (Damping results)

Figure 6 – 9 shows the damping results for the shaker tests. Damping tends to decrease with increasing excitation frequency.

6.4 Non-linear System Verification

In this project, several tests have been carried out, using the shaker, to verify the linearity of the system. In this case, 1-rubber, 2-rubbers and 3-rubbers tests are performed at different voltage inputs, which are 0.25V and 0.5V. The results obtained at different voltage input are compared. The voltage represents the force applied to the system.

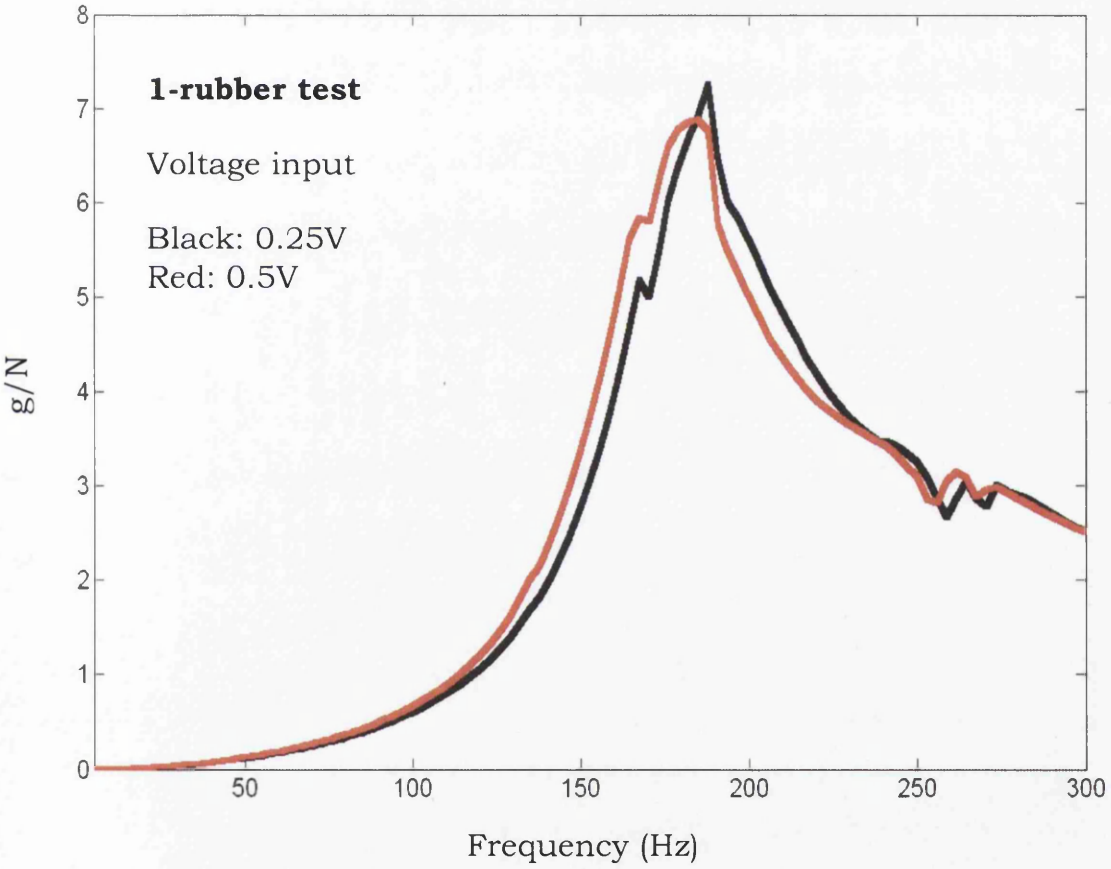

Figure 6 – 10 Different voltage input shaker test (1-rubber test)

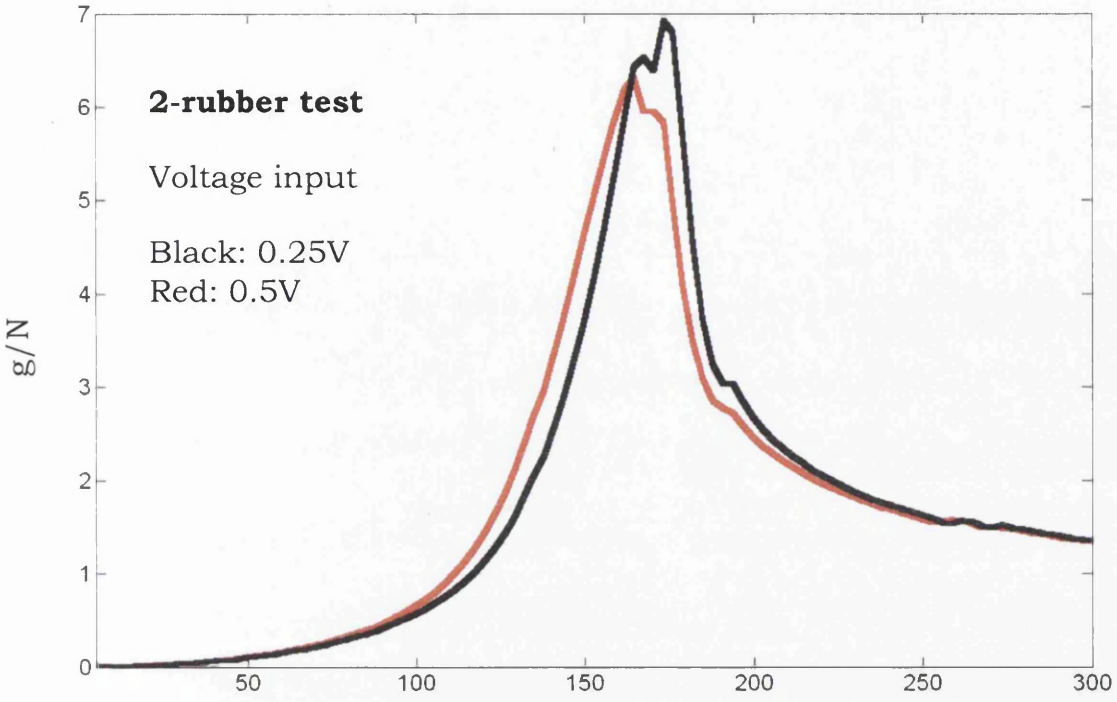

Figure 6 – 11 Different voltage input shaker test (2-rubber test)

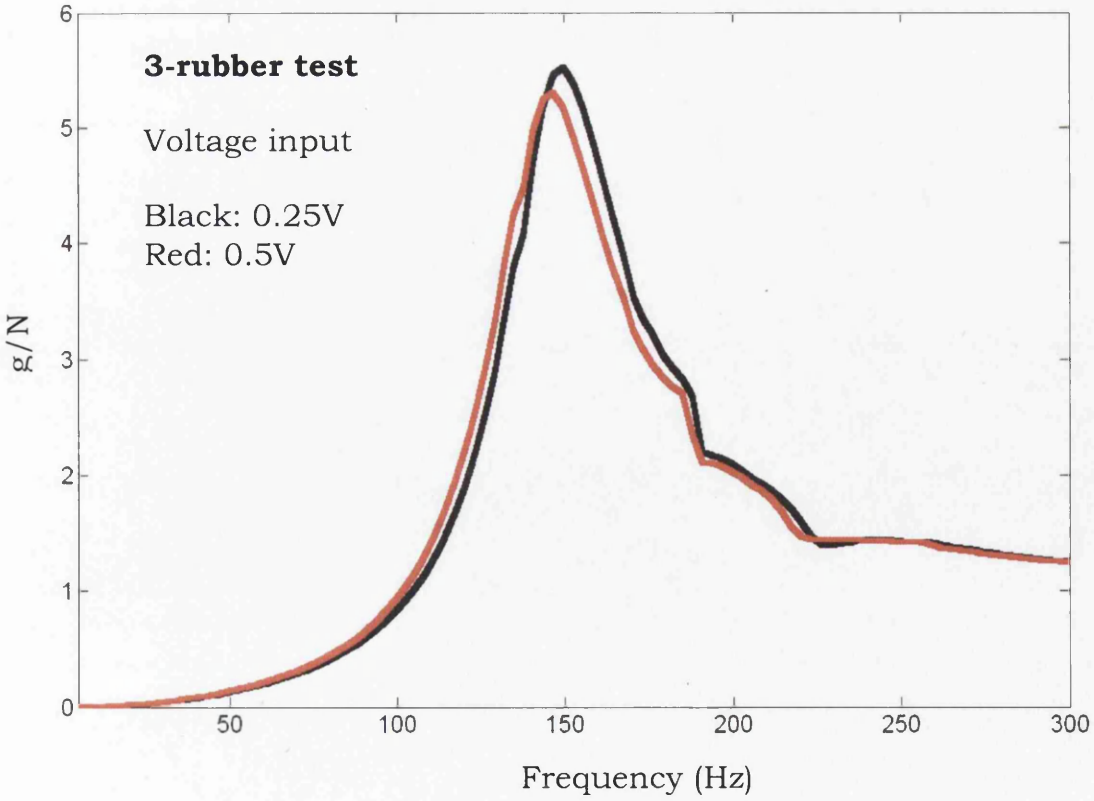

Figure 6 – 12 Different voltage input shaker test (3-rubber test)

The overall results indicate that the acceleration of the system is slightly different when a different voltage input was applied to the system. Theoretically, the acceleration increases with increment of force supplied. The results obtained are a transfer function (g/N) of acceleration over the excitation force. Therefore, for a linear system, when the applied force is changed, the transfer function (g/N) should remain the same. Nevertheless, in this case, it was found that the transfer function (g/N) decreased when the force applied is increased. Here, it was concluded that the system is non-linear and this explained why the response amplitude didn't increased linearly when more rubbers were applied to the system.

6.5 Discussion

Results obtained using the identification theory given in Chapter 3 together with the data acquired from the shaker test have been discussed in this chapter. Here, the overall results showed that stiffness tends to increase on increasing the excitation frequency. In addition, damping tends to decrease on increasing the excitation frequency.

The experimental results indicate that the noise is less if compared to the run-down and hammer test. This is due to the tracking filter function in the *vss* program that is able to reduce the noise of the system. Due to the reduction of noise during the experiment, the results obtained are accurate even when the excitation frequency is low. In this case, the signal/noise ratio is high, therefore, the experimental results of shaker test is accurate even when the acceleration is low. It was mentioned previously that the results from hammer test and run-down test are less accurate at low frequencies because the accelerations are low which lead to low signal/noise ratio. Furthermore, in this case, for the hammer test, the time averaging is low; hence it was more affected by system noise.

From the set of results presented in Figure 6 – 7, the response amplitude for the 3-rubbers test is the highest followed by 2-rubbers and 1-rubbers. Furthermore, the 1-rubber test achieved the highest natural frequency followed by 2-rubbers and 3-rubbers test. This can be explained by the flexibility of the system. The elastomer layers were added in series, which is shown in Chapter 4. Therefore, the flexibility of the system increased. The vibration increases on increasing the flexibility of the system. At the same time, the natural frequencies decrease on increasing the flexibility of the system. From the general dynamic theory, natural frequency is varying with the stiffness (flexibility) of the system. The flexibility, which means the stiffness of the system, is shown in Figure 6 – 8. The results show that the 1-rubber system is the stiffest when compares with 2-rubber and 3-rubber system. The 3-rubbers

system is the most flexible system; hence, the vibration that occurred in the 3-rubber test is the highest.

The corresponding damping results are shown as damping ratio in Figure 6 – 9. Here, the damping ratio decreases on increasing the excitation frequency. From both stiffness and damping results, it is seen that 1-rubber test had the highest stiffness and damping followed by 2-rubbers and 3-rubbers test. The reason has been discussed in Chapter 5. When the elastomers are added in series, the reciprocals will add and therefore the damping will reduce. Hence, when more layer of elastomers are applied to the system, the system becomes more flexible and the damping reduces. This explains why the 3-rubber system had the lowest damping properties.

CHAPTER 7

VERIFICATION OF THE HAMMER TEST RESULTS

In this chapter, the corresponding hammer test and shaker test results are compared in order to verify the hammer test results. It has previously stated that the shaker test is a far more accurate way of measuring dynamic response. However, it is a relatively complex process whereas the hammer test is relatively simple, but possibly less accurate. Also the space required for a hammer test is far less than that for a shaker test. The aim here is to compare the result in order to confirm, or otherwise, that reasonable results can be achieved by the hammer test and hence validate its use in these circumstances, where space may be limited.

The response amplitude results of 1-rubber, 2-rubbers and 3-rubbers tests performed using hammer and shaker tests are shown in Figure 7 – 1 to Figure 7 – 3. As mentioned in previous chapter, the motion involved in hammer and shaker tests is rotational motion (to a first approximation), hence, the displacements are presented in radians (rad) rather than millimetres (mm).

The difference between the hammer tests and the shaker tests is the type of excitation forces applied to the system. For the hammer test, impact excitation is supplied to the system by using a specially designed hammer. For a shaker test, swept-sine excitation produced by the

vibration generator (shaker) is applied to the system. Both hammer test and shaker test response amplitude results are presented.

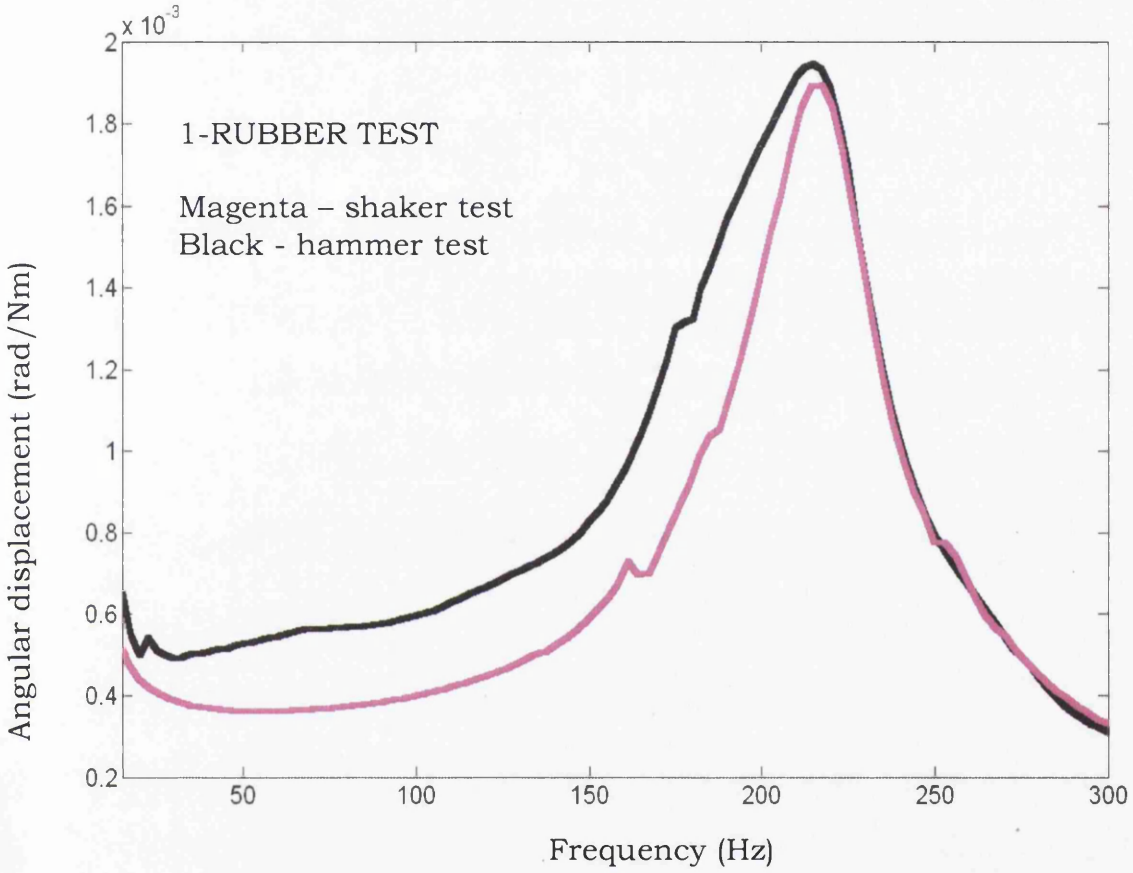

Figure 7 – 1 1-rubber tests (Hammer and shaker tests)

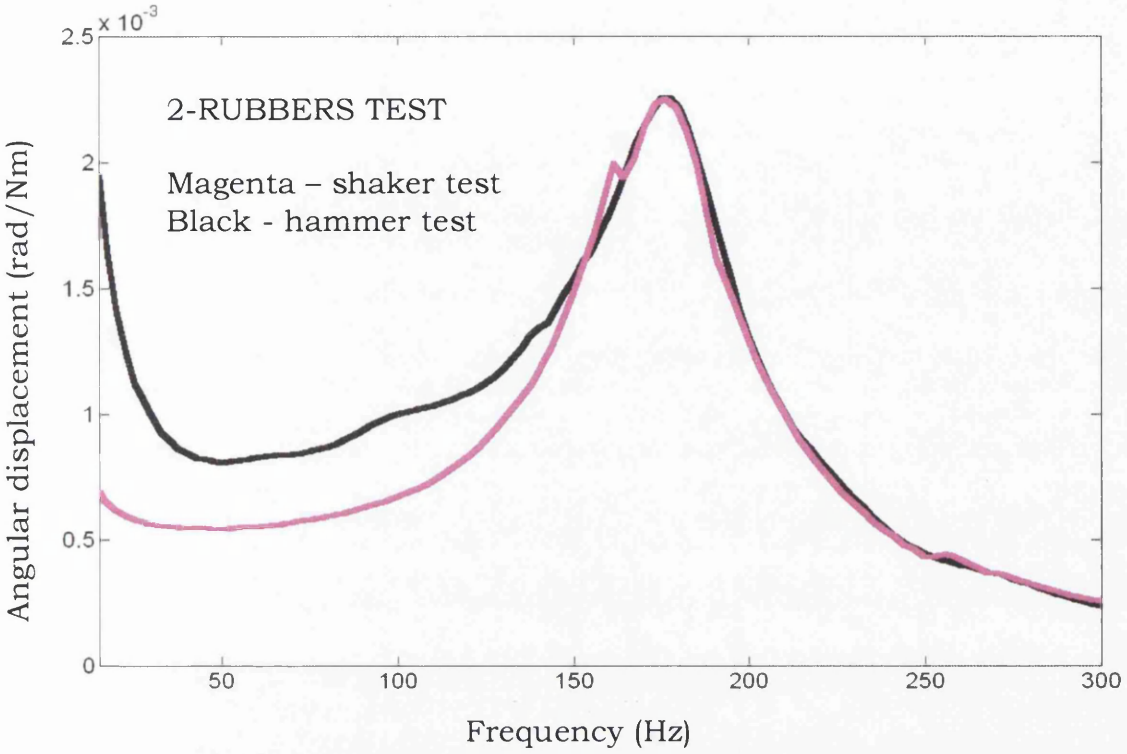

Figure 7 – 2 2-rubber tests (Hammer and shaker tests)

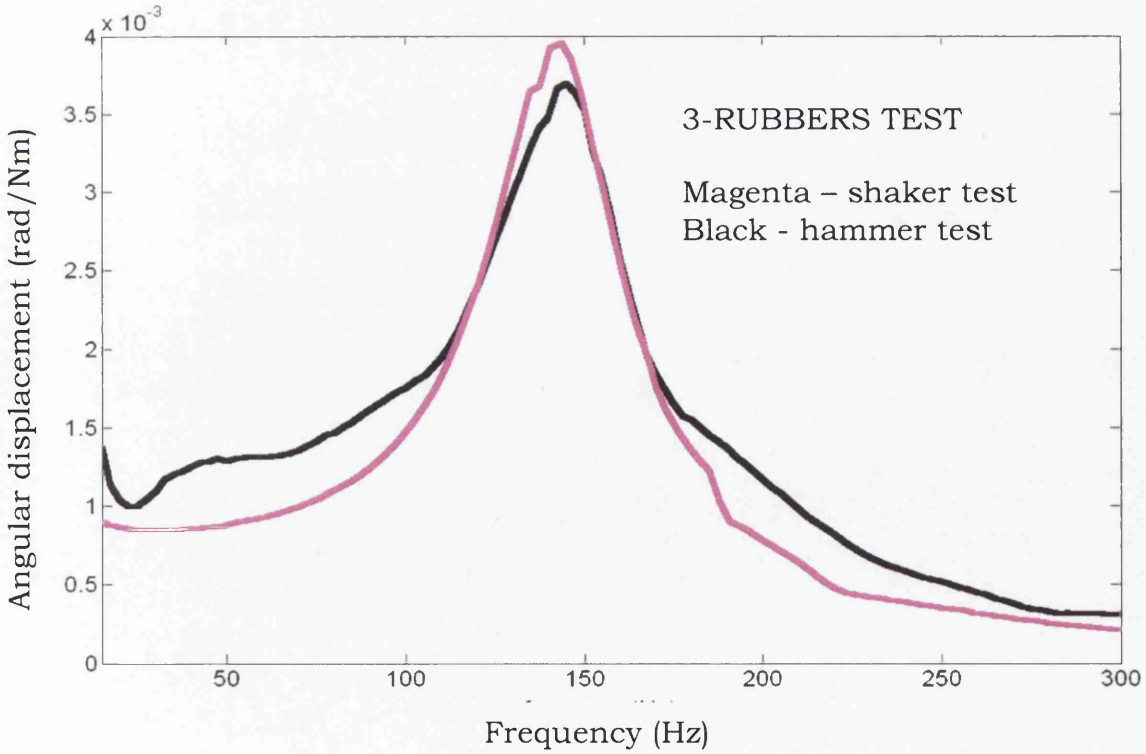

Figure 7 – 3 3-rubber tests (Hammer and shaker tests)

There is good comparison between the experimental results from the hammer test and those from the shaker test and this justifies the precision of the experimental result obtained. For the sets of results presented in this section, the result obtained from hammer and shaker test are approximately identical. This will be discussed further in the next chapter. Both hammer and shaker test results are showing a similar trend of curve. In conclusion, the results obtained from the simple hammer test are reliable.

CHAPTER 8

SUMMARY AND CONCLUSIONS

8.1 Summary of Results

In this present study, topics of importance to the research into the dynamic properties of elastomers in academic and industrial communities have been addressed including a review of the relevant literature and an overview of the associated combination of experimental and theoretical techniques.

Using measured bearing responses and known excitation forces, it is possible to estimate the influence of the dynamic properties of elastomers on machine behaviour. The models showed some predictive capacity with respects to the thickness of elastomer used in the system; however, the response amplitude at low frequency was often seriously in error. It is believed that this is due to noise. The signal to noise ratio is very small when the acceleration is low. Therefore, the experimental results obtained at low frequency in this work are less accurate.

It has been shown that the dynamic characteristics of elastomers can have a significant influence on machinery. Having designed a suitable rig for the experiments, the measured response amplitude and excitation force together with the identification theory was used to determine the stiffness and damping properties of an elastomer. The

influence of elastomers on machine behaviour has been quantified in this project.

Different experiments were carried out to accomplish the aim of this project. The results obtained from run-down, hammer and shaker tests are summarised. Here, the accuracy of the hammer test results was verified by the shaker tests. It was found that the simple hammer test results are comparable with the more complex shaker test results.

From all the experimental results obtained, a statement is made that the vibration tends to increase when more elastomers are applied to the system. The system becomes more flexible when more layers of elastomers are used. Here, the stiffness results represent the flexibility of the system. In this case, the results showed that the stiffness reduced when the number layer of elastomers increased, which is in good agreement with the results obtained by Chang [10]. In the early years, the literature from NASA [12] stated that the size of the elastomer has a significant influence on the dynamic stiffness of the system. It was found that stiffness reduces with the increment of height (thickness) which is in good agreement with the findings in this work. Furthermore, the overall results show that the natural frequency of the system increases with stiffness. This is in good agreement with the work reported by Bormann and Gasch [14] who obtained similar findings using different method as illustrated in their paper.

In particular, the stiffness increased on increasing the excitation frequency and the damping decreased on increasing the excitation frequency. F. Petrone et al. [16] had reported that stiffness tends to increase and damping tends to decrease on increasing the excitation frequency, which is a good agreement with the trend of graph in this

work. The results obtained by F. Petrone are shown in Figures 8 – 1 & 2 which support the findings in this work. Furthermore, Lapčik et al. [9] reported that the dynamic stiffness of recycled rubber increases with frequency. The stiffness result obtained by Lapčik et al is shown in Figure 8 – 3 that also supports the findings of this work.

Presently, applications of elastomers are receiving a great deal of attention in both academic and industrial communities. Dynamic systems suffering from instability or resonance problems often lack sufficient damping to reduce the vibration to an acceptable level. Elastomers are particularly suitable to provide the necessary damping for rotors. However, applications of elastomers must be appropriate, especially in terms of the shape and size of the dampers (elastomers) which is one of the major factors that affect the machine behaviour. Richards and Singh [6] reported that the size and shape of rubbers have a significant influence on the vibration of the system. In this work, it was found that the number layers of elastomer (or thickness) affect the damping characteristics of the system. An increase of the number layers of elastomers is actually reducing the damping of the system.

Here, it was also suggested that the system might be non-linear from observations of the experimental results obtained. Hence, several tests are carried out to verify the linearity of the system. A shaker test was performed for this purpose at different voltage input (force applied). The results showed that the system is non-linear. This explained why the case 2 (2-rubber test) is not exactly 2/3 of the amplitude of case 3 (3-rubber test). Case 1 is not exactly 1/3 of the amplitude of case 3 because of non-linearity. There are many factors that can cause non-linearity to the system. For example, in this case, a layer of steel plate/shim was applied to the system between the elastomers; this prevented the

elastomer layers from experiencing high lateral deformation [10]. Because of this characteristic, the bearing has a high vertical stiffness when the elastomers are bonded to the interleaving steel plate/shim. A layer of steel shim between the rubber layer can actually increase the vertical (lateral) stiffness while maintaining the horizontal flexibility [10]. Therefore, the more interleaving steel plate/shims are applied to the system, the lower the elastomers deformation occurs.

Typically, elastomers show a non-linear elastic and dissipative behaviour. These mean that the stiffness and damping properties are non-linear function of the displacement. The same non-linear behaviour occurs with respect to frequencies when the elastomers are excited with periodic forces [16]. Friction between the rubber and steel shim occurred when a movement takes place, which decreases the stiffness of the system. A friction force is required to overcome the resistance offered by the friction between the surfaces. The total reaction forces in between the elastomers and steel plate/shim have different expressions according to whether there is adherence on both sides, sliding on both sides, or adherence on one and sliding on the other side [16]. This reaction force will reduce the stiffness of the system by a certain factor depends on the adherence or sliding case [16] . This is a further explanation for the non-linearity of the system.

The identification of the dynamic properties of elastomers has been successfully achieved, with measured parameters matching very closely in most cases. The identification method was tested in a wide range of conditions. The influence of dynamic properties on machine behaviour was studied, and found to be significant. The results obtained in this work are summarized in Table 8 – 1. Table 8 - 1 shows that the response amplitude of 3-rubbers test is the highest follow by 2-rubbers

and 1-rubbers tests. The natural frequency of 1-rubber tests is the highest follow by 2-rubbers and 3-rubbers tests. Damping decrease when the number layer of elastomers increases. Stiffness decreases when the number layer of elastomers increases.

		1 RUBBER	*2 RUBBERS*	*3 RUBBERS*
RUN-DOWN TEST	Natural frequency (Hz)	AH - 26.4 BH – 25 BV – 25	AH – 26.7 BH – 25.5 BV – 25.5	AH – 27 BH – 26.2 BV – 26.2
	Peak amplitude (m)	AH – 4.1×10^{-6} BH – 2.45×10^{-6} BV – 2.1×10^{-6}	AH – 4.2×10^{-6} BH – 2.475×10^{-6} BV – 2.187×10^{-6}	AH – 4.25×10^{-6} BH – 2.5×10^{-6} BV – 2.21×10^{-6}
HAMMER TEST	Natural frequency (Hz)	146.5	178	216.6
	Peak amplitude (m)	0.0038	0.0023	0.002
	Damping ratio, ζ	0.044	0.0167	0.0066
SHAKER TEST	Natural frequency (Hz)	145.4	176.7	218
	Peak amplitude (m)	0.0039	0.00225	0.0019
	Damping ratio, ζ	0.034	0.019	0.0047

Table 8 – 1 Results summary of Run-down, Hammer and Shaker tests

UNIVERSITY OF WALES SWANSEA LIBRARY

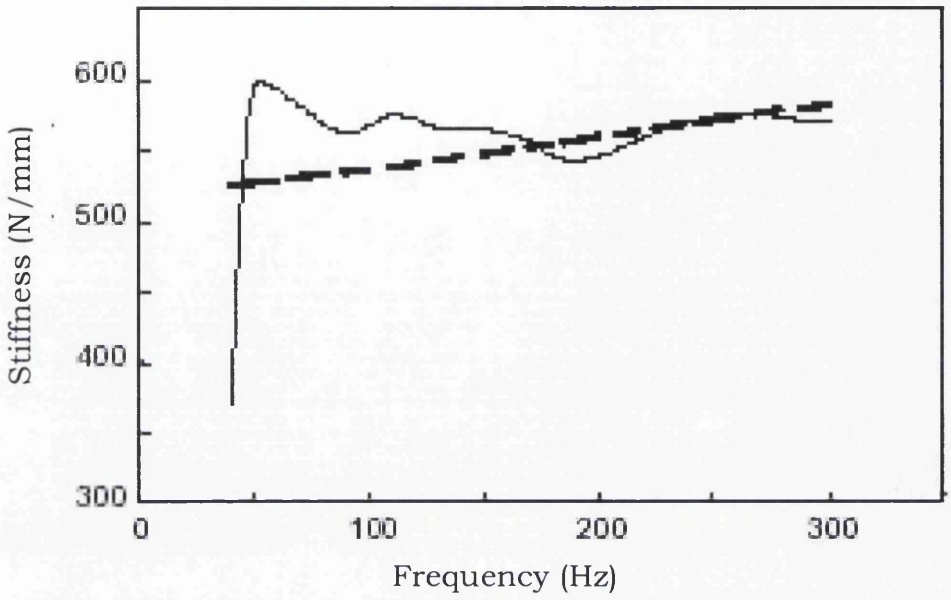

Figure 8 – 1 Dynamic stiffness versus excitation frequency
(Result obtained by F. Petrone et.al [16])

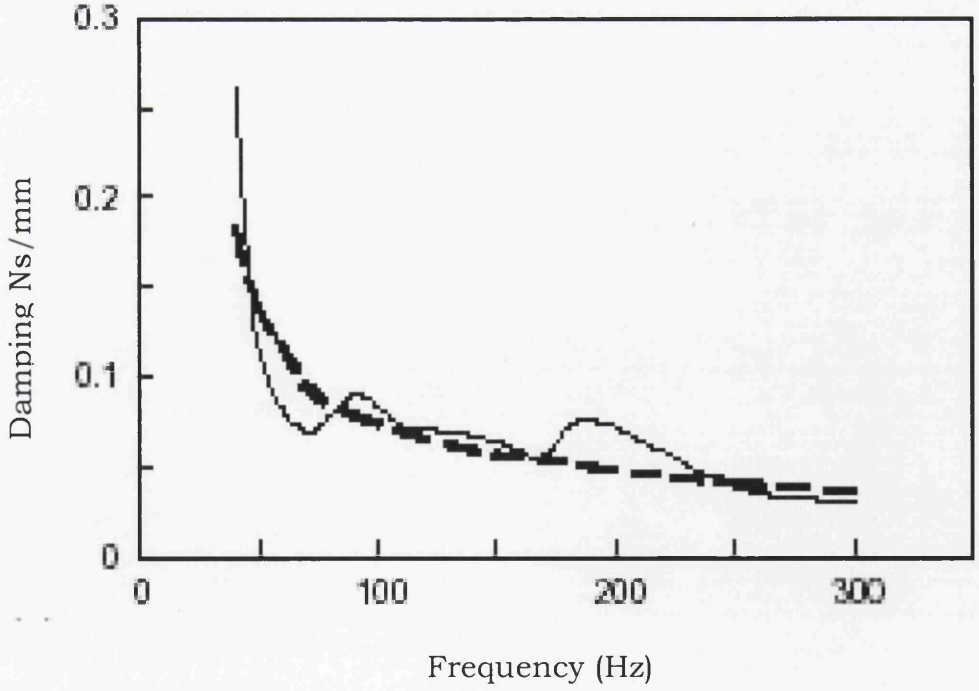

Figure 8 – 2 Viscous damping coefficients versus excitation frequency
(Result obtained by F. Petrone et.al [16])

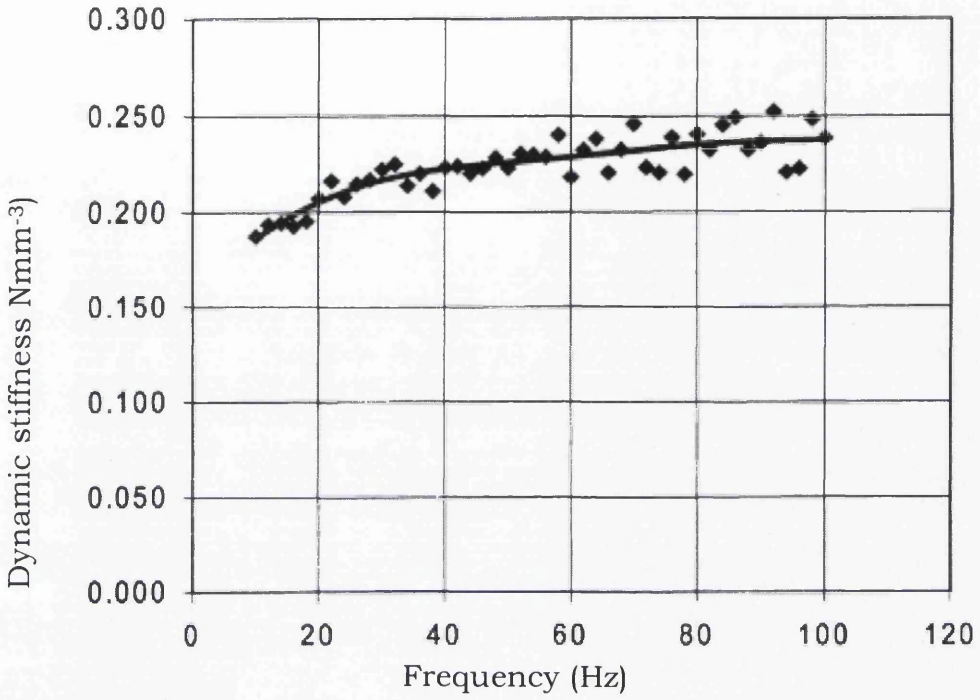

Figure 8 – 3 Dynamic stiffness versus excitation frequency
(Result obtained by L. Lapčik Jr et.al [9])

8.2 Conclusions

In this thesis, the effect of the dynamic properties of elastomers on machine behaviour has been addressed, including a review of the relevant literature. An overall summary of the experimental results obtained has also been presented. As discussed in this thesis, the application of elastomers in industry is extremely broad, for example, as dampers and isolators. Therefore, the influence of elastomers on machine behaviour is an important issue. However, their qualification is still an ongoing research topic. Hence, techniques for property identification under operating conditions were developed in this research work. Broadly the studies have been concentrated on the objective of studying and quantifing the influence of elastomer thickness on machine behaviour.

An identification method for estimating both stiffness and damping properties has been presented. For the objective, the proposed methods have been qualified initially on a run-down test. Later on, it proceeded to hammer test and shaker test. A total of three types of experiment were performed in this study. For machines involving elastomers, it has been shown that the inclusion of elastomers in machinery can have a significant influence on the dynamic behaviour of the system. Here, a conclusion is made that the size of elastomers, in term of thickness, has a significant influence on machine behaviour. Stiffness and damping properties of the system reduced with the increased of number layers of elastomer.

The response of the system was observed for a number of layers of elastomer in the system. The vibration increases when more layers of elastomers are applied. It has been shown that the system is non-linear,

as the response amplitude of the system does not increase linearly with the number of layers of elastomer. As expected, the natural frequencies of the system vary with the stiffness properties, while the system is flexible, the natural frequency is lower.

As has also been shown that the hammer test results compared reasonably well with shaker test results. Therefore, the identification method may be regarded as having been broadly successful with further work required to improve the predictive capacity of the estimated models. It is hoped that the work discussed above, which is of practical relevance to the application of elastomers as dampers in machinery, will form a basis for the implementation of these ideas and results, and thus play a part in improving the vibration conditioning of machinery.

8.3 Recommendations for Future Work

As far as future work in this field is concerned, the following recommendations are made:

(i) Extension of the work to larger, multi-degree-freedom models. The motion of the system can be considered as both horizontal and rotation allowing for the representation of the system as a two-degree-of-freedom system.

(ii) The proposed method should be performed for a higher range of frequencies.

(iii) Shear and tensile/compressive effects should be included in the identification method.

(iv) The identification of a modal model for the objective of this work should be developed and the usefulness of the identified model should be compared with the present method.

REFERENCES

[1] *F. Findik, R. Yilmaz and T. Köksal*, 2003, "Investigation of mechanical and physical properties of several industrial rubbers", Material and Design 25(2004), pp. 269-276.

[2] *Ana Lúcia N. Silva, Marisa C. G. Rocha and Fernanda M. B. Coutinho*, 2002, "Study of Rheological Behaviour of Elastomer/polypropylene blends", Polymer Testing 21(2002), pp. 289-293.

[3] *C. Louis, J. F. Chailan, P. Bartolomeo and J. L. Vernet*, "Morphological, thermal and mechanical properties of rubber and polysulfone blends", Polymer Testing 42(2001), pp. 7101-7115.

[4] *Zheng Ming Huang, S. Ramakrishna and A. A. O. Tay*, 2000, "Modeling the stress/strain behaviour of a knitted fabric-reinforced elastomer composite", Composites Science and Technology 60(2000), pp. 671-691.

[5] *R. Y. Tan and I. W. Weng*, 1995, "Identification of dynamic properties of isolated structures", Engineering Structures, Vol 18, No.3, pp. 240-246.

[6] *C. M. Richards and R. Singh*, 2001, "Characterization of Rubber Isolator Nonlinearities in the context of Single and Multi-Degree-Of-Freedom Experimental Systems", Journal of Sound and Vibration, 247(5), pp. 807-834.

[7] *S. Kim and R. Singh*, 2001, "Multi-Dimensional Characterization of Vibration Isolators over a Wide Range of Frequencies", Journal of Sound and Vibration, 245(5), pp. 877-913.

[8] *M. Sjőberg and L. Kari*, 2003, "Testing of Nonlinear Interaction Effects of Sinusoidal and Noise Excitation on Rubber Isolator Stiffness" , Polymer Testing 22(2003), pp. 343-351.

[9] *L. Lapčik Jr, P. Ausustin, A. Pištěk and L. Bujnoch*, 2001, "Measurement of the Dynamic Stiffness of Recycled Rubber based Railway Track Mats according to the DB-TL 918.071 Standard", Applied Acoustics 62(2001), pp. 1123-1128.

[10] *Cheng Hsiung Chang*, 2002, "Modeling of Laminated Rubber Bearings using an analytical stiffness matrix", International Journal of Solids and Structure 39 (2002), pp. 6055-6078.

[11] *M. Imbimbo and A. De Luca*, 1998, "F.E Stress Analysis of Rubber Bearings under Axial Loads", Computer and Structured 68(1998), pp. 31-39.

[12] *J. A. Tecza, M. S. Darlow and A. J. Smalley*, 1979, "Development of Procedure for Calculating Stiffness and Damping of Elastomers in Engineering Applications", Part V, NASA-CR- 159552.

[13] *M. S. Darlow and A. J. Smalley*, 1978, "Development of Procedure for Calculating Stiffness and Damping of Elastomers in Engineering Applications", Part IV, NASA-CR-135355.

[14] *Bormann A and Gasch R*, 2003, "Damping and Stiffness Coefficients of Elastomer Rings and Their Optimised Application in Rotor

Dynamics: Theoretical Investigations and Experimental Validation", Sixth International Conference, IFToMM Australia, pp. 628-636.

[15] *A. F. El-Bassiouny,* 2004, "Effect of Non-lineariarities in Elastomeric Material Dampers on Torsional Oscillation Control", Applied Mathematics and Computation, Article in press.

[16] *F. Petrone, M. Lacagnina and M. Scionti,* 2004, "Dynamic Characterization of Elastomers and Identification with Rheological Models", Journal of Sound and Vibration, 271(2004), pp. 339-363.

[17] *S. Edwards,* 1999, "An Investigation Of Rub, Unbalance And Shaft Bow In Rotordynamics Systems", PhD Dissertation, University Of Wales Swansea.

[18] *Fyfe. K. R. and Munck,* E.D.S., 1997, "Analysis of Computed Order Tracking", Mechanical Systems and Signal Processing, 11(2), pp. 187-205.

[19] *K. M. Bossley, McKendrick, R. J. Harris, C. J. and C. Mercer,* 1999, "Hybrid Computed Order Tracking", Mechanical Systems and Signal Processing, 13(4), pp. 627-641.

[20] *VSI Rotate 2.0,* 2000, Vold Solutions Inc., USA.

[21] *Siglab*: 1998, User Guide Version 3.0. DSP Technology Inc., USA

[22] *Matlab*: 1999, A User Guide, The Mathworks Inc., Version 5.3.1